Anti-cancer Effect of *Andrographis paniculata, Ziziphus spina-christi,* and *Vernonia extensa* and its Combination with Piperine Free *Piper nigrum* Extract on Cancer Cell Lines

Muhammad Faisal

A Thesis Submitted in Fulfillment of the Requirements for the Degree of Master of Science in Biomedical Sciences

Prince of Songkla University

2020

Anti-cancer Effect of *Andrographis paniculata, Ziziphus spina-christi,* and *Vernonia extensa* and its Combination with Piperine Free *Piper nigrum* Extract on Cancer Cell Lines

Muhammad Faisal

A Thesis Submitted in Fulfillment of the Requirements for the Degree of Master of Science in Biomedical Sciences

Prince of Songkla University

2020

Thesis Title	Anti-cancer Effect of *Andrographis paniculata, Ziziphus spina-christi*, and *Vernonia extensa* and its Combination with Piperine Free *Piper nigrum* Extract on Cancer Cell Lines
Author	Mr. Muhammad Faisal
Major Program	Biomedical Sciences

Major Advisor

……
(Assoc. Prof. Dr. Potchanapond Graidist)

Examining Committee :

……Chairperson
(Assist. Prof. Dr. Narissara Lailerd)

……..Committee
(Assoc. Prof. Dr. Potchanapond Graidist)

……..Committee
(Assist. Prof. Dr. Yaowapa Sukpondma)

The Graduate School, Prince of Songkla University, has approved this thesis as fulfillment of the requirements for the Master of Sciences Degree in Biomedical Sciences

……
(Prof. Dr. Damrongsak Faroongsarng)
Dean of Graduate School

This is to certify that the work here submitted is the result of the candidate's own investigations. Due acknowledgement has been made of any assistance received.

……Signature
(Assoc. Prof. Dr. Potchanapond Graidist)
Major advisor

……Signature
(Mr. Muhammad Faisal)
Candidate

I hereby certify that this work has not been accepted in substance for any degree, and is not being currently submitted in candidature for any degree.

……Signature
(Mr. Muhammad Faisal)
Candidate

Thesis Title	Anti-cancer Effect of *Andrographis paniculata*, *Ziziphus spina-christi*, and *Vernonia extensa* and its Combination with Piperine Free *Piper nigrum* Extract on Cancer Cell Lines
Author	Mr. Muhammad Faisal
Major Program	Biomedical Sciences
Academic Year	2019

ABSTRACT

Andrographis paniculata, *Ziziphus spina-christi*, *Vernonia extensa*, and *Piper nigrum* have biological activities in anti-cancer activity. This study was carried out to investigate the anti-cancer activity of three plants individually and the interaction of combination among three plants leaves and PFPE as a novel anti-cancer regimen as well as to analyze the apoptosis and multi-caspase activities induced by the combination. The study results demonstrated that dichloromethane extract of *A. paniculata* leaves exhibited anti-proliferation on colorectal cancer cell lines (HT-29 and SW-620) with an IC_{50} values of 8.93 ± 0.52 µg/ml and 7.49 ± 0.04 µg/ml, respectively. The GC-MS analysis suggests that major volatile constituents group of this extract of *A. paniculata* leaves are alcohols group (1-heptatriacotanol), and steroids (androsta-1,4-dien-3-one, 6,17-dihydroxy-, (6β,17β) and γ-sitosterol). The dichloromethane extract of *Z. spina-christi* and *V. extensa* showed the highest cytotoxicity on MCF-7 and A2780 cells with an IC_{50} values of 13.35 ± 0.30 µg/ml and 14.64 ± 1.51 µg/ml, respectively. The major volatile compounds group of *Z. spina-christi* are including fatty acids (palmitic acid, linolenic acid, and linoleic acid), terpenes (neophytadiene), and fatty alcohols (n-tetracosanol-1). The dichloromethane extract of *V. extensa* exhibited the highest cytotoxicity in MCF-7 and A2780 cells with IC_{50} at 15.58 ± 1.81 µg/ml and 10.08 ± 0.04 µg/ml, respectively. The major volatile compounds of dichloromethane extract of *V. extensa* are fatty acids (palmitic acid, linolenic acid, and linoleic acid), and terpenes (neophytadiene and phytol). Thereafter, the combination study was carried out using dichloromethane extract of *A. paniculata*, *Z. spina-christi*, and *V. extensa* leaves, combined with PFPE each dichloromethane extract at various ratio (IC_{50}: IC_{50}; IC_{50}:$0.5IC_{50}$; $0.5IC_{50}$:IC_{50}, and $0.5IC_{50}$:IC_{50}) (where IC_{50} as a baseline). The

combination among the dichloromethane extract of *V. extensa* leaves and PFPE showed a synergistic interaction on MCF-7 cell lines with a CI value of 0.34 ± 0.06; 0.36 ± 0.14, and 0.44 ± 0.14, respectively. As a further investigation, the combination of dichloromethane extract of *V. extensa* and PFPE was tested in apoptosis and multi-caspase activities assessed by Annexin V-FITC and Multi-caspase assays. The results showed that combination of dichloromethane extract of *V. extensa* leaves with PFPE at ratio IC_{50}:IC_{50} induced caspases cascade and leading to apoptosis with time-dependent on MCF-7 cell lines. In conclusions, dichloromethane extract of *A. paniculata*, *Z. spina-christi*, and *V. extensa* represented a potential anti-cancer treatment in the individual extract. The combination of dichloromethane extract of *V. extensa* and PFPE could be a promising anti-cancer regimen in combating breast cancer cell lines.

ACKNOWLEDGEMENT

In the name of Allah, the most gracious, the most merciful. Herewith, I would like to express my gratitude to my family which is my purpose of life in this world and might be gathered in the afterlife.

I wish to show my respectfulness and gratitude to my advisor Associate Professor Dr. Potchanapond Graidist. For all those the valuable knowledge I procured and learned from her by conducting a research project with high efficiency and effectiveness. I never forget her patience, justify, and encourage teaching to prepare myself for every crucial and critical moment in the future.

Thereafter, I wish to express my thanks to the examination committee: Assistant Professor Dr. Narissara Lailerd of the Faculty of Medicine, Chiang Mai University, and Assistant Professor Dr. Yaowapa Sukpondma of the Faculty of Science, Prince of Songkla University.

I wish to give the biggest thanks to all staff and student in Department of Biomedical Sciences, Faculty of Medicine, and Prince of Songkla University, and also my advisor's research team, Miss Thidarath Rattanaburee (Ph.D. candidate) and Mr. Tanotnon Tanawwattanasuntorn (Ph.D. candidate), particularly Dr. Aman Tedasen (post-doctoral fellow), Miss Sirinapa Dokduang (research assistant), and Mrs. Saowanee Muangchanburee (scientist) for their selfless help, kindness, and understanding.

Muhammad Faisal

CONTENTS

CONTENTS (Continued)

CONTENTS (Continued)

CONTENTS (Continued)

CONTENTS (Continued)

LIST OF TABLES

LIST OF TABLES (Continued)

LIST OF FIGURES

LIST OF FIGURES (Continued)

LIST OF FIGURES (Continued)

LIST OF ABBREVIATIONS AND SYMBOLS

5-FU	=	5-Fluorouracil
AC	=	Adenocarcinoma
AJCC	=	American Joint Committee on Cancer
AMH	=	Anti-Mullerian Hormone
AP	=	*Andrographis paniculata*
APC	=	Adenomatous Polyposis Coli
ARID1A	=	AT-Rich Interaction Domain 1A gene
ARO	=	Action of Aromatase
ATCC	=	American Type Culture Collection
ATG	=	Autophagy-related Genes
ATM	=	Ataxia Telangiectasia Mutated gene
BAX	=	Bursa-Cell Lymphoma-2 Associated X Protein
BCL-2	=	Bursa-Cell Lymphoma 2
BEP	=	Bleomycin, Etoposide, Platinol
BRAF	=	B-Rapidly Accelerated Fibrosarcoma proto-oncogene
BRCA	=	Breast Cancer Gene
CASP8	=	Caspase-8
CCND1	=	Cyclin D1
CHK	=	Checkpoint Kinase protein
CI	=	Combination Index
cIAP	=	Cellular Inhibitor of Apoptosis Protein
CL	=	Corpus Luteum
CNS	=	Central Nerves System
c-SRC	=	Cellular-Sarcoma proto-oncogene
cyt c	=	Cytochrome *c*
DCC	=	Deleted in Colorectal Carcinoma
DCIS	=	Ductal Carcinoma *in situ*
DEAP	=	Dichloromethane Extract of *Andrographis paniculata* leaves
DEVE	=	Dichloromethane Extract of *Vernonia extensa* leaves
DEZSC	=	Dichloromethane Extract of *Ziziphus spina-christi* leaves

LIST OF ABBREVIATIONS AND SYMBOLS (Continued)

DISC	=	Death-Inducing Signaling Complex
DMEM	=	Dulbecco's Modified Eagle's Medium
DMSO	=	Dimethyl Sulfoxide
DNA	=	Deoxyribose Nucleic Acid
DR3, 4, 5, 6	=	Death Receptor 3, 4, 5, 6
DRI	=	Dose Reduction Index
EAAP	=	Ethyl Acetate extract of *A. paniculata*
EGF	=	Epidermal Growth Factor
EGFR	=	Epidermal Growth Factor Receptor
ER	=	Estrogen Receptor
ERBB2	=	Erythroblastic-B2 Receptor Tyrosine Kinase 2
ERK1/2	=	Extracellular Signal-Regulated Kinases 1 and 2
FDAP	=	Freeze dried extract of *Andrographis paniculata* leaves
FDVE	=	Freeze dried extract of *Vernonia extensa* leaves
FDZSC	=	Freeze dried extract of *Ziziphus spina-christi* leaves
FGFR2	=	Fibroblast Growth Factor Receptor 2
FigIα	=	Facto de linea Germinal alpha
FIGO	=	The International Federation of Gynecology and Obstetrics
FOLFIRI	=	Folinic Acid (leucovorin), Fluorouracil, Irinotecan
FOLFOX	=	Folinic Acid (leucovorin), Fluorouracil, Oxaliplatin
FSH	=	Follicle-Stimulating Hormone
GC	=	Germ Cells
GC-MS	=	Gas Chromatography-Mass Spectrometry
GnRHR	=	Gonadotrophin Releasing Hormone Receptor
GSK-3	=	Glycogen Synthase Kinase-3
HER2	=	Human Epidermal Growth Factor Receptor 2
HIV	=	Human Immunodeficiency Virus
HPCC	=	Hereditary Non-Polyposis Colon Cancer
HRAS	=	Harvey-Rat Sarcoma gene
i.e	=	id est (Latin), for example

LIST OF ABBREVIATIONS AND SYMBOLS (Continued)

IBC	=	Inflammatory Breast Cancer
IC_{50}	=	Median Inhibitory Concentration
IDC	=	Invasive Ductal Carcinoma
IFN-γ	=	Interferon-Gamma
IGF1R	=	Insulin Like Growth Factor 1 Receptor
IL-2	=	Interleukin-2
ILC	=	Invasive Lobular Carcinoma
KitL/kit	=	Kinase Tyrosine Ligand
KRAS	=	Kirsten Rat Sarcoma gene
LA	=	Luminal A
LB	=	Luminal B
LCIS	=	Lobular Carcinoma *in situ*
LH	=	Luteinizing Hormone
LSP1	=	Lymphocyte Specific Protein-1
MAP	=	Mutated Y Human-Associated Polyposis
MAP3K1	=	Mitogen-Activated Protein Kinase Kinase Kinase 1
MAPK	=	Mitogen-Activated Protein Kinase
MAPK-PP	=	Mitogen-Activated Protein Kinase Phosporylated
MEAP	=	Methanol Extract of *Andrographis paniculata*
MLH1	=	Mutated L Homolog 1
MSH2	=	Mutated S Homolog 2
Mt	=	Mutated
mTOR	=	Mammalian Target of Rapamycin
MTT	=	3-(4,5-Dimethylthiazol-2-yl)-2,5-Diphenyltetrazolium Bromide
$NaHCO_3$	=	Sodium Bicarbonate
NF1	=	Neurofibromatosis type I
NF-*k*B	=	Nuclear Factor Kappa B
NRAS	=	Neuroblastoma Rat Sarcoma
NTs	=	Neurothropins

LIST OF ABBREVIATIONS AND SYMBOLS (Continued)

OECD	=	Organisation for Economic Co-operation and Development
P16INK4a	=	Cyclin-Dependent Kinase Inhibitor 2A
PFPE	=	Piperine Free *Piper nigrum* Extract
PGCs	=	Primordial Germ Cells
PIK3CA	=	Phosphatidylinositol 3-kinase catalytic alpha polypeptide
PJS	=	Peutz-Jeghers Syndrome
PMFs	=	Primordial Follicles
PR	=	Progesterone Receptor
PTEN	=	Phosphatase and Tensin homolog
RIP1	=	Receptor Interacting Protein 1
RNA	=	Ribonucleic Acid
ROS	=	Reactive Oxygen Species
RPMI	=	Roswell Park Memorial Institute
SMAD2, -4	=	S-Mothers Against Decapentaplegic
STK11	=	Serine/Threonine Kinase 11
TDLUs	=	Terminal Duct Lobular Units
TGFBR2	=	Transforming Growth Factor-Beta Receptor 2
TGF-β	=	Transforming Growth Factor-Beta
TNBCs	=	Triple Negative Breast Cancers
TNM	=	Tumor, Node, Metastasis
TNRC9	=	Trinucleotide Repeat Containing 9
TP53	=	Tumor Protein 53
TRAIL	=	Tumor Necrosis Factor-Related Apoptosis-Inducing Ligand
VE	=	*Vernonia extensa*
VEGFR	=	Vascular Endothelial Growth Factor
v-SRC	=	Virus of Sarcoma
WHO	=	World Health Organization
WNT-1	=	Wingless Integrated -1
WT	=	Wild type
ZSC	=	*Ziziphus spina-christi*

LIST OF ABBREVIATIONS AND SYMBOLS (Continued)

α	=	Alpha
γ	=	Gamma
β	=	Beta

CHAPTER 1
INTRODUCTION

1.1 Background and Rationale

Over 18 million mortalities worldwide were caused by cancer. A report from the *GLOBOCAN 2018* breast and colorectal cancer were the top three cancer cases worldwide (Bray *et al.*, 2018). On the other hand, ovarian cancer exerted the highest death rate compared to breast, endometrial, and cervical cancer (The World Ovarian Cancer Coalition, 2018). Notably, in Indonesia, breast and ovarian cancer were the top three cancer incidences in women, and colorectal cancer gave the high incidences under lung cancer for men (WHO, 2019). Meanwhile, in Thailand, breast cancer was the top three cancer incidences (11.4% all cancer cases). Colorectal cancer was responsible for 8.1% cancer mortalities. Ovarian cancer in Indonesia and Thailand showed the highest death rate compared to breast and colorectal cancers (The Global Cancer Observatory, 2019).

Nowadays, clinicians treat cancer patients with several ways consists of surgery, radiotherapy, and chemotherapy (including immunotherapy, hormone therapy, and targeted therapy). Surgery effectively works for many types of cancer in the early stage (National Cancer Institute, 2015b). Radiotherapy is an adjuvant therapy using high dose radiation-based to devastate cancer cells and shrink tumors (National Cancer Institute, 2019b). Chemotherapy is a treatment for cancer patients using the drugs to kill the entire cells inside the body (systemically) which have specific mechanisms such as stimulates the immune systems (immunotherapy) and hormones (hormone therapy) as well as hit the growth cancer modulator proteins (targeted therapy) (National Cancer Institute, 2019c; American Cancer Society, 2019d; National Cancer Institute, 2020). Presently, doxorubicin, 5-fluorouracil, and cisplatin are determined as the first line of chemotherapeutic drugs for breast, colorectal, and ovarian cancer, respectively (Paridens *et al.*, 2000; Masi *et al.*, 2004; Rose, 2016).

Generally, using chemotherapy drugs is required to consider deeply due to some disadvantages such as recurrence of cancer, drug resistance which are leading to the ineffectiveness of the treatment (Wang *et al.*, 2019). Chemotherapeutic drugs could eradicate cancer cells, but frequently harming the healthy fast-growing cells

(bone marrow, hair follicles in the skins, cells in the oral, digestive tract, and reproductive cells). Furthermore, chemotherapeutic drugs might cause severe toxicity to the vital organ (heart, nerve, liver, and kidney) (Sak, 2012; Pérez-herrero and Fernández-medarde, 2015).

To date, there are numerous plant species reported by their biological activities. *Andrographis paniculata* (Family Acanthaceae: Green Chiretta), *Ziziphus spina-christi* (Family Rhamnaceae: Sidr), and *Vernonia extensa* (Family Asteraceae: Bitter leaf) are well-known medicinal plants (Ponglux *et al*., 1992; Okhuarobo *et al*., 2014; Aati *et al*., 2019). Recognized as a medicinal plant species, *A. paniculata* leaves possess some biological activities including anti-oxidant (Lin *et al.*, 2009), anti-inflammatory effects (Liu *et al.*, 2007), immunomodulatory effect (Sheeja, Shihab and Kuttan, 2006), hepatoprotective effect (Shi *et al.*, 2008), anti-microbial (Kunwar, Shrestha and Bussmann, 2010) and anti-viral (Calabrese *et al.*, 2000). Meanwhile, the aerial part of *Z. spina-christi* species was reported to possess antioxidant, anti-bacterial, anti-fungal, anti-diabetic, analgesic effect (Asgarpanah and Haghighat, 2012), anti-angiogenic (Abu-raghif, Jasim and Hanoon, 2017). *V. extensa* leaves have been used traditionally by the citizen of Northern Thailand as an immunity enhancer (Ponglux *et al.*, 1992). Nevertheless, some biological activities from *Vernonia* were investigated as an anti-malarial (Abosi and Raseroka, 2003), anti-microbial, anti-parasitic activities (Akinpelu, 1999; Krief, Hladik and Haxaire, 2005), anti-oxidant (Farombi and Owoeye, 2011).

Surprisingly, three plants were reported to possess a high cytotoxic effect against several cancerous cell lines. Methanolic extract of *A. paniculata* leaves inhibited half of the cell number (IC_{50}) with the concentration as 5.3 µg/ml, 10 µg/ml, and 3.1 µg/ml to HeLa (cervical cancer) cell lines, HT-29 (colon cancer) cell lines and P388 (leukemia cell line), respectively (Siripong *et al.*, 1992; Kumar *et al.*, 2004). Furthermore the ethanolic extract of *A. paniculata* leaves exerted IC_{50} value at 14.01 µg/ml to Hl-60 (leukemia cell line) (Cheung *et al.*, 2005). Moreover, the ethanolic extract of *Z. spina-christi* leaves gave IC_{50} value at 20 µg/ml to MCF-7 (Farmani *et al*., 2016). Subsequently, a recent study revealed that dichloromethane extract of *V. extensa* leaves at 30 µg/ml concentration possess cytotoxicity to, HuCCA-1 (cholangiocarcinoma cells), MOLT-3 (leukemic cells), HepG2 (liver carcinoma cells),

and A549 (lung cancer) with a percentage of inhibition at 91%, 100%, 95.6%, and 89%, (Thongnest *et al*., 2019). The exploration of natural sources as a cancer treatment has been interesting since the various chemical compounds possessed in natural sources. Therefore, the first part of this study was carried out to investigate the anti-cancer activity of promising medicinal plants.

Moreover, piperine-free *Piper nigrum* extract (PFPE) was used as the combination treatment of *A. paniculata*, *Z. spina-christi*, and *V. extensa.* Previously, a study conducted by Sriwiriyajan and colleagues, PFPE exhibited a denotable potency in several cell lines including MCF-7, MDA-MB-468, MDA-MB-231, ZR-75-1, and SK-N-SH, which are indicated by IC_{50} values 7.45 µg/ml, 18.19 µg/ml, 22.67 µg/ml, 13.85 µg/ml, and 21.51 µg/ml, respectively (Sriwiriyajan *et al*., 2016). According to Tedasen and colleagues investigation, PFPE showed cytotoxicity towards cholangiocarcinoma cell lines, KKU-100, KKU-M213, KKU-M055, and TFK-1, with IC_{50} at 17.79 µg/ml, 13.70 µg/ml, 16.74 µg/ml, and 15.30 µg/ml, respectively (Tedasen *et al*., 2020). Interestingly, PFPE did not show the cytotoxicity in non-cancerous fibroblast cell lines (L-929 cell lines) (Tedasen *et al*., 2020). Furthermore, an *in vivo* study by rat models suggested that the PFPE showed an anti-cancer effect without inducing toxicity to several vital organs (Sriwiriyajan *et al*., 2016). High cytotoxicity on cancer cell lines and reported active as an organ protector in rat models convinced this study by using this extract as a combination.

Presently, the combination treatment has become a common technique in clinical practice. Several contributions previously demonstrated that the combination treatment using *A. paniculata* and *Z. spina-christi* towards cancer cell lines. The combination of *A. paniculata* and *Silybum marianum* extract demonstrated a synergistic effect (Singh *et al.,* 2013). The primary constituent of *A. paniculata* named andrographolide could increase the cytotoxicity of paclitaxel, 5-fluorouracil, topotecan, doxorubicin, and cisplatin (Yang *et al.,* 2009; Sukumari-Ramesh *et al.,* 2011; Yuan *et al.,* 2016; Hodroj *et al.,* 2018). The combination of *Z. spina-christi* extract and termite shelter tubes showed a synergistic effect in cancer cell lines (Madlum *et al.,* 2015). The purposes of harnessing the combination are to attack the cancer cells in more than one pathway and decrease the doses of either two compounds or a single compound.

In purpose to analyze deeply the anti-cancer activity of the combination, the apoptosis and multi-caspase assay were performed. The anti-cancer drugs induce cellular damage which arrests the cell cycle with apoptosis as an outcome. Nevertheless, cancer cells may escape the apoptosis process while exposed by a single anti-cancer drug (Mohammad *et al*., 2016). The combination of anti-cancer promising extract might hit more than one apoptotic-associated proteins which bring the cancer cells to face the apoptosis pathway. Correlated with apoptosis, caspases are recognized as initiators and executors proteins of apoptosis. The activation of these proteases could lead to apoptosis on cancer cell lines (McIlwain *et al*., 2013). Then, the analysis of apoptosis and multi-caspases activities could be an effective way to evaluate whether the combination has the anti-cancer potency through apoptosis or not. Therefore, the final study was aimed to evaluate the anti-cancer activity of plant extracts and its combination with PFPE on the induction of apoptotic and multi-caspase activities.

1.2 Review of literature

1.2.1 Cancer development

Theoretically, cells can divide by themselves modulated by the genes. One of the genes, the *TP53* gene (the guardian of genomes), is a versatile controller of cellular mechanisms. When the DNA damage, ataxia telangiectasia mutated gene (*ATM*) promptly sends a signal to the *TP53* gene to encode the proteins for arresting the cell cycle. If the damage could not be repaired, the cells activate the apoptosis mechanism, and the cells have been underlying self-destruction. Meanwhile, the mutant *TP53* could not encode the protein to stop the cell division. As a result, the cells will be aggregated and become benign tumors. Afterward, the multi-mutation may occur into benign tumor cells and become the malignant tumor cells or cancer cells. Sooner or later, the malignant tumor cells concurrently collaborate with the angiogenic receptor to the cancer invasion. In consequence, the tumor cells massively migrate and invade to the other sites through the blood vessels or lymph nodes with terms metastasize (OECD, 2007). Furthermore, the cancer progression could be a basic understanding to determine suitable cancer treatment, as shown in Figure 1.

The alterations have not come merely from the genetic factors but also the environment, which is predisposing the genes structures of somatic cells.

Carcinogen, an exogenous factor related to DNA damaging and leads to cancer progression. Carcinogens are known as the most ubiquitous and hazardous risk factors, consists of chemicals (arsenic, benzene, isopropyl alcohol, and benzidine) and radiations (radon, x-rays, and γ-rays) (American Cancer Society, 2019a).

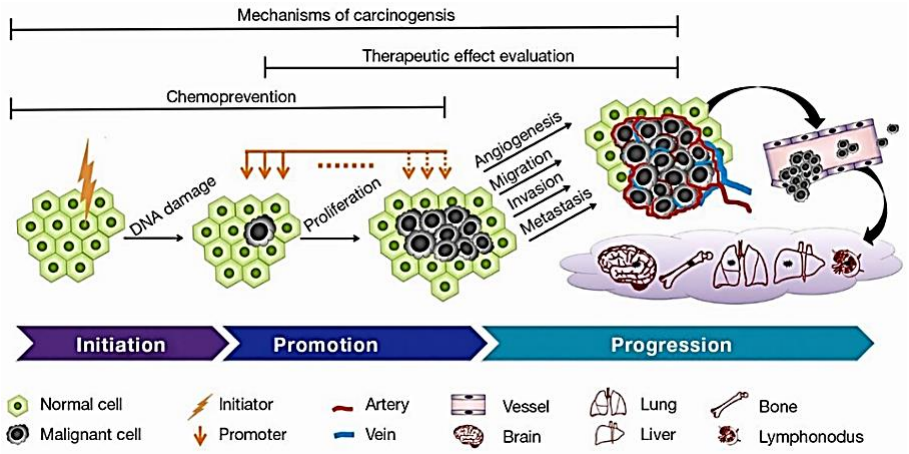

Figure 1. Scheme of cancer progression (Liu *et al.*, 2015)

1.2.2 Cancer treatment

Nowadays, clinicians treat cancer patients with several ways consists of surgery, radiotherapy, immunotherapy, hormone therapy, targeted therapy, and chemotherapy. Surgery is commonly used for many types of cancer which effectively works in the early stage of cancers (National Cancer Institute, 2015b). Radiotherapy is an adjuvant therapy which is using high dose radiation-based to eradicate cancer cells and shrink tumors while the low dose only for imaging inside the body system. Practically, radiotherapy is used as an adjuvant for the surgery, chemotherapy, and immunotherapy effectivity (National Cancer Institute, 2019b). Immunotherapy is a way to remedy cancer which stimulates the immune system such as white blood cells and lymph systems to eliminate the cancer cells. This therapy can be used in both the early and advanced stages of cancers (National Cancer Institute, 2019c). Hormone therapy or endocrine therapy is a cancer treatment, only used to inhibit hormone-related cancer. This therapy is harnessed the hormone to regulate the hormonal that associated with cancer growth such as progesterone and estradiol. Targeted therapy is a cancer therapy targeting the growth of cancer modulators. This therapy is capable to control the immune system devastate cancer cells, to stop cancer cells from proliferating, and to

stop cancer cells from forming the blood vessels (angiogenesis) (National Cancer Institute, 2020). Chemotherapy is a treatment for cancer patients which using the drugs to eradicate the entire cells inside the body (systemically) (American Cancer Society, 2019d).

To date, many different types of chemotherapeutic drugs have been explored and harnessed to treat cancer including topoisomerase inhibitors, antimetabolites, mitotic inhibitors, alkylating agents, anti-tumor antibiotics, and corticosteroids. First, topoisomerase inhibitors could disrupt specifically to topoisomerase enzymes, which effectively treat ovarian, leukemia, colorectal, gastrointestinal, and pancreatic cancers. Topoisomerase I inhibitors are including irinotecan and topotecan and topoisomerase II inhibitors are etoposides, mitoxantrone, and teniposide. There are two types of topoisomerase including topoisomerase I and II, then the inhibitors separated into the two types as well. Second, antimetabolites drugs, a chemotherapy drug that could disrupt DNA duplication, consequently cells are not able to divide. These drugs are often to treat leukemia, breast, ovarian, and intestinal cancers. Antimetabolites drugs examples are including 5-fluorouracil, capecitabine, azacytidine, gemcitabine, floxuridine, decitabine, and trifluridine. Third, mitotic inhibitors drug type is a type commonly obtained from natural products and usually used treat breasts, leukemias, lymphomas, and myelomas. The mechanisms are to stop all cells in multiplying to form new cells. Examples of these chemo drugs are docetaxel, paclitaxel, cabazitaxel, vincristine, vinblastine, and vinorelbine. Alkylating drugs are employing in all phases of the cancer cell cycle. Fourth, alkylating drugs are used to treat various types of cancers including lung, breast, ovary, leukemia, lymphoma, Hodgkin disease, myeloma, and sarcoma. Alkylating chemotherapy drugs examples are including carboplatin, cisplatin, oxaliplatin, dacarbazine, altretamine, cyclophosphamide. Fifth, anti-tumor antibiotics are working in altering the DNA inside cancer cells to block them from growing and dividing. This type of chemotherapy drug consists of doxorubicin, bleomycin, epirubicin, daunorubicin, valrubicin, and idarubicin. The last is corticosteroids or steroids are normally functions as natural hormones or hormone-like drugs. Prednisone, methylprednisolone, and dexamethasone are examples of corticosteroids for treating cancer cells (American Cancer Society, 2019c).

1.2.3 Breast cancer

1.2.3.1 Breast cancer prevalence

Breast cancer was the second leading cancer type worldwide refers to the number of new cases in 2018. According to death cases, breast cancer was the fifth deadly cancer type and new cancer cases, approximately 2,088,849 cases (11.6% of cancer cases), and 626,679 death cases (6.6% of cancer death cases). Furthermore, the Asian region was the first leading number of breast cancer, both incidences, and mortalities, 911,014, and 310,577, respectively (WHO, 2018). Particularly in Indonesia, breast cancer was the first rank in cancer incidences (58,256 of 348, 809 cases) and the second rank of mortalities (22,692 of 207,210 mortalities) (WHO, 2019).

1.2.3.2 Normal breast anatomy

The mature breast consists of approximately 15-20 branches, each branch to the inside of lobules with approximately 100 ductal lobular units (TDLUs) in which producing milk. The milk is carried from lobules to the nipple by the ducts (Figure 2a). There are two main epithelium cell types in human breasts, luminal epithelial cells, and myoepithelial cells (Figure 2b) (Deugnier *et al.*, 2002). Due to breasts are located near axillary nodes, supraclavicular nodes, infraclavicular nodes, and lymph nodes vessels, the breasts are associated with the lymphatic circulation, as shown in Figure 3 (Kalimuthu *et al.*, 2015).

1.2.3.3 Breast cancer progression

Breast cancer develops due to several risk factors, including menstruation, genetics and inheritance, hormone, and hormonal (American Cancer Society, 2017a). Both women in early menstruation and late menopause after 54 years old are the most susceptible to breast cancers (Mcpherson, Steel, and Dixon, 2000). Moreover, late pregnancy (after 35 years old) could be a risk factor for breast cancer. Excess of estrogen also possibly enhances the risk of breast cancer occurs (Martin and Weber, 2000). In contrast, a suitable proportion of physical activity could reduce 20-30% risk of breast cancer (Lee, 2003).

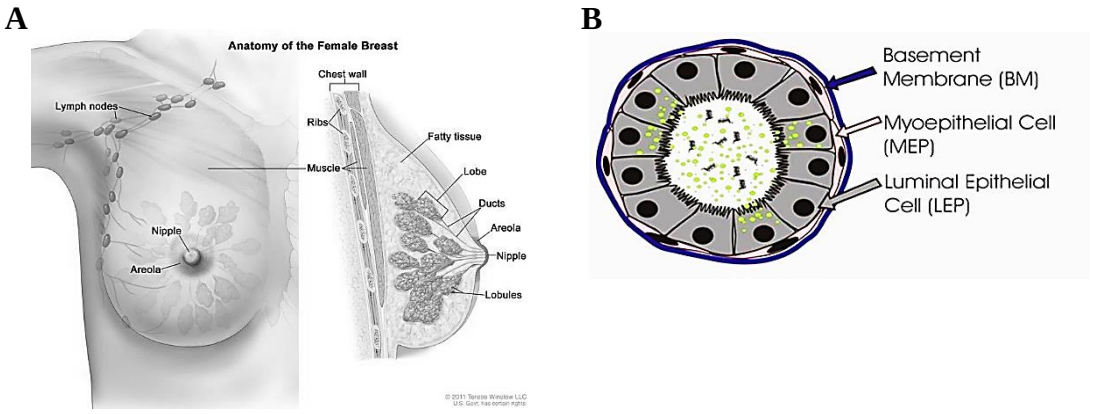

Figure 2. Scheme of breast tissue, **a)** scheme of healthy breast tissues (National Cancer Institute, 2011), **b)** scheme of an intersection of the normal breast (Adriance *et al.*, 2005)

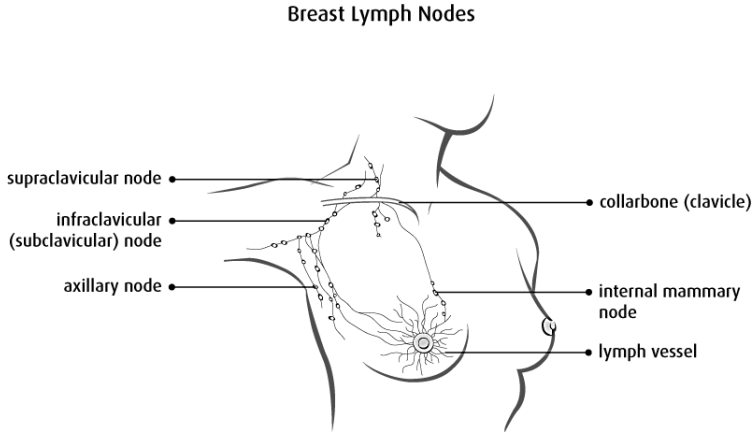

Figure 3. Scheme of interconnection among breasts and lymph nodes (Canadian Cancer Society, 2019)

In essence, the life of healthy breast cells is controlled by oncogenes (mutated-vulnerable genes) and tumor suppressor genes, which are the most important genes to control cell fate, apoptosis, promote proliferation, and tumor mass (Croce, 2008; Dang, 2012). Several vulnerable tumor suppressors could increase the mutation rate to cell germline, consisting of *BRCA1*, *BRCA2*, and *TP53*. Several other studies have identified several mutated genes that associated with breast cancers, including fibroblast growth factor receptor (*FGFR2*), thymocyte selection-associated high mobility group box 9 (*TNRC9*), mitogen-activated kinase kinase kinase 1 (*MAP3K1*), lymphocyte-specific protein (*LSP1*), *caspase-8* (*CASP8*), *PI3KCA*, *PTEN*, *TP53*, and *NF-kB* (Cox *et al.*, 2005; Easton *et al.*, 2007; Stacey *et al.*, 2007; Hunter *et al.*, 2012).

1.2.3.4 Clinical breast cancer types

There are several clinical types of breast cancer consists of ductal carcinoma in situ (DCIS), lobular carcinoma in situ (LCIS) (Figure 4), as well as invasive ductal carcinoma (IDC), invasive lobular carcinoma (ILC), and inflammatory breast cancer (IBC). Non-invasive breast cancer is also known in medical stage 0. In women with DCIS, the abnormal cells are solely growing in the milk-producing duct. The second type, invasive breast cancer, IDC (invasive ductal carcinoma) and ILC (invasive lobular carcinoma). IDC is the most frequent invasive breast cancer types in which 80% of cancer cases. IDC begins to proliferate in the milk ducts canal, penetrate through the wall, and grows into surrounding breast tissue. This type of cancer can spread (metastasize) into several parts of the body via the lymphatic system and blood vessels. Invasive lobular carcinoma (ILC) begin to proliferate in the milk-reservoir glands (lobules). This type is only 10% in which invasive breast cancer cases and more robust to detect using mammograms than IDC (American cancer society, 2017b).

1.2.3.5 Molecular subtypes of breast cancer

Based on the hormone status, a study reported that breast cancer could be discriminated for 5 main intrinsic subtypes including Luminal A (ER+ and PR+), Luminal B (ER+ and PR+/-), HER2-like (HER2 +), Basal Like and Claudin-low (ER, PR, and HER negative) (Table 1).

Table 1. The molecular subtypes of breast cancer and its characters

Molecule subtype	Hormone receptor	p53 mutant	Ki-67 level	Reference(s)
Luminal A	ER+, PR+, HER2-	13%	low	Loi *et al.*, 2007; Sørlie *et al.*, 2001; Holliday and Speirs, 2011
Luminal B	ER+, PR+/-, HER2-	40%	high	
HER2-like	ER-, PR-, HER2+	71%	high	
Basal-like	ER-, PR-, HER2-	82%	high	
Claudin-low	ER-, PR-, HER2-	-	low	

ER: Estrogen receptor; HER2: human epidermal growth factor receptor 2; PR: progesterone receptor

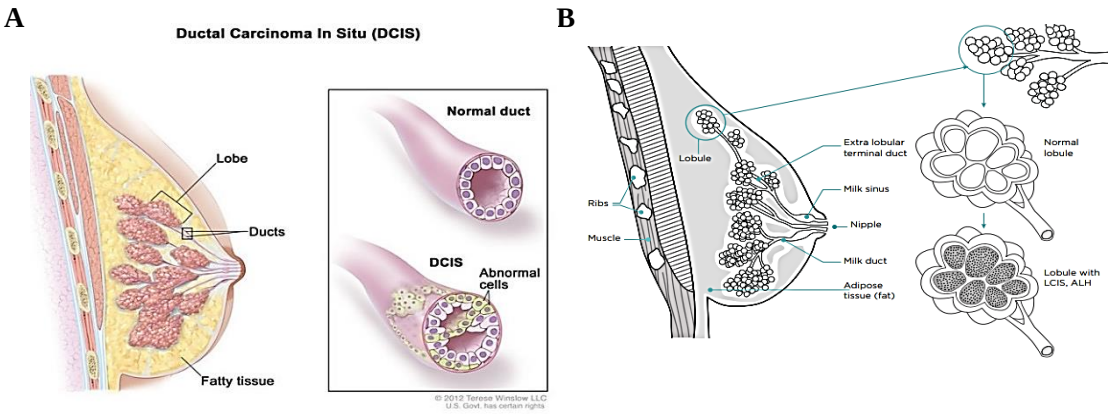

Figure 4. Scheme of non-invasive breast cancer types, **a)** ductal carcinoma in situ (DCIS) (National Cancer Institute, 2015a), **b)** lobular carcinoma in situ (LCIS) (Breast Screen Victoria, 2018)

About 70% of breast cancers are HER2 positive and show a better prognosis than HER2 negative breast cancers. Moreover, luminal subtype (Luminal-A and -B) also show its abundance, 90-95% of tumors are luminal A and B subtypes (Prat *et al.*, 2015). As a comparison, luminal B has higher expression of Ki-67 protein than luminal A as well as worse prognosis than luminal A (Sørlie *et al.*, 2001; Prat *et al.*, 2015). Basal-like and Claudin-low tumors have the worst prognosis, while luminal A has a better prognosis. Basal-like and Claudin-low tumors are also known as Triple Negative Breast Cancers (TNBCs), about 86% of this subtype of breast cancer showed a negative result in three receptors (ER, PR, and HER2). TNBCs subtype makes up 10 to 20% of all breast cancers (Prat *et al.*, 2013). TNBCs are classified as Basal-like, Claudin-low, and MBC. Tumors with HER2 overexpression are found in 15% to 25% of invasive breast cancers, and they show a worse prognosis than luminal subtype but have a sensitivity to therapy for HER2-targeted (Figure 5). (Dai *et al.*, 2017a).

1.2.3.6 Breast cancer treatment

Presently, breast cancer treatment has been explored and applied commercially (surgery, chemotherapy, radiotherapy, hormone therapy, and targeted therapy). Every treatment has a strategy based on tumor status and grade. Subsequently, an adjuvant treatment like surgery is beneficial when employed, along with chemotherapy and radiotherapy. A combination of chemotherapy, hormone, and targeted therapies is usually used commercially (American Cancer Society, 2017c).

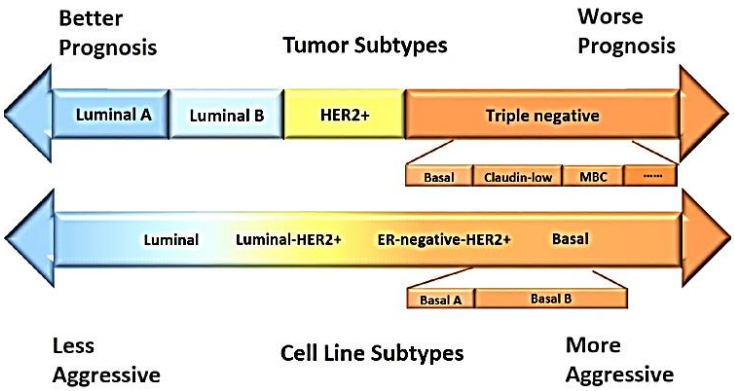

Figure 5. Prognosis comparison of different cell line subtypes (Dai *et al.*, 2017a)

Several pathways of targeted chemotherapeutic drugs into cells to inhibit topoisomerase I and II or RNA polymerase II, and interrupt cell cycles, such as doxorubicin, taxane, and docetaxel. Concisely, topoisomerase I and II are responsible for cleavage single or double DNA strands. As a result, apoptosis also would be proceeded after the inhibition of DNA condensation and mitosis failure (Earnshaw and Heck, 1985). Moreover, RNA polymerase I plays a crucial role in the gene transcription process and involved in cell proliferation (Cramer *et al.*, 2000).

Based on the molecular subtype, luminal A and B tumors are ER, PR positive, and HER2 negative. ER is positive in breast cancer metastasis due to the progression of angiogenesis caused by the collaboration of ER and Vascular Endothelial Growth Factor Receptor (*VEGFR*) as shown in Figure 6. Interestingly, this hormone therapy might improve the life span of patients (Leary and Dowsett, 2006).

Vice versa, progesterone Receptor (PR) positive is associated with WNT-1 and cyclin D1 (CCND1) to mediate cell adhesion together with cell proliferation and cell survival. By the activation of WNT-1, matrix metalloproteinase could generate and produce a free Epidermal Growth Factor (EGF), as shown in Figure 7. ER/PR positive breast cancer could be remedied by several chemotherapeutic drugs by blocking estrogen receptors from stimulating breast cancer cells to grow, such as tamoxifen, fulvestrant, and aromatase inhibitor (American Cancer Society, 2017c).

HER2 positive breast cancer type was frequently occurred, about 1 in 5 women with breast cancer and mostly linked with more aggressive clinical cancer staging (Korkaya and Wicha, 2013). Furthermore, the cancers could grow up and spread aggressively more than HER2 negative (Figure 8) (American Cancer Society, 2018a).

Several commonly used chemotherapeutic drugs such as trastuzumab, pertuzumab, and lapatinib are targeting EGFR and IGFR.

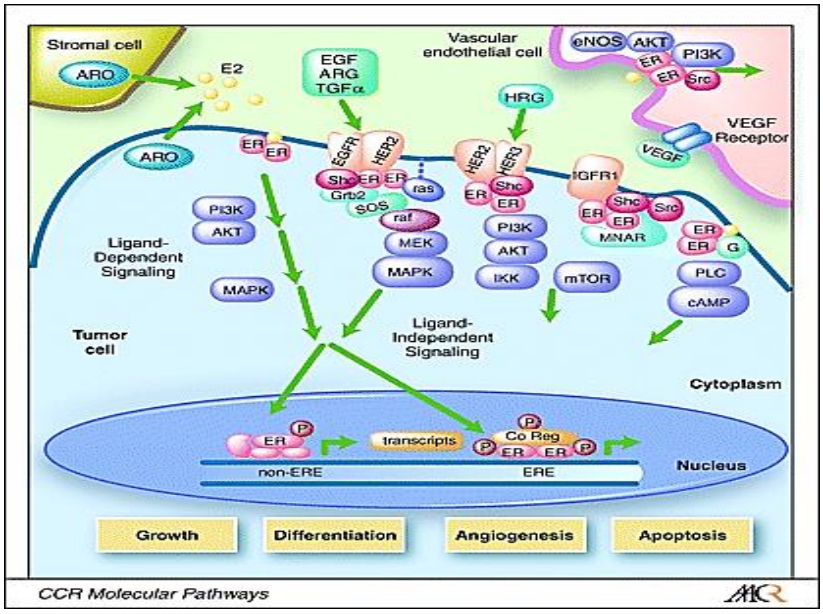

Figure 6. Scheme of interaction of estrogen and growth factor receptor signalling in human tumors, ARO: action of aromatase; EGF: epidermal growth factor; HER: human epidermal growth receptor; mTOR: the mammalian target of rapamycin; E2: estradiol; PI3K-AKT: phosphatidylinositol-3-kinase and protein kinase B; ERE: estrogen receptor element (Pietras and Márquez-Garbán, 2007)

Scientifically, the mechanisms and details of the drugs are classified by cancer cell cycle and inhibition of proliferation to control cancer development. The drugs were summarized in Table 2. In the circumstances, administrating chemotherapeutic drugs might cause some adverse effects since they have a lack of specificity. The drugs can kill tumors as well as healthy cells and lead to the benign or severe side effects comprising of blood clots, uterine, stroke, bone marrow suppression, liver, heart damage, and kidney toxicity (American Cancer Society, 2017e). Indeed, exploring chemotherapeutic drugs associated with the signaling molecules requires to be undertaken for improving breast cancer treatment. The different mutated genes and molecular pathways were described in Figure 9.

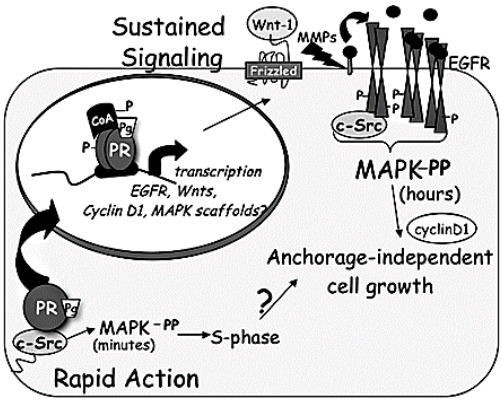

Figure 7. Scheme of Progesterone/PR-mediated MAPK signaling, PR: Progesterone Receptor; EGFR: Epidermal Growth Factor Receptor; c-SRC: steroid receptor coactivator; WNT: Wingless/Integrated; MAPK-PP: Mitogen-Activated Protein Kinase Phosphorylated (Faivre and Lange, 2007)

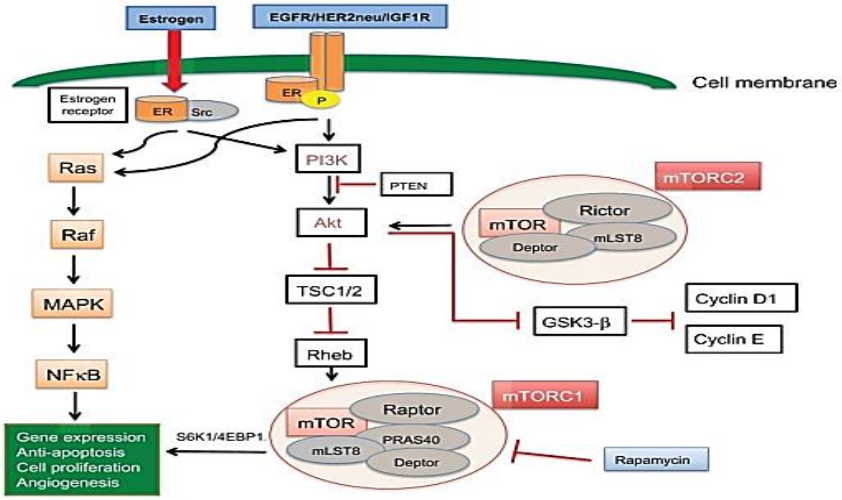

Figure 8. Scheme of EGFR/HER2/IGF1R membrane tyrosine kinase receptors lead to anti-apoptosis, cell proliferation, and angiogenesis, EGFR: epidermal growth factor receptor; mTOR: mammalian target of rapamycin; HER2: human epidermal growth factor receptor-2; PI3K: phosphatidylinositol 3-kinase, MAPK: mitogen-activated protein kinase (Paplomata and O'regan, 2014)

1.2.3.7 Breast cancer cell lines

The first human breast cancer cell lines, BT-20, was successfully established in 1958 by Lasfargues and Ozzello. The cancer cell lines, mainly breast cancer cell lines, have been used as a worthwhile tool for medical researchers to explore breast cancer drug development through its signaling pathway. However, the genetics

of each cell is uniquely different. Therefore, the researchers have to concern carefully the properties of each cell line that were chosen in the designed research (Lasfargues and Ozzello, 1958).

Based on the subtype, the most frequently used breast cancer cell lines type luminal A are MCF-7, T-47D, and ZR-75-1. UACC-812, ZR-75-27, and ZR-75-30 cell lines are included in the Luminal B type. Triple-negatives (TN) consists of MDA-MB-231, MDA-MB-468, and Hs578T (Dai *et al.*, 2017a). Generally, the commonly used cell lines are MCF-7, MDA-MB-231, MDA-MB-468, T-47D, and ZR-75-1. Several properties of human breast cancer cell lines in this study were summarized in Tables 3 and 4.

Table 2. Several drugs for breast cancer treatment and its molecular mechanisms

Treatment	Drugs	Cancer type	Mechanism of drugs	Reference(s)
Chemotherapy	Doxorubicin (Adriamycin®)	All types	Inhibit Topoisomerase-II and RNA polymerase II	Logan *et al.*, 1989
	Taxanes	All types	Bind beta-subunit of tubulin and causes mitosis failure	Crown and O'Leary, 2000
	Docetaxel	All types	Accumulate tubulin and mitosis failure	Cortes and Pazdur, 1995
Hormone therapy	Tamoxifen	All types, particularly for ER+ (Luminal subtype)	Block Estrogen Receptors	American Cancer Society, 2017d
	Fulvestrant	Luminal subtype		
	Aromatase Inhibitor	Luminal, HER2-like	Stop estrogen production	
Targeted therapy	Trastuzumab (herceptin)	HER2-like	Monoclonal antibody binding extracellular HER2 domain	American Cancer Society, 2018a
	Pertuzumab (perjeta)	HER2-like		
	Lapatinib (tykerb)	Luminal B, HER2-like	HER2 targeted drug	

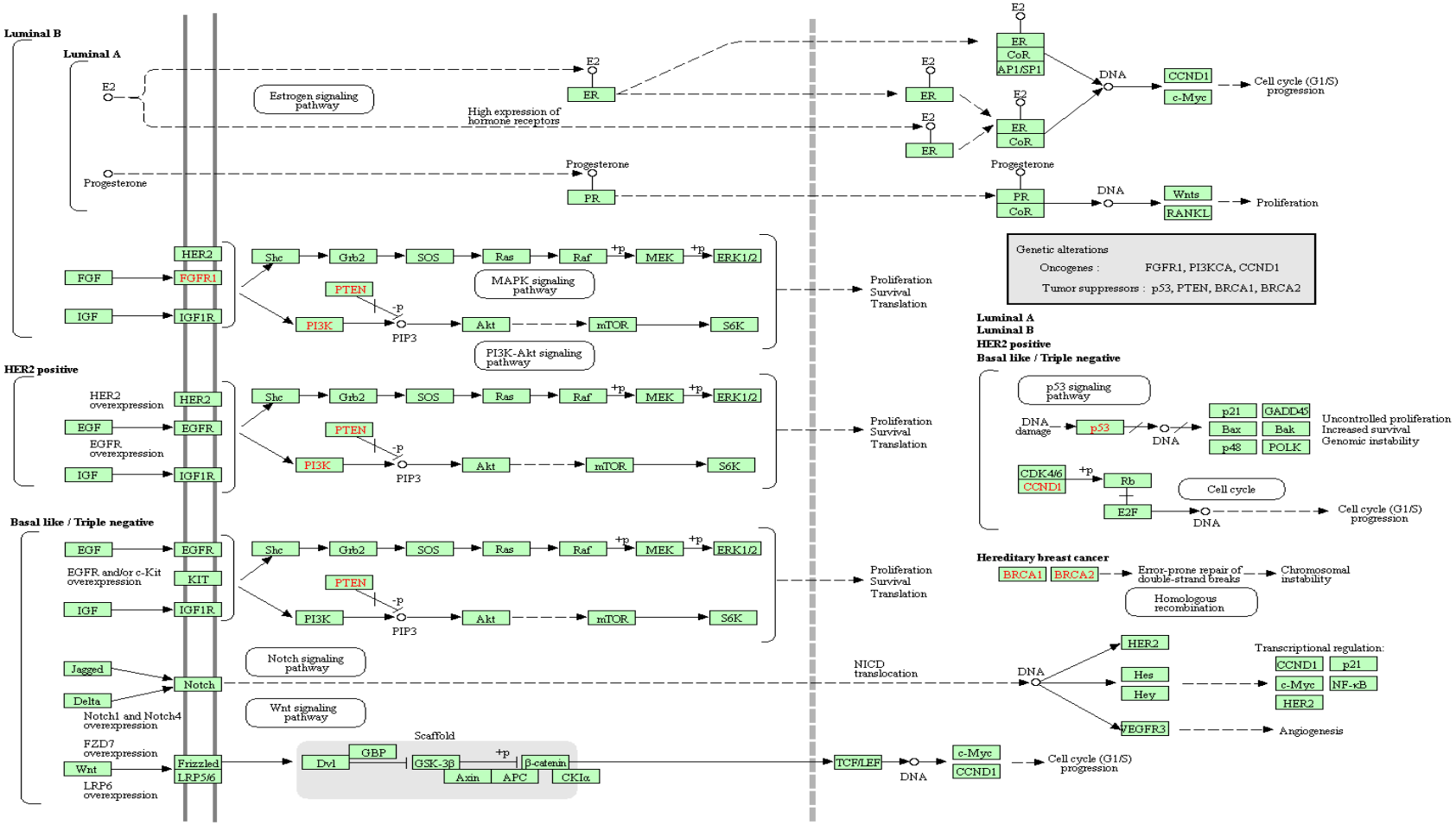

Figure 9. Mechanisms of proteins signalling pathway based on its molecular subtypes of breast cancer cell lines (Kanehisa Laboratories, 2018a)

Table 3. Several properties of used breast cancer cell lines

Cell line	Cancer		Hormone Receptor				Chemotherapy Response	Reference(s)
	Type	Subtype	ER	PR	HER2	Ki-67		
MCF-7	IDC	LA	+	+/-	-	90%	Response	Subik *et al.*, 2010
MDA-MB-231	AC	TNBC	-	-	-	100%	Response	

IDC: invasive ductal carcinoma type; AC: adenocarcinoma type, cancer originated from glands such as duct and lobule; LA: luminal A subtype; TNBC: triple-negative breast cancer; ER: estrogen receptor; PR: progesterone receptor; HER2: human epidermal growth factor receptor 2

Table 4. Several under mutation genes of used breast cancer cell lines

Cell line	Histology	Mutated Gene				Reference(s)
		KRAS	*CDKN2A*	*BRAF*	*TP53*	
MCF-7	Adenocarcinoma	WT	Mt	WT	WT	American Type Culture Collection, 2014
MDA-MB-231	Adenocarcinoma	Mt	Mt	Mt	Mt	

WT: wild type (no mutation); Mt: mutated; *KRAS*: K-Ras; *CDKN2A*: cyclin-dependent kinase inhibitor 2A; *BRAF*: B-Raf; *TP53*: The protein 53 (p53); EGFR: epidermal growth factor receptor

1.2.4 Colorectal cancer

1.2.4.1 Colorectal cancer prevalence

In 2018, colorectal cancer was the third rank of cancer incidences worldwide, about 1.8 million cases (10.2% of the total incidences), and responsible for 881,000 deaths. By the gender, colorectal cancer was responsible as the third rank mortalities in men, approximately 10.9%. Moreover, in Indonesia, colorectal cancer was responsible for 29,357 cancer incidences and 16,034 deaths (Bray *et al.*, 2018; WHO, 2019).

1.2.4.2 Normal colorectal anatomy

Colorectal constructed as two parts of the human large intestines is separated by the colon and rectum. Colon size is about a 60 to 72 inches long tube, which connects the small intestine to the rectum (Underhill, 1955). There are disparate parts of the colon, including ascending colon, which plays a role in reabsorption the fluid; transverse colon, which canalize the ascending colon with the descending colon (right to left body); the descending colon, which transfers the food to the sigmoid colon

(Jayasekeran, Holt and Bourke, 2013). The sigmoid colon is “S” shaped like and connects among colon and rectum (Syamala and Prasad, 2016). The rectum is a final part of human digestion (Jayasekeran, Holt, and Bourke, 2013). Anatomy of the colorectal was described in Figure 10.

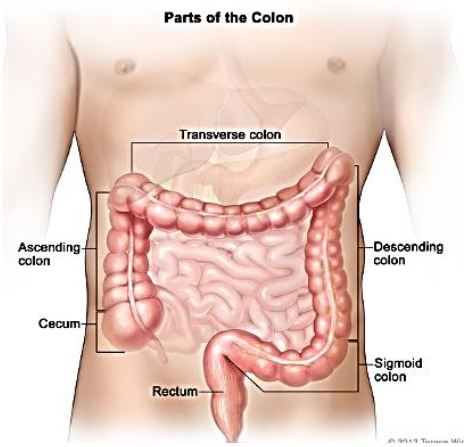

Figure 10. Scheme of parts of the colorectal (Cancer Quest, 2018)

1.2.4.3 Colorectal cancer progression

Basically, colorectal cancers mostly initiated grow from the inner lining of the colon or rectum, literally known as a polyp (precancerous cells). There are some stages before the polyp becomes malignant cancers (Figure 11) (American Cancer Society, 2018b). This type of cancer caused almost a million death cases worldwide (Bray *et al.*, 2018). American Cancer Society reported that several risk factors require to be concerned, such as physical activity, healthy diet, smoking, and alcohol consumption. However, some uncontrolled risk factors such as the personal history of inflammatory bowel disease, and family or personal profile of colorectal cancer or adenomatous polyps need to be more noticed. Approximately 2-4% of Lynch syndrome (non-polyposis colon cancers) is the most frequent case that occurred in colorectal cancer. This syndrome is mostly caused by MutL homolog 1 (*MLH1*) or MutS Homolog 2 (*MSH2*) gene mutation, which has a role as on amelioration damaged DNA. Furthermore, another type of syndrome known as Familial Adenomatous Polyposis (FAP), which accounted for 1% of all colorectal cancers (American Cancer Society, 2018b). The mutation causes other rare inherited syndromes such as Peutz-Jeghers syndrome (PJS) and MYH-associated polyposis (MAP) in Serine/Threonine Kinase 11

(*STK11*) and MYH-associated polyposis (MAP) genes, respectively (National Center for Advancing Translational Sciences, 2015).

Other findings also reported the mutation of different genes related to the development of colorectal cancer. Firstly, tumor suppressor genes such as *APC, DCC, TP53, SMAD2, SMAD4,* and *p16INK4a,* are included in the FAP tumors type as 80% of sporadic tumors. The genes play a role as both controllers of proliferation and apoptosis (Llor *et al.*, 2005). Secondly, proto-oncogenes such as *KRAS* and *NRAS* may predispose 35-42% of colorectal cancer and mostly in advanced adenomas (Leslie *et al.*, 2002; Cheng and Lai, 2003; Llor *et al.*, 2005).

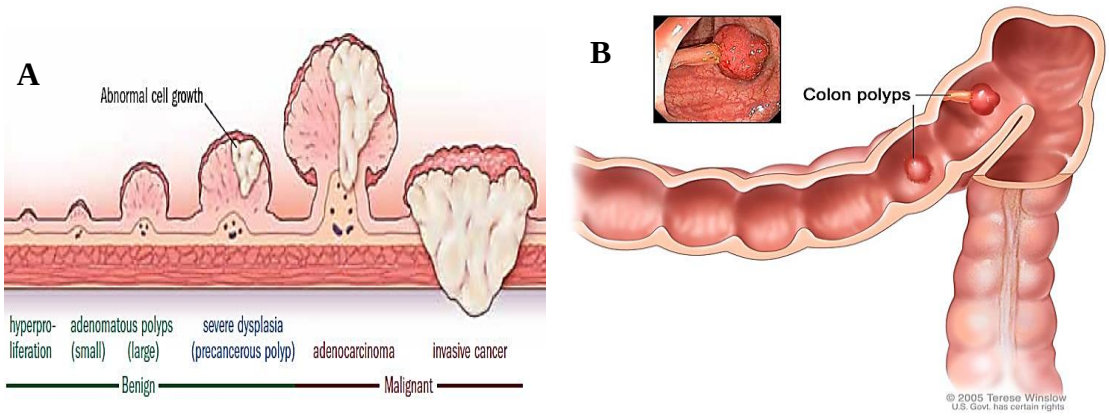

Figure 11. Scheme of the polyp development, **a)** polyp develops from precancerous to be adenocarcinoma (Harvard Medical School, 2013), **b)** polyps grow in the transverse colon (National Cancer Institute, 2018)

1.2.4.4 Clinical colorectal cancer type

There are several stages of colorectal cancer, including stage 0, -I, -IIA, -IIB, -IIC, -IIIA, -IIIB, -IIIC, and IV. When stage 0 (*in site* carcinoma) has occurred, malignant cells are found in the inner layer of healthy tissue and growing to sub-mucosa and occasionally spread to the muscle layer (stage I). In stage II, there are three types of colorectal progression, 1) stage IIA, wherein cancer has spread thoroughly to the muscle layer of the colon wall to the serosa, 2) stage IIB, cancer has migrated to the serosa yet not spread to the other organs surround colorectal, 3) More than another stage II, IIC, cancer has spread through outside the serous to proximal organs. In stage III, cancers have invaded the lymph nodes. In the final stage (stage IV), in this stage, cancer has spred to all body through lymph nodes and blood vessels, as known as metastasis

(American Cancer Society, 2018b). Colorectal cancer staging described in Figure 12 and Table 5.

1.2.4.5 Colorectal cancer treatment

Presently, several treatments that already invented and applied by medical researchers and paramedics, including surgery therapy, radiation therapy, chemotherapy, targeted therapy, and immunotherapy. Occasionally, the therapies could be combined in the case of some stages based on its malignancy. In stages 0 and 1, the cancers are still in the inner lining, required surgical therapy. Occasionally, the cancers may recurrence, thus need to do a colectomy (intersect the infected part of colorectal). While the cancers have invaded the muscular and outer layer, they need to merge the surgery with adjuvant chemotherapy such as adrucil (5-FU) and oxaliplatin. Stages 3 and 4 are the advanced stage of this disease. Hence, the chemotherapeutic drugs are favorably combined along with targeted drugs, such as FOLFOX (leucovorin, 5-FU, and oxaliplatin) and FOLFIRI (leucovorin, 5-FU, and irinotecan) regimens. Theoretically, the FOLFOX regimen inflicts DNA damage and cell cycle arrest to the cancer cells. Meanwhile, FOLFIRI is a regimen to kill the cancers through two pathways, DNA damaging and inhibiting DNA topoisomerase I (Ishihara *et al.*, 2010). Interestingly, the two regimens contain leucovorin as a protector of healthy cells from cytotoxicity of methotrexate as well as increase the effect of 5-FU (BC Cancer Agency Cancer Drug Manual, 2006).

Due to the metastasized cancer mostly migrate and invade into the other organs, the metastasized cancer requires blood vessels to transport the nutrient for its colony, called by angiogenesis (Ellis, 2006). For anticipating angiogenesis, hormone therapy is an appropriate decision to kill metastasized cancers. A summary regarding colorectal treatment based on the cancer stage was showed in Table 6. Moreover, an explanation described the correlation among the cancer progression, altered genes, and its pathways (Figure 13).

Table 5. Comparison of Dukes, Astler Coller and TNM colorectal staging (Akkoca *et al.*, 2014)

Progression	Dukes	Astler-Coller	TNM
Tumor invasion to the mucosa	A	A	Tis, N0
Tumor invasion only into the submucosa, not going to lymph node	A	B1	T1, N0
Tumor invasion only to the submucosa and lymph node	C	C1	T1, N1-2
Tumor begins to invade to the muscle layer but not going to lymph node	A	B2	T2, N0
Tumor begins to invade to the muscle layer and going lymph node	C	C1	T2, N1-2
Whole of the muscle layer but no to lymph node	B	B2	T3, N0
Whole of the muscle layer and lymph node	C	C2	T3, N1-2
Tumors have invaded to the surround organs but no to lymph node	B	B2	T4, N0
Tumors have invaded to the surround organs and lymph node	C	C2	T4, N1-2
Distant metastasize	D	D	T1-4, N0-2, M1

A: Tumor limited to mucosa; B1: Tumor limited to the submucosa, no lymph node invasion; B2: Tumors confined to the muscle layer, no lymph node invasion; C1: The tumor did not exceed the bowel wall, lymph node metastasis; C2: Tumor exceeded the intestinal wall, and lymph node metastasis; D: distant metastases; Tis: Carcinoma in situ; T1: Tumor invades submucosa; T2: Tumor invades muscularis propria; T3: Tumor invasion to subserosa or to pericolic/perirectal tissue; T4:Tumor invasion to neighboring organs or structures and/or visceral peritoneum is perforated; N0: no lymph node metastases; N1: 1-3 lymph node involvement; N2: 4 or more lymph node involvement; M1: Distant metastasis

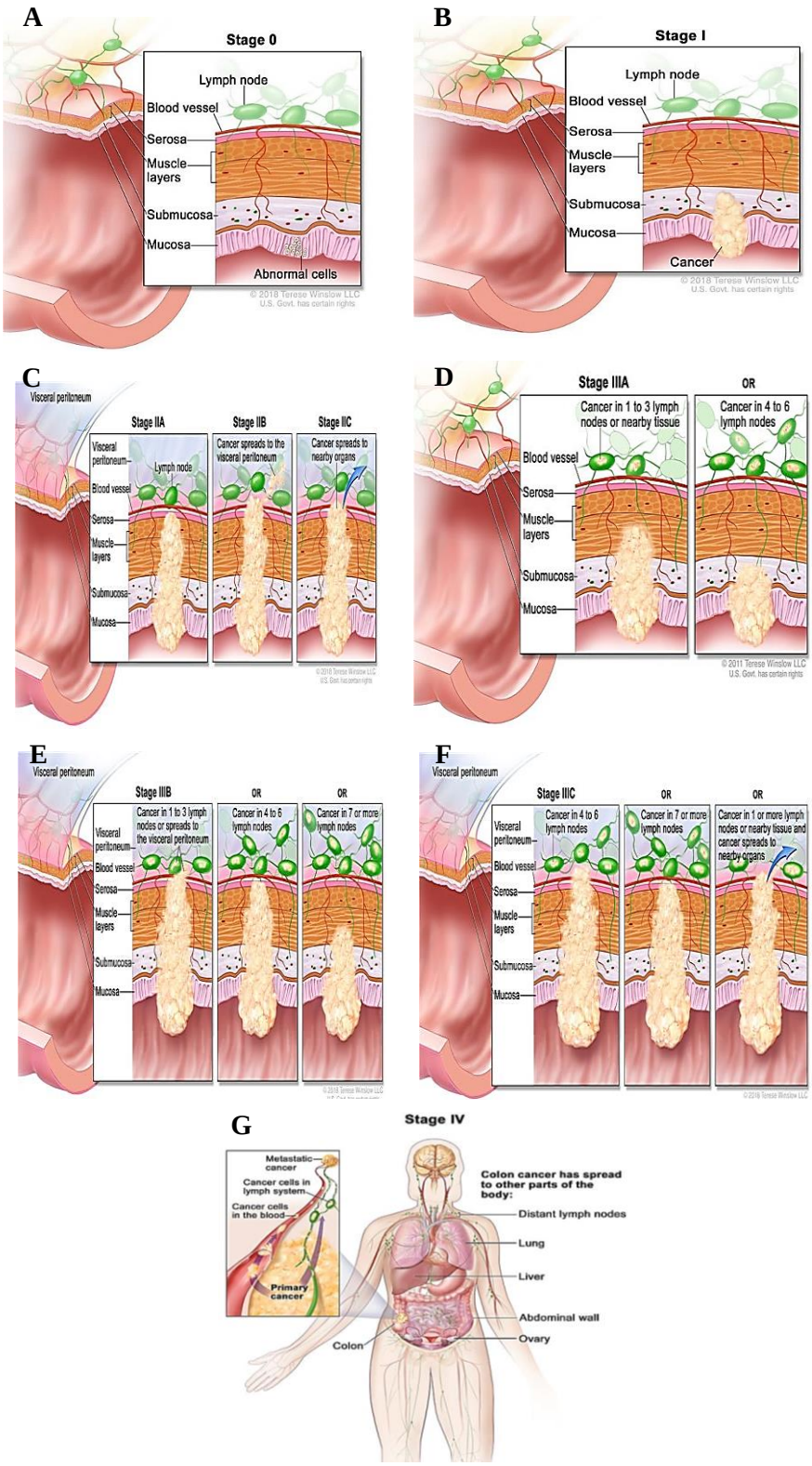

Figure 12. Scheme of colorectal staging, **a)** stage 0, **b)** stage I, **c)** stage IIA, IIB and IIC, **d)** stage IIIA, **e)** stage IIB, **f)** stage IIIC, **g)** stage IV (National Cancer Institute, 2019a)

1.2.4.6 Colorectal cancer cell lines

A commencing study by Leibovitz and colleagues, sustainable cell lines have emerged from approximately 10% of over 163 specimens endeavor (Leibovitz *et al.*, 1976). Clinically, colorectal cancer invades and metastasizes which leads to malignancy. Several studies have recognized both invasive and non-invasive cell lines (Bresalier *et al.*, 1987; Schlecte *et al*., 1990). The genetic alteration of cell lines could be a consideration to make an accurate decision in targeted therapy. Several cell lines are encountered by multiple gene alterations, which are *APC, TP53, BRAF, SMAD4, KRAS,* and *PIK3CA*, as the central altered genes on colorectal cell lines. A brief description regarding used human colorectal cancer cell lines was summarized in Table 7.

Table 6. Several treatments of colorectal cancer and its molecular mechanisms

Stage	Treatment	Drugs/Regimen	Mechanism of drugs	Reference(s)
0	Surgery	No drugs used	-	American Cancer Society, 2018c
I	Surgery	No drugs used	-	
II	Surgery and adjuvant chemotherapy	5-Fluorouracil	Disrupt DNA and RNA synthesis	American Cancer Society, 2018c
		Oxaliplatin	Inhibit DNA replication and transcription and cell cycle arrest	American Cancer Society, 2018c; Mehmood, 2014
III	Surgery and adjuvant chemotherapy	FOLFOX regimen including leucovorin, 5-FU, and oxaliplatin	Inhibit and disrupt DNA and RNA transcription, synthesis and cell cycle arrest	American Cancer Society, 2018c; Pardini *et al.*, 2011; Mehmood, 2014
		CAPEOX regimen including capecitabine and oxaliplatin	Inhibit DNA and RNA synthesis including transcription and induces cell cycle arrest	American Cancer Society, 2018c; Schellens, 2007
IV	Surgery and adjuvant chemotherapy	FOLFOX regimen including leucovorin, 5-FU, and oxaliplatin	Inhibit and disrupt of DNA and RNA transcription and synthesis and cell cycle arrest	American Cancer Society, 2018c; Pardini *et al.*, 2011; Mehmood, 2014
		FOLFIRI regimen including leucovorin, 5-FU, and irinotecan	Disrupt DNA and RNA synthesis and inhibit the action of topoisomerase I	American Cancer Society, 2018c; Ishihara *et al.*, 2010
IV	Targeted therapy	Bevacizumab	Inhibit VEGF and inhibit the progression of angiogenesis	American Cancer Society, 2018c; Ellis, 2006

Table 6. Several treatments of colorectal cancer and its molecular mechanisms (continued)

Stage	Treatment	Drugs	Mechanism of drugs	Reference(s)
IV	Targeted therapy	Cetuximab	Bind with EGFR and inhibit cell-cycle arrest, apoptosis, and angiogenesis	American Cancer Society, 2018c; Bou-Assaly and Mukherji, 2010

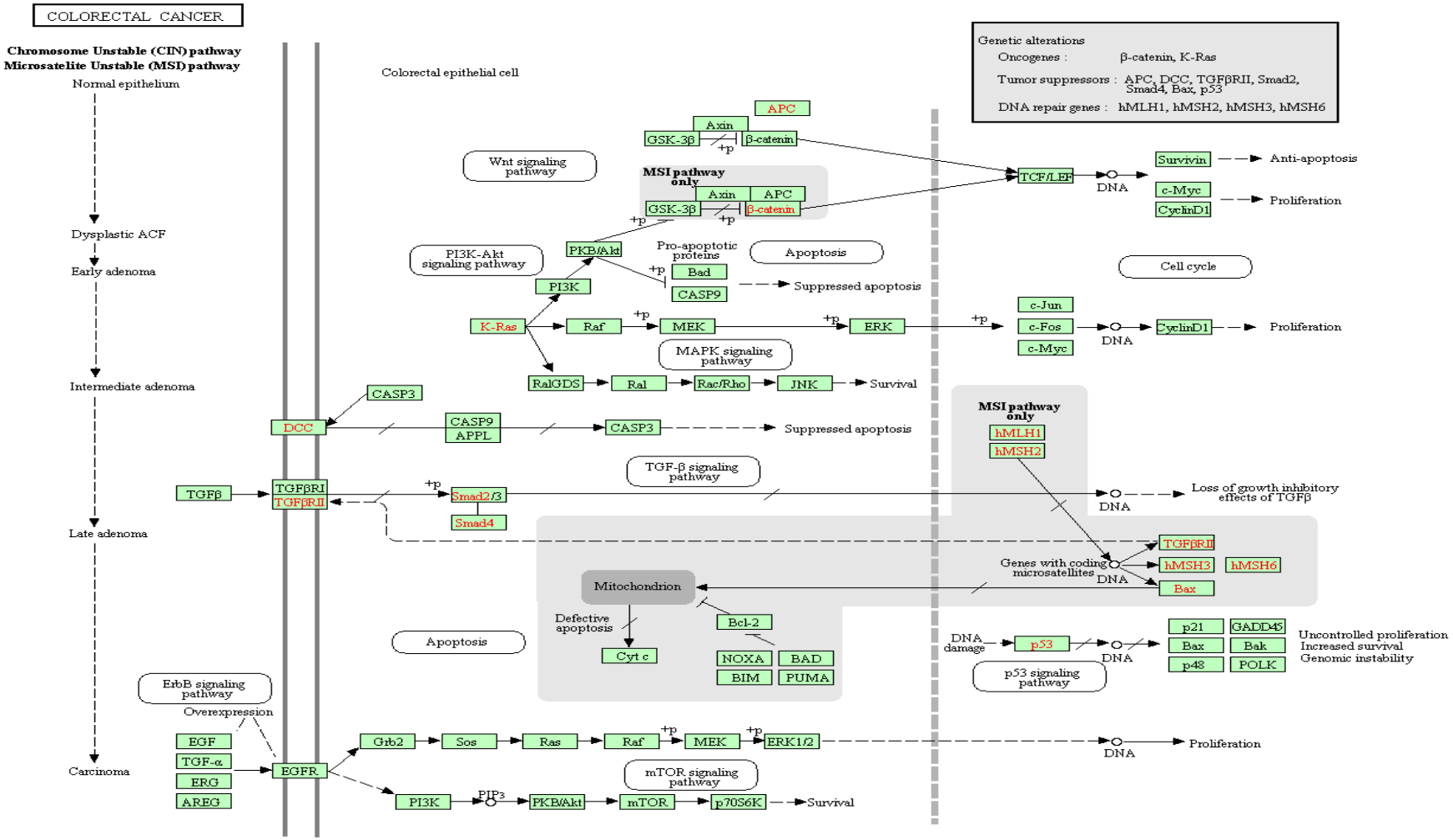

Figure 13. Signalling pathway of colorectal cancer based on its malignancy (Kanehisa Laboratories, 2018b)

Table 7. Cell lines derived from human colorectal cancers used in this study

Cell line	Histology	Mutated Gene						Dukes stage	Reference(s)
		APC	***SMAD4***	***TP53***	***PIK3CA***	***KRAS***	***BRAF***		
HT-29	Adenocarcinoma	Mt	Mt	Mt	Mt	WT	Mt	B	American Type Culture Collection, 2014; Ehrig *et al.*, 2013
SW-620	Adenocarcinoma	Mt	Mt	Mt	WT	Mt	WT	C	

Mt: mutated; WT: wild type (no mutation); *APC*: Adenomatous Polyposis Coli; *SMAD4*: the mothers against DPP homolog; *TP53*: The protein 53 (p53); *PIK3CA*: phosphatidylinositol-4,5-bisphosphate 3-kinase catalytic subunit alpha; *KRAS*: one of the ras family; *BRAF*: B-Raf

1.2.5 Ovarian cancer

1.2.5.1 Ovarian cancer prevalence

Ovarian cancer was not a common cancer type worldwide. Ovarian cancer was accounted for 295,414 incidences (1.6% of all cancer type) and 184,799 mortalities (1.9% of all cancer type) (Bray *et al.*, 2018). This type of cancer mainly develops in older women who more or equal to 63 years old. Moreover, ovarian cancer is more frequent occurred in caucasian women than Afro-American women (American Cancer Society, 2019b). In Indonesia, ovarian cancer was the third leading of cancer incidences (13,310 incidences) under breast cancer cases position (58,256 cases) and cervix and uterine cancer (32,469 incidences) (WHO, 2019).

1.2.5.2 Normal ovarian anatomy

The ovaries are located on the middle surface of the pelvic wall, which connects to the oviduct, as shown in Figure 14 (Ramirez-Gonzalez *et al.*, 2016). Ovaries are reproductive organs that have shape ovoid, almond-shaped, and smooth surface in early reproductive age and the size (adult ovaries) about 3 to 5 cm in length, 1.5-3 cm in width, and 0.2–0.6 inch in thickness. However, the size of ovaries depends on its age, hormonal status, menstrual cycle, and the contents of follicular derivatives. The ovarian stroma consists of fibroblasts, arteries, veins, smooth muscle cells, lymphatics, follicles, and nerves. Based on the histological aspect, ovaries contain three zones based on their layers starting from the outer cortex, the highly vascular inner medulla, and the hilum.

The cortex is the layer constructed by follicles, corpus luteal, fibroblasts, and smooth muscle (Clement, 1987).

An ovary produces one ovum that established from oocytes. Oocytes are covered by the follicles. Follicles progressively mature through primordial, primary, and secondary stages before retrieving an antral cavity. The antral cavity of a follicle that about 0.08-0.20 inch in diameter, which appeared on the menstrual cycle. After the pubertal period, follicle-stimulating hormone (FSH) and luteinizing hormone (LH) are released from the hypothalamus through the pituitary (Forabosco *et al.*, 1991; Gougeon, 1996). During the menstrual cycle, several follicles are developed to be mature, but only one follicle can complete the process. During the menstrual cycle, only one antral follicle will be ovulated while all the other follicles will be undergone as atresia (Gougeon, 2004). Figure 14 displays the general female reproductive system.

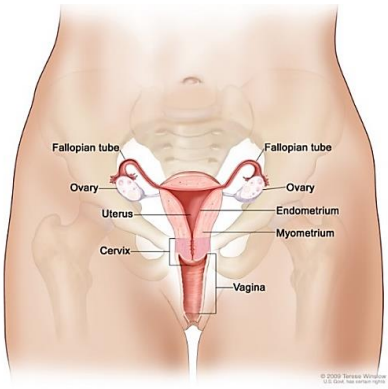

Figure 14. Female reproductive system (National Cancer Institute, 2018)

As described in Figure 15, primordial germ cells (PGCs) are defined by the BMP signaling pathway, then growth and migrate to the gonad, and construct germ cells clusters. The clusters are forced to form primordial follicles (PMFs), each holding a single oocyte (purple) hemmed by a flattened layer of pre-granulosa cells (blue). This process is negatively regulated by the estradiol (E2) and AMH and is controlled by activin, neurotrophins (NTs), FigIα, KitI/kit, FOXL2, and NOTCH signaling. Mostly PMFs remain quiescent, yet a selected subpopulation is activated to further process into primary follicles in a process regulated by both intra- and extra-oocyte factors. The shift from primary to the secondary follicle is followed by germ cells (GC) proliferation and encapsulation of the follicle by the theca cells (green). Secondary pre-antral follicles depend much on TGF-β signaling. Antral follicles require gonadotropin hormones such

as FSH and LH for their survival and ovulation. The LH flow triggers ovulation, while the remaining GC undergo terminal differentiation to form the corpus luteum (CL) (Rimon-Dahari *et al.*, 2016).

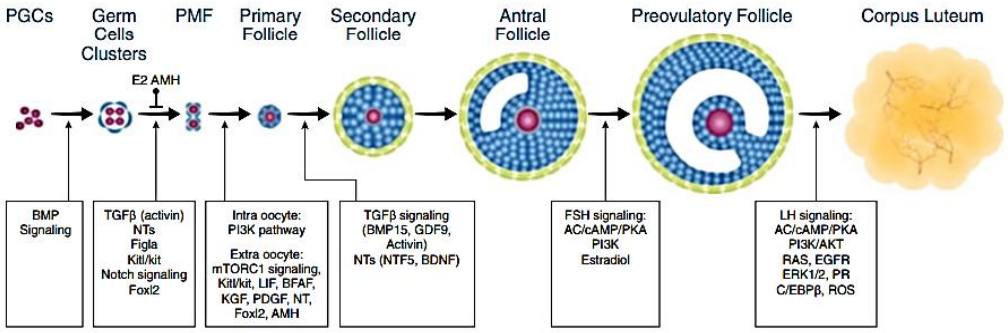

Figure 15. Scheme of ovarian folliculogenesis (Rimon-Dahari *et al.*, 2016)

1.2.5.3 Ovarian cancer development

Ovarian cancer may be caused by some risk factors, such as getting older, obesity, late pregnancy, harnessing fertility treatment, taking hormone therapy after menopause, having ovarian cancer inheritance, and holding a descendant of ovarian, breast or colorectal cancer. Around 2 persons from 40 people who are suffering from ovarian cancers are a part of inheritance syndromes from inherited changes (*mutations*) in specific genes (American Cancer Society, 2018d).

The involvement of genes related to specific syndromes also increases the ovarian cancer risk factors consisting of *BRCA1* and *BRCA2,* which are related to breast and ovarian cancer syndrome. *PTEN* is recognized as Cowden disease, which promotes the risk factor of endometrial and ovarian cancer. *MLH1*, *MLH3*, *MSH2*, *TGFBR2*, *MSH6*, *PMS1*, and *PMS2*, which are associated to hereditary non-polyposis colon cancer (HPCC); *STK11*, which is related to digestive tracts and also promoted risk of ovarian cancer (both epithelial ovarian cancer and a type of stromal tumor named sex cord tumor with annular tubules); *MUTYH*, which is related to the colon and small intestine (American Cancer Society, 2018d).

1.2.5.4 Clinical ovarian cancer types

Two systems are deciphering of ovarian cancer stage, the FIGO (International Federation of Gynecology and Obstetrics) order and the AJCC

(American Joint Committee on Cancer) TNM staging order are the same refers to the basic. The staging system was summarized in Table 8.

1.2.5.5 Molecular subtypes of ovarian cancer

Based on the position, ovarian cancer has developed from three origins, including stromal ovary, epithelial ovary, and germ-cell (Figure 16). Banerjee and Kaye deciphered regarding the subtypes of ovarian cancer. There are two types of ovarian cancer consisting of epithelium and non-epithelial. Several epithelial ovarian cancer types are high-grade serous, low-grade serous, mucinous, clear cell, and endometrioid. Moreover, the non-epithelial ovarian cancer type is sex-cord stromal, and so on (Figure 17).

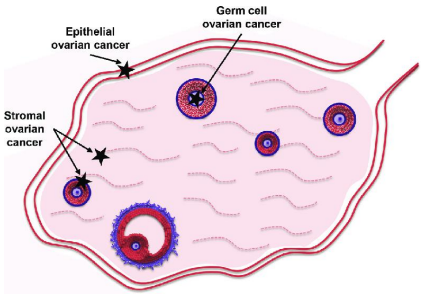

Figure 16. Scheme of ovarian cancer types (Ptak, Hoffmann and Rak, 2017)

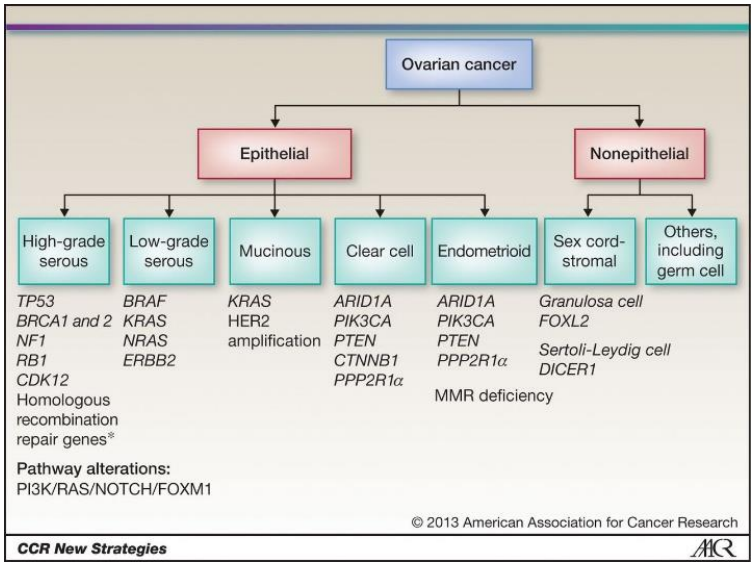

Figure 17. Classification of ovarian cancer molecular subtypes (Banerjee and Kaye, 2013)

Table 8. Ovarian cancer staging based on AJCC (American Joint Committee on Cancer, 2018) and FIGO (Mutch and Prat, 2014)

AJCC stage	FIGO stage	Stage grouping	Description
I	I	T1 N0 M0	- Cancer still exists only in the ovary (or ovaries) or fallopian tube(s) (T1). - Cancers have not migrated to nearby lymph nodes (N0) or to distant sites (M0).
IA	IA	T1a N0 M0	- Cancer exists in one ovary, and the tumor is invaded within the ovary, or the cancer is inside one fallopian tube and is only inside the fallopian tube. No cancer exists on the outer surfaces of the ovary or fallopian tube and emerged in the fluid (ascites) or washings from the pelvis and abdomen (T1a). - Cancers have not distributed to nearby lymph nodes (N0) or to distant sites (M0).
IB	IB	T1b N0 M0	- The cancer is in both ovaries and fallopian tubes but not on the outer surfaces. No cancer cells emerge in the fluid (ascites) or washings from the abdomen and pelvis (T1b). - Cancers have not migrated to nearby lymph nodes (N0) or to distant sites (M0).
IC	IC	T1 N0 M0	There are three of - The tissue (capsule) around the tumor broke during surgery, which could allow cancer cells to leak into the abdomen and pelvis. (called by IC1). - Cancer is on the exterior surface of at least one of the ovaries, fallopian tubes, or the capsule (tissue surrounding the tumor) has damaged before surgery (which could allow cancer cells to spill into the abdomen and pelvis). (called by IC2). - Cancer cells are found in the ascites or washings from the abdomen and pelvis (called by IC3). - Cancers have not migrated to nearby lymph nodes (N0) or to distant sites (M0).

Table 8. Ovarian cancer staging based on AJCC (American Joint Committee on Cancer, 2018) and FIGO (Mutch *et al.*, 2014) (continued)

AJCC stage	FIGO stage	Stage grouping	Description
II	II	T2 N0 M0	- Cancer cells are existed in one or both ovaries or fallopian tubes and spread to other organs, including the uterus, bladder, the sigmoid colon, or the rectum) within the pelvis or there is primary peritoneal cancer (T2). - Cancers have not migrated to nearby lymph nodes (N0) or to distant sites (M0).
IIA	IIA	T2a N0, M0	- Cancer has invaded the uterus or the fallopian tubes or the ovaries (T2a). - Cancers have not migrated to nearby lymph nodes (N0) or to distant sites (M0).
IIB	IIB	T2b N0, M0	- Cancer has spread to other pelvic tissues (the bladder, the sigmoid colon, or the rectum) (T2b). - Cancers have not migrated to nearby lymph nodes (N0) or to distant sites (M0).
IIIA2	IIIA2	T3a N0 or N1 M0	- Cancer has spread to the peritoneal lymph glands and spread or grown nearby the other organs in the pelvis. There is no cancer visible to the naked eyes, but tiny accumulated of cancer are found in the line of the abdomen when examining in the lab (T3a). - Cancers may or may not spread to the retroperitoneal lymph nodes only (N0 or N1) but still not spread to distant sites (M0).
IIIB	IIIB	T3b N0 or N1 M0	- Cancer has spread to the peritoneal lymph glands and spread or grown nearby the other organs in the pelvis. The accumulated cancer may be seen in the naked eyes (T3b). - Cancers may or may not spread to the retroperitoneal lymph nodes only (N0 or N1) but still not spread to distant sites (M0).
IIIC	IIIC	T3c N0 or N1	- Cancer has migrated to the peritoneal lymph glands and spread or grown nearby the other organs in the pelvis. The accumulated cancer may be seen in the naked eyes and its size larger than 2 cm and may be reached the outside of the liver or spleen (T3c).

Table 8. Ovarian cancer staging based on AJCC (American Joint Committee on Cancer, 2018) and FIGO (Mutch *et al*., 2014) (continued)

AJCC stage	FIGO stage	Stage grouping	Description
IIIC	IIIC	M0	- Cancers may or may be not migrated to the retroperitoneal lymph nodes only (N0 or N1) but still not spread to distant sites (M0).
IVA	IVA	Any T Any N M1a	- Cancer cells are arrested in the fluid around the lungs (called a malignant pleural effusion) with no other areas of cancer spread consisting of liver, spleen, intestine, or lymph nodes outside the abdomen (M1a).
IVB	IVB	Any T Any N M1b	- Cancer has migrated to the inside of the spleen or liver, to lymph nodes other than the retroperitoneal lymph nodes, and/or other organs or tissues such as the lungs and bones (M11b).

1.2.5.6 Ovarian cancer treatment

Presently, various treatments of ovarian cancer have been invented related to its type and stage. Chemotherapy is a generic drug that can eliminate cancer cells depends on its mechanism. Over time, scientists have invented some notable and novel drugs that retard some receptors such as EGFR and VEGF (Banerjee and Kaye, 2013; American Cancer Society, 2018e). Furthermore, other treatments also have been explored explicitly for each type of ovarian cancer and the stage.

As known as the hereditary tumor suppressor gene, theoretically, *BRCA1* can trigger estrogen receptor alpha (ER-α). As a result, cancers are continuing to proliferate, but cell proliferation could be ceased due to ER-β (apoptosis controller) increased (Wada-Hiraike *et al.,* 2005). Furthermore, estrogens showed its role as an enhancer of *TP53* tumor suppressor protein. Reproductive hormones, including estrogen, progesterone, and androgen, possibly play a role as the carcinogen modulator by using special hormone receptors (Ho, 2003). Therefore, a hormone therapy, which utilizing tamoxifen known as an estrogen antagonist. Tamoxifen could inhibit the estrogen receptor from suppressing cancer proliferation (Shahbaz, 2016). Some treatments based on both types and stages were summarized in Table 9.

Table 9. Treatments of ovarian cancer based on its type or stage

Treatment	Type of ovarian cancer	Ovarian cancer stage	Drugs/Regimen	Mechanism	Reference(s)
Surgery and chemotherapy	Germ cell tumors	ND	BEP regimen including bleomycin, etoposide, and cisplatin/platinol	The DNA damage caused by lipid peroxidation, inhibition of DNA Topoisomerase II, and oxidative stress	Khaidakov, Manjanatha, and Aidoo, 2002; Montecucco, Zanetta and Biamonti, 2015; Dasari and Tchounwou, 2014
	Invasive epithelial ovarian cancers	Stage IA and IB (grade 2 and 3) and IC	Carboplatin and paclitaxel	Inhibit replication and transcription which causes DNA damage caused by and also induce apoptosis through inactivation of BCL-2, IL-1β, and TNF-α	de Sousa, Wlodarczyk and Monteiro, 2014; Yusuf *et al.*, 2003
		Stage IIA and IB	Carboplatin and paclitaxel		
		Stage III	Carboplatin and paclitaxel		
Surgery, targeted therapy, and chemotherapy	Invasive epithelial ovarian cancers	Stage III	Carboplatin and paclitaxel bevacizumab	Inhibit replication and transcription which causes DNA damage and inactivation of BCL-2, IL-1β, and TNF-α and inhibition of angiogenesis	de Sousa, Wlodarczyk and Monteiro, 2014; (Yusuf *et al.*, 2003); Ellis, 2006

Table 9. Treatments of ovarian cancer based on its type or stage (continued)

Treatment	Type of ovarian cancer	Ovarian cancer stage	Drugs/Regimen	Mechanism of drugs	Reference(s)
Surgery and hormone therapy	Stromal tumors of the ovary	Stage IV	Bevacizumab and palliative care (sometimes followed by chemotherapeutic drugs, carboplatin, and paclitaxel)	Counter the EGFR effect via Gonadotropin-releasing hormone receptor (GnRHR) activation	Wilson *et al.*, 2007
			Goserelin	Counter the EGFR effect via Gonadotropin-releasing hormone receptor (GnRHR) activation	Furman, 2017
			Tamoxifen	Inhibit estrogen	Shahbaz, 2016
			Aromatase inhibitor (letrozole, anastrozole, and exemestane)	Blocking of the aromatase enzyme (enzyme for altering other hormones to be estrogen)	American Cancer Society, 2018e

Table 9. Treatments of ovarian cancer based on its type or stage (continued)

Treatment	Type of ovarian cancer	Ovarian cancer stage	Drugs/Regimen	Mechanism	Reference(s)
Surgery alone	Germ cell tumors	ND	No drugs used	Ovarian cystectomy (removing infected part of an ovary)	American Cancer Society, 2018f
	Borderline epithelial tumors (atypical proliferating tumors)	ND	No drugs used		
	Stromal tumors of the ovary	Stage I	No drugs used		
	Invasive epithelial ovarian cancers	Stage IA and IB (grade 1)	No drugs used		American Cancer Society, 2018f

1.2.5.7 Ovarian cancer cell lines

In the 1970s, the first characterization of cultured ovarian cancer cells was reported while the continuous derivative ovarian adenocarcinoma cell lines (Ioachim, 1975). There are other appropriate features of cell lines related to ovarian cancer, such as hormone receptor status, drug sensitivity, and response to growth factor (EGF and TGFβ). Moreover, a report regarding ovarian cancer types and related mutated genes were described in Table 10.

1.2.6 Cell death mechanisms

1.2.6.1 Apoptosis

Apoptosis is recognized as cell suicide, a process that occurred mostly in eukaryotes and synonymously as programmed cell death. Apoptosis typically occurs without energy, natural, and genetically controlled process. Moreover, this event occurs during normal cell turn over, tissue homeostasis, embryogenesis, induction, and maintenance of immune tolerance, development of the nervous system, and endocrine-dependent tissue atrophy (Abud, 2004). The principle of apoptosis, according to the morphological feature, is DNA and cell shrinkage, as shown in Figure 18 (Hotchkiss *et al.*, 2009). There are two paths to mediate apoptosis, extrinsic pathway (death receptors mediated) and intrinsic pathway or mitochondrial-mediated (Ghatage *et al.*, 2012).

Table 10. Cell lines derived from human ovarian cancers used in this study

Cell line	Histology	Mutated Gene							Ovarian Cancer Types	Reference(s)
		TP53	***NF1***	***PIK3CA***	***HRAS***	***ARID1A***	***PTEN***	***ERBB2***		
A2780	Adenocarcinoma	WT	WT	Mt	WT	Mt	Mt	WT	Endometrioid Carcinoma (ENOCa)	Anglesio *et al.*, 2013
SKOV-3	Adenocarcinoma	Mt	Mt	Mt	Mt	Mt	WT	Mt	High-Grade Serous Carcinoma (HGSC)	

Mt: mutated; WT: wild type (no mutation); NF11: neurofibromatosis type 1; *TP53*: The protein 53 (p53); *PIK3CA*: phosphatidylinositol-4,5-bisphosphate 3-kinase catalytic subunit alpha; *HRAS*: H-Ras; *ERBB2*: Erb-b2 receptor tyrosine kinase 2; *PTEN*: phosphatase and tensin homolog; *ARID1A*: AT-rich interaction domain 1A

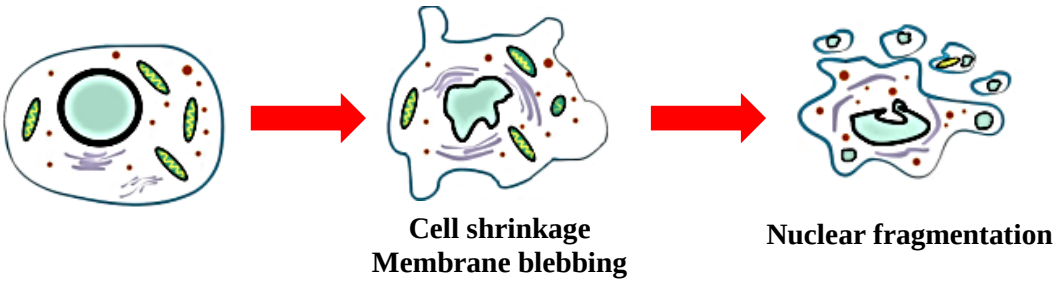

Figure 18. Scheme of morphological features of apoptosis (adapted from Tan *et al.*, 2014)

1.2.6.1.1 Extrinsic pathway (death receptors mediated)

Run due to the death receptors; the extrinsic pathway has several signaling receptors such as TNF-receptor 1, FAS, DR3, DR4, DR5 and DR6, which are known as Tumor Necrosis Factor (TNF) family. Several ligands, TNF-α, lymphotoxin, FAS Ligand (FASL), and TNF-Related Apoptosis-Inducing Ligand (TRAIL) undergo conformationally alters that allow them to communicate with specialized intracellular adaptor proteins, known as FAS-associated death domain (FADD) and TNFR-associated death domain (TRADD). FADD/TRADD, together with Death-Inducing Signaling Complex (DISC) stimulates initial apoptosis *cas-8* (CASP-8). The final step is execution by *caspase-3*/*-6*/*-7* (Gómez-Sintes *et al.*, 2011).

1.2.6.1.2 Intrinsic pathway (mitochondrial-mediated)

This pathway is provoked by intracellular signals, such as hypoxia, radiation, viral infections, and determined as DNA damage. Damaged cells give the signal to *ATM* and *CHK*, which trigger p53 proteins to recruit BAX as the DNA damage consequences. Bax proteins stimulate the mitochondria to release cytochrome-c (*cyt-c*), and this process mediated by Bcl families such as Bcl-2 and Bcl-xl. *Cyt-c* binds with protein APAF, and its binding activates the pro-*cas-9* into *cas-9*. Thus, the forming apoptosome and leading to *cas*-3 activation and led to cell death (Gómez-Sintes *et al.*, 2011). The intrinsic and extrinsic pathways were briefly described in Figure 19.

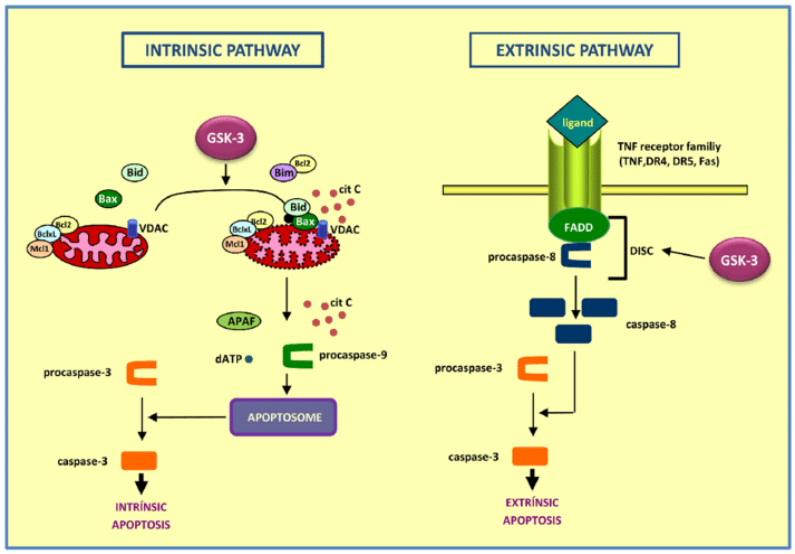

Figure 19. Model of intrinsic and extrinsic pathways related to the function of GSK-3 (glycogen synthase kinase-3) (Gómez-Sintes *et al.*, 2011)

1.2.6.2 Necrosis

Necrosis is known as an unmodulated form of dead cells caused by disadvantage or detrimental conditions. Based on the morphological, necrosis has several distinctive characters including cell swelling, damaged organelles, and then overturning of the intracellular contents throughout the extracellular milieu, as shown in Figure 20 (Vandenabeele *et al.*, 2010). The necrosis is mediated by the tumor necrosis factor receptor (TNFR) binding with TNFR1. This binding affirms the recruitment of several signaling molecules, including the TNFR-associated death domain (TRADD), the receptor-interacting protein 1 (RIP1), a cellular inhibitor of apoptosis proteins (cIAP1 and cIAP2), TNFR-associated factor 2 (TRAF2) and TRAF5, leading to the formation complex 1. Subsequently, the secondary signaling complex, consisting of TRADD, RIP1 and RIP3, fas-associated death domain (FADD), and *cas-8*. However, due to the inactivating of *cas-8* probably trigger RIP1 and RIP3 to be phosphorylated and became necrosis (Figure 21) (Tan *et al.*, 2014).

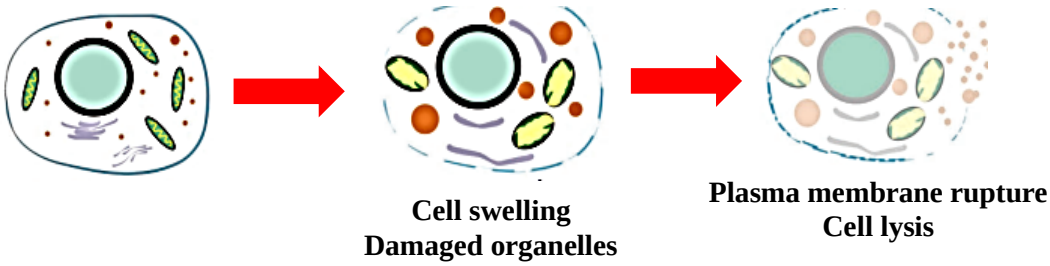

Figure 20. Scheme of morphological features of necrosis (adapted from Tan *et al.*, 2014)

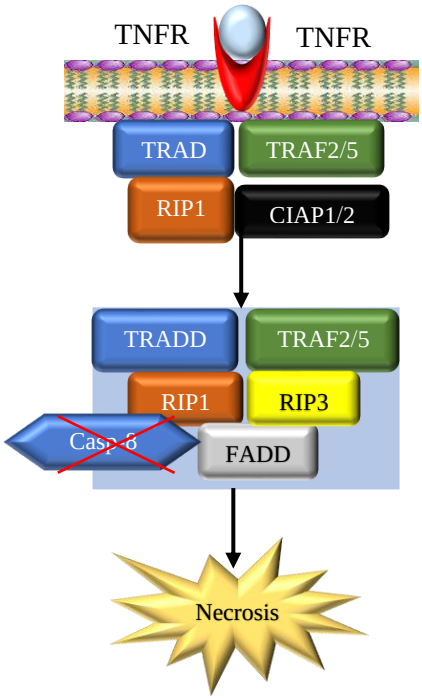

Figure 21. Scheme of necrosis pathway (adapted from Tan *et al.*, 2014)

1.2.6.3 Autophagy

Different to the other programmed cell deaths, autophagy is known as a self-mortality process caused by diverse stresses, consists of nutrient deficiency, organelle damage, hypoxia, reactive oxygen species (ROS), endoplasmic reticulum (ER) stress, and also drug treatment (Chen, He and Lu, 2018). In autophagy, the foreign and undesired cytoplasmic materials and organelles are captured in double-membrane vesicles called autophagosomes. The autophagosomes merge with lysosomes for degrading the cargo in the recycling process (Figure 22) (Rosenfeldt and Ryan, 2009).

The formation of autophagosomes is constructed by the command of autophagy-related (ATG) proteins. There are critical components involved in

generating the autophagosome such as Beclin-1, and microtubule-associated protein 1 light chain 3 (LC3). Moreover, Bcl-2 negatively regulates autophagy by interacting with Beclin-1 and disrupted the autophagy process (Pattingre *et al.*, 2005). Interestingly, the mammalian target of rapamycin (mTOR) also plays its function as a modulator of autophagy in both normal and cancer cells (Jung *et al.*, 2010). The autophagy pathway was described briefly in Figure 23.

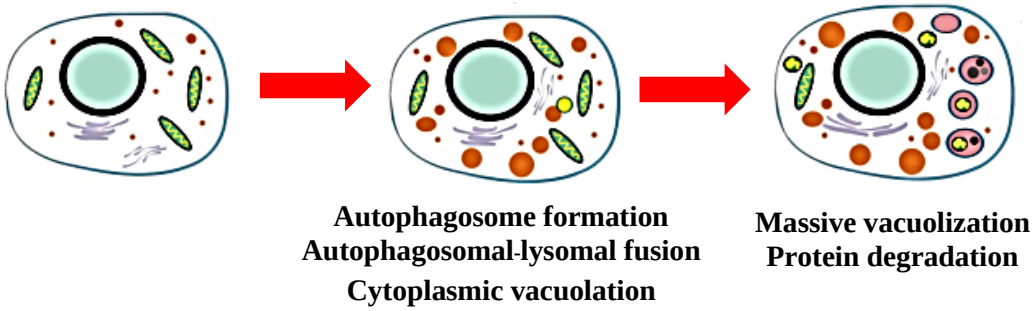

Figure 22. Scheme of morphological alteration of autophagy (adapted from Tan *et al.*, 2014)

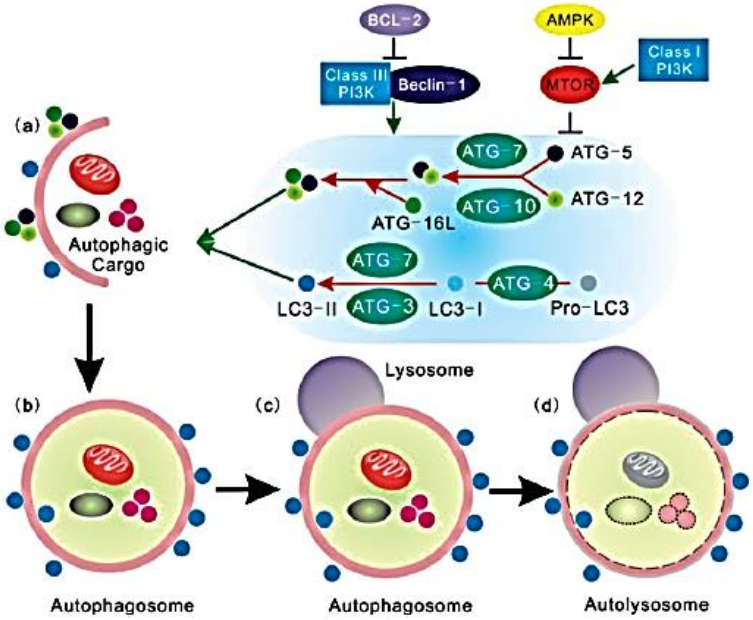

Figure 23. Scheme of autophagy pathway (Tan *et al.*, 2014)

1.2.7 *A. paniculata* (Burm.f.) Nees.

1.2.7.1 General information

Classification of *A. paniculata*

Kingdom : Plantae
Divisi : Tracheophyta
Class : Magnoliopsida
Order : Lamiales
Family : Acanthaceae
Genus : Andrographis
Species : *A. paniculata* (Burm.f.) Nees
(Global Biodiversity Information Facility, 2017a)

A. paniculata is recognized as lateral branching, an annual shrub plant with sharp quadrangular branching and height 1 meter. This plant has lanceolate leaves with 5 to 8 cm long. Moreover, this plant has small flowers with a color covering from white to rose-pink as shown in Figure 24 (Thakur *et al*., 1989).

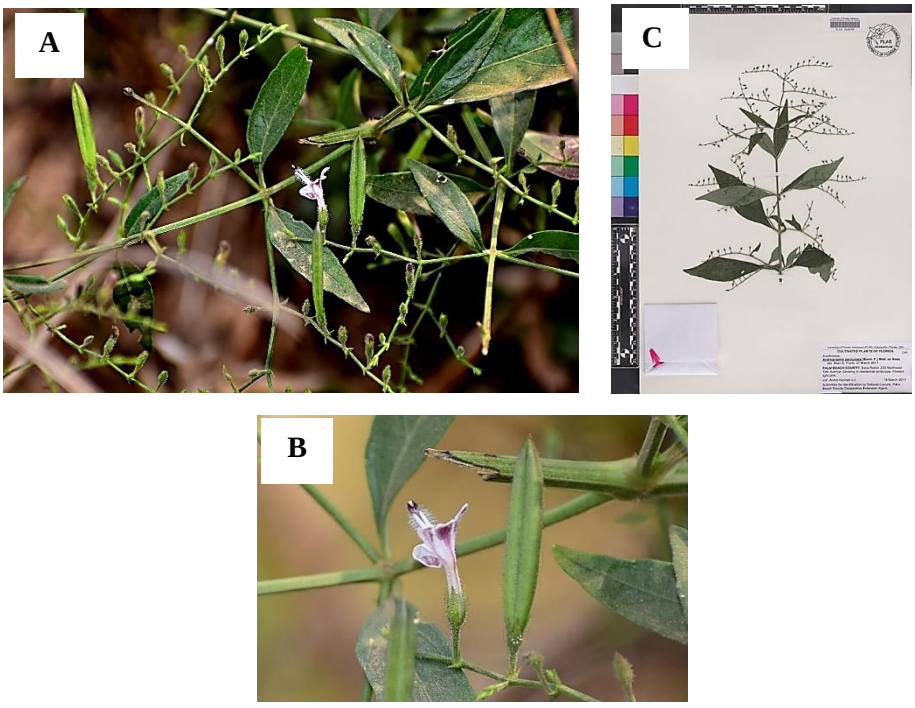

Figure 24. *A. paniculata* plant, **a)** plant morphology (Singhamahapatra, 2019a), **b)** flower (Singhamahapatra, 2019b), **c)** specimen (Davis, 2017)

A. paniculata (family: Acanthaceae) is grown in many Asian countries such as South East Asia (including to Myanmar, Peninsular Malaysia, Laos, Vietnam, Indonesia, the Philippine), India, Nepal, Australia, North America, Dominica, Venezuela, Hawaii Island, and also Southern China (Figure 25). In Indonesia itself, *A. paniculata* was widely distributed to the Indonesian society either in single or combined with other natural sources into a caplet (Widyawati, 2007).

Figure 25. Distribution map of *A. paniculata* (Global Biodiversity Information Facility, 2017a)

1.2.7.2 Chemical compounds of *A. paniculata*

A study about phytochemical screening that was conducted by Malahubban and Lalitha colleagues, methanol crude extract of *A. paniculata* contains alkaloids, saponins, flavonoids, tannins, terpenoids, steroids (Malahubban *et al.*, 2013). General chemical compounds of *A. paniculata* are steroids, phenols, terpenoids, alkaloids, saponins, flavonoids, and diterpenes (Nyeem *et al.*, 2017). Moreover, a dominant constituent of this plant is known as andrographolide included in the diterpenoid group, and its derivatives were described in Figure 26.

1.2.7.3 Biological activities of *A. paniculata* extracts

One of the medicinal values of this plant is its active chemical compounds such as andrographolide and neo-andrographolide, which are two examples of diterpenoids. Based on a study of andrographolide revealed that this compound could remedy colic pain, fever, sore throat, loss of appetite, irregular stools and diarrhea, herpes, and other chronic infectious diseases (Mishra, Sangwan, and Sangwan, 2007; Niranjan, Tewari and Lehri, 2010).

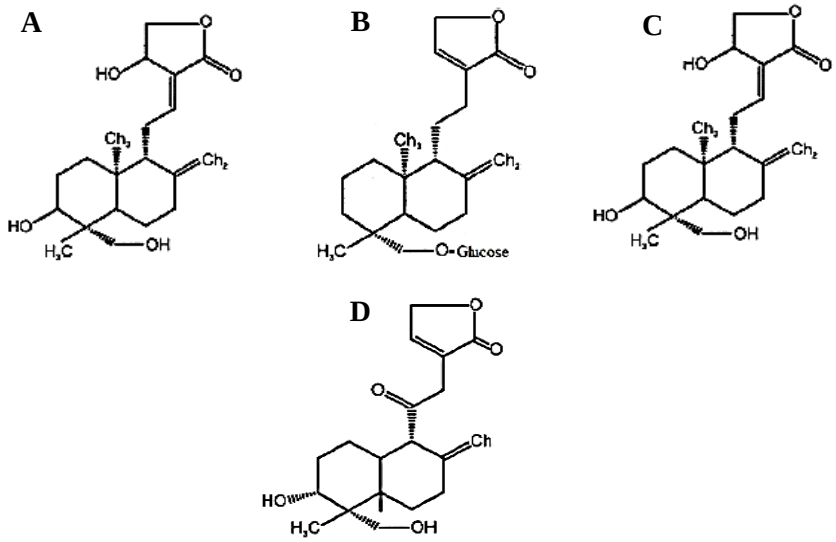

Figure 26. Several diterpene lactones contained in *A. paniculata*, **a)** andrographolide, **(b)** neoandrographolide **(c)** 14-Deoxy-11,12-didehydroandrographolide, **(d)** 14-deoxy-11-oxoandrographolide (Anju *et al.*, 2012)

Other chemical constituents isolated from *A. paniculata* also have been reported by several scientists. Dehydro-andrographolide could remedy the inflammation by reducing the histamine, dimethyl benzene, and adrenaline (Deng, 1978). Interestingly, other chemical constituents, 12-didehydroandrogapholide; andrograpanin; 14-deoxyandrographolide and 5-hydroxy-7,8-dimethoxyflavone showed a potency as anti-virus of HIV (Reddy *et al.*, 2005). This plant species indicated its potency to neutralize the effect of rattlesnake venom (Samy *et al.*, 2008). Furthermore, this plant extract showed a protective feature to human body systems such as hepatoprotective, immune protection, and protection of peroxidative substances (Niranjan *et al.*, 2010).

1.2.7.4 Anti-cancer effect of *A. paniculata* extracts

As a pioneer of the research regarding the potency of *A. paniculata*, Siripong, and colleagues gave a contribution to get the evidence through a study using methanolic extract to obtain the diterpenoid compound. From this study, the results suggested that the methanolic extract could inflict significant cytotoxic effect against KB (human epidermoid leukemia) and P388 (lymphocytic leukemia) cell lines, with ED_{50} less than 20 µg/ml. A study regarding *A. paniculata* was also performed by Kumar

and colleagues, the methanolic extract of *A. paniculata*, which fractioned into methanol, petroleum ether, dichloromethane, aqueous. This finding suggested that dichloromethane and methanol crude extract of *A. paniculata* more significantly inhibited the proliferation of HT-29 (colon cancer cell line), indicated by IC_{50} 20 µg/ml, but exhibited low cytotoxic effect with the ether and water extract (Kumar *et al.*, 2004). One year after that, Cheung and research team also conducted a study using ethanol extract against human promyelocytic leukemia cells (HL-60) and cervical contaminant carcinoma (KB/HeLa derivative) that exhibited potent cytotoxicity to HL-60 and otherwise, low cytotoxicity to KB (Cheung *et al.*, 2005).

Terpenoids are the major compound of natural products and become a reservoir of anti-cancer therapy (Huang *et al.*, 2012). Furthermore, tannins and phenols also showed anti-cancer activity by down-regulating of cyclins A and B1, arresting cell-cycle in the S phase, and causing apoptosis through the intrinsic pathway (Yildirim and Kutlu, 2015). A few mechanisms of action from cardiac glycosides to suppress cancer cell viability were reviewed by Pongrakhanaon. Theoretically, cardiac glycosides can impede Nuclear Factor-kB (NF-kB) pathway and Mitogen-Activated Protein Kinases (MAPKs) pathway (two of several factors to trigger DNA replication of cancer cell) and also upregulation triggered cancer apoptosis (Pongrakhananon, 2013).

Less than one decade, Sagadevan and Suzuki colleagues reported that methanol extract of *A. paniculata* could inhibit behalf of mammary adenocarcinoma (MCF-7) as well as human oral squamous cell carcinoma (HSC) population by concentration 57.33 and 28 µg/ml, respectively. Some publications reported the mild effect of the water extract of *A. paniculata* (Sagadevan *et al.*, 2013; Suzuki *et al.*, 2016). The aqueous crude extract gave low cytotoxic effect against mice mammary adenocarcinoma, neuroblastoma (IMR-32), and also human colon cancer (HT-29), with IC_{50} more than 250 µg/ml (Suzuki *et al.*, 2016); (Rajeshkumar *et al.*, 2015). Ethanol extract of *A. paniculata* was investigated by Singh and Padmalochana's research team. They found low cytotoxic effect against MCF-7, SiHa, HT, HepG2, and Hep2 cell line indicated by the percentage of inhibition 16.04%, 24.06%, 12.42%, 28.22%, and 10.31%, respectively (Singh *et al.*, 2013; Padmalochana, 2017). An in vivo study, an ethanolic extract of *A. paniculata* increased the life span of mice administered with thymoma cells (Sheeja *et al.*, 2006). Nugrahaningsih and the colleague also conducted

a study, using C3H mice, *A. paniculata* showed programmed cell death (apoptosis) towards mammary adenocarcinoma (Nugrahaningsih *et al.*, 2013).

Several previous studies reported the mechanism of action by some chemical constituents of *A. paniculata*. Varma and research team reviewed that andrographolide could inhibit the cancer growth by inducing apoptosis, necrosis, cell-cycle arrest, or cancer cell (Varma, Padh, and Shrivastava, 2011). Other constituents were explored by Kumar and colleagues. using andrographolide, 14-Deoxy-11,12-didehydroandrographolide and 14-Deoxyandrographolide for appraising the behalf population inhibitory concentration (GI_{50}) against a wide array of cancer type such as breast, CNS, colon, lung, melanoma, ovarian, prostate, and renal (Kumar *et al.*, 2004).

From the chromatographic fractionation, *A. paniculata* leaves were isolated into refined andrographolide which was investigated to be highly toxic against the cancer cell lines such as acute myeloid leukemia (Cheung *et al.*, 2005; Chen *et al.*, 2017), human liver cancer cell lines (Chen *et al.*, 2012), ovarian cancer cell lines, breast cancer cell lines (Tan *et al*., 2005; Sukardiman, Widyawaruyanti, and Zaini, 2007; Jada *et al*., 2008), gastric cancer cells (Jiang *et al.*, 2007), colon cancer cells (Jada *et al.*, 2008; Wang *et al.*, 2016), glioma cell line (Agarwal, 2015), lung cancer cell line (Tan *et al.*, 2005; Lim *et al.*, 2015).

Almost two decades, several studies of andrographolide tried to resolve the global issues about the malignancy of variant types of cancer cell lines. The previous study reported the effectiveness of andrographolide against variant types of cancer cell lines and derivates of andrographolide (14-Deoxy-11,12-di-dehydroandrographolide) against human breast cancer (T-47D) (Cheung *et al.*, 2005; Tan *et al.*, 2005; Jada *et al.*, 2008; Dai, Wang and Pan, 2017b), whereas criteria of effectiveness IC_{50} values are not more than 4 µg/ml. Other studies also reported the potency of andrographolide consecutively by more than one previous decade through the last two years (2007-2018) (Sukardiman *et al*., 2007; Shi *et al*., 2008; Manikam and Stanslas, 2009; Chen *et al*., 2012; Luo *et al*., 2014; Agarwal, 2015; Yuan *et al*., 2016, 2018; Doi *et al*., 2017; Khan *et al*., 2018; Liu and Chu, 2018; Sarkar *et al*., 2018).

Several previous studies demonstrated the mechanisms of andrographolide on cancer cell lines. Andrographolide and its analogs exert anti-cancer activities directly to the cell-cycle arrest at G0/G1 phase via induction of cell-cycle

inhibitory protein and decreased expression of cyclin-dependent kinase (Rajagopal *et al.*, 2003; Satyanarayana *et al.*, 2004; Cheung *et al.*, 2005; Jada *et al.*, 2007; Shi *et al.*, 2008). Ji and Manikam reported that Andrographolide obviously could inhibit human hepatoma cell growth through activating c-Jun N-terminal kinase or inducing cell differentiation (Ji *et al.*, 2007; Manikam and Stanslas, 2009). Moreover, andrographolide might repress an oncogene v-Src-induced transformation and down-regulates v-Src protein expression via the attenuation of the ERK1/2 signaling pathway (Liang *et al.*, 2007).

1.2.7.5 Anti-cancer effect of the combination with *A. paniculata*

Several studies using the combination of *A. paniculata* were successfully conducted by several research teams. The combination of *A. paniculata* with *S. marianum* extract showed higher cytotoxicity to MCF-7 (breast cancer), SiHa, and HepG2 (cervical cancer cell lines) than single treatment (Singh *et al.*, 2013).

Andrographolide of *A. paniculata* also showed its capacity as a promising anti-cancer compound. Andrographolide significantly increased cytotoxicity of chemotherapeutic drugs. Yang and colleagues achieved that andrographolide gave more significant cytotoxic than 5-fluorouracil alone. The increasing of cytotoxicity was indicated by the upregulating of *cas-3, -9, -8,* cytochrome-c, and p53 proteins. expressions (Yang *et al.*, 2009). Moreover, andrographolide increases the cytotoxicity of doxorubicin and cisplatin through the down-regulation of anti-apoptotic genes (Bcl-2 and Bcl-xl), apoptotic mediator genes (Bax) (Sukumari-Ramesh *et al.*, 2011). For the combination with paclitaxel, andrographolide could predispose higher cytotoxicity than paclitaxel alone, indicated by increasing reactive oxygen species (ROS) (Yuan *et al.*, 2016).

Table 11. Anti-cancer effect of *A. paniculata* leaves prepared with various solvents against several cancer cell lines (effective criteria is less than 20 µg/ml)

Type of solvent	Cell lines	Effective concentration	Reference(s)
Methanol	KB (human HeLa contaminant Carcinoma/Papilloma)	IC_{50} = 5.3 µg/ml	Siripong *et al.*, 1992
	P388 (human myelogenous leukemia cell)	IC_{50} = 3.1 µg/ml	
	HT-29 (human colon cancer cell)	IC_{50} = appx 10 µg/ml	Kumar *et al.*, 2004
	MCF-7 (human mammary gland adenocarcinoma)	IC_{50} = 57.33 µg/ml	Sagadevan *et al.*, 2013
	HSC (human oral squamous cell carcinoma)	IC_{50} = 28 µg/ml	Suzuki *et al.*, 2016
Aqueous	HT-29 (human colon cancer cell)	IC_{50} = appx > 100 µg/ml	Kumar *et al.*, 2004
	IMR-32 (Neuroblastima)	IC_{50} = appx 250 µg/ml	Rajeshkumar *et al.*, 2015
	Hep2 Cell line (human HeLa contaminant carcinoma)	IC_{50} = 250 µg/ml	Padmalochana, 2017
	C3H (mice mammary adenocarcinoma) at concentration: 500 µg/ml; 1000 µg/ml; 15000 µg/ml	Mean apoptotic indices: 1.37; 2.03; 2.53	Nugrahaningsih *et al.*, 2013
Dichloromethane	HT-29 (human colon cancer cell)	IC_{50} = appx 10 µg/ml	Kumar *et al.*, 2004
Ethanol	Hl-60 (human acute promyelocytic leukemia)	IC_{50} = 14.01 µg/ml	Cheung *et al.*, 2005
	KB (human HeLa contaminant Carcinoma/Papilloma)	IC_{50} = 131.40 µg/ml	
	CNE-3 (human nasopharyngeal carcinoma)	IC_{50} = 150.27 µg/ml	
	H4-II-E (rats liver hepatoma)	IC_{50} = 223.88 µg/ml	
	IMR-32 (neuroblastima)	IC_{50} = appx 200 µg/ml	Rajeshkumar *et al.*, 2015
	HT-29 (human colon cancer)	IC_{50} = appx 200 µg/ml	
	Hep2 Cell line (human HeLa contaminant carcinoma)	IC_{50} = appx 200 µg/ml	Padmalochana, 2017

Table 11. Anti-cancer effect of *A. paniculata* leaves prepared with various solvents against several cancer cell lines (effective criteria less than 20 µg/ml) (continued)

Type of solvent	Cell lines	Effective concentration	Reference(s)
70% Ethanol extract concentration at 100 µg/ml	MCF-7 (human mammary gland adenocarcinoma)	% Inhibition: 16.04%	Singh *et al.*, 2013
	SiHa (human cervix squamous cell carcinoma	% Inhibition: 24.08%	
	HT-29 (human colon cancer)	% Inhibition: 12.42%	
	Ovcar (human ovarian carcinoma)	% Inhibition: 51.12%	
	HepG2 (liver hepatocellular carcinoma)	% Inhibition: 28.22%	
Ethyl acetate	T-47D (human invasive ductal carcinoma)	IC_{50} = appx 10 µg/ml	Sukardiman *et al.*, 2014
	HeLa	IC_{50} = appx 25 µg/ml	
	WiDr (human colon colorectal adenocarcinoma)	IC_{50} = appx 15 µg/ml	
Petroleum ether	HT-29 (human colon cancer cell)	IC_{50} = appx 90 µg/ml	Kumar *et al.*, 2004
Acetone	IMR-32 (Neuroblastima)	IC_{50} = appx 250 µg/ml	
	HT-29 (human colon cancer)	IC_{50} = appx 200 µg/ml	
	Hep2 Cell line (human HeLa contaminant carcinoma)	IC_{50} = appx 250 µg/ml	Padmalochana, 2017

1.2.8 *Z. spina-christi* (L.) Desf.

1.2.8.1 General information

Classification of *Z. spina-christi*

Kingdom : Plantae
Divisi : Tracheophyta
Class : Magnoliopsida
Order : Rosales
Family : Rhamnaceae
Genus : Ziziphus
Species : *Z. spina-christi* (L.) Desf.
(Global Biodiversity Information Facility, 2017b)

Z. spina-christi species has the shrub to tree form which size of 5 to 10 m. Compared to the other species of *Ziziphus*, *Z. spina-christi* has light brown spines (Figure 27a). *Z. spina-christi* leaves are formed as simple, narrowly ovate-lanceolate, and alternate with a size of 0.4-1.38 inches in width and 0.4 to 3.54 inches in length. The flowers of *Z. spina-christi* are greenish-yellow and located in the terminal of the leaves (Figure 27a). Moreover, the fruits form is globe drupe with 0.4 to 0.59 inches in diameter (Saied *et al.*, 2008) as shown in Figure 27b.

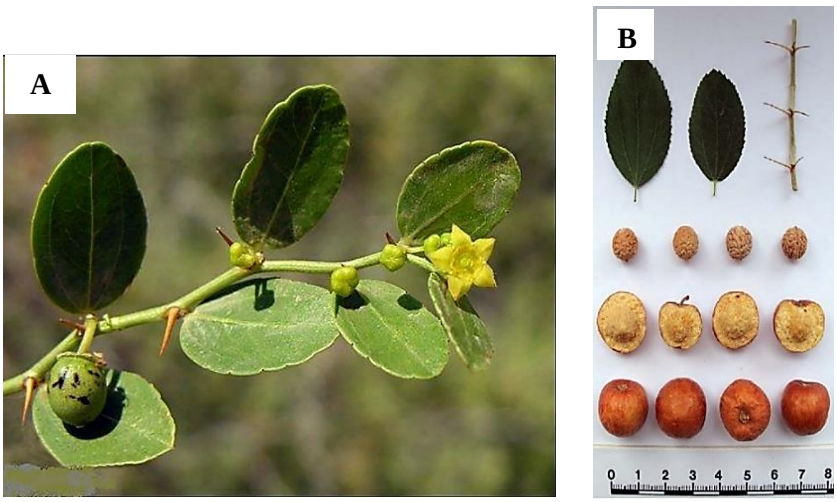

Figure 27. *Z. spina-christi*, **a)** leaves and flowers (Asgarpanah and Haghighat, 2012); **b)** leaves, spinal barks and fruits (Saied *et al.*, 2008)

As described in Figure 28 below, *Z. spina-christi* is a native plant of the Middle East to the south of the Euphrates and widely distributed to Saharan Oases across Africa to the Sahel (Nkafamiya *et al*., 2013). Yet the *Ziziphus* genus is frequently used in traditional medicine in the two continents such as Africa as shown in Figure 28, and this species also introduced in Indonesia. This species is also known in two religions, Moslems and Hebrews, due to its historical record in the Middle East. According to the Muslim perspective, *Z. spina-christi* is respected and regarded as close to "holy tree", which is mentioned twice in the Holy Quran at Surah XXXIV (Saba – The City of Saba), Verse: 15-16 and Surah LVI (Al-Waqia – The Inevitable Event), Verse: 27-34 (Dafni *et al*., 2005).

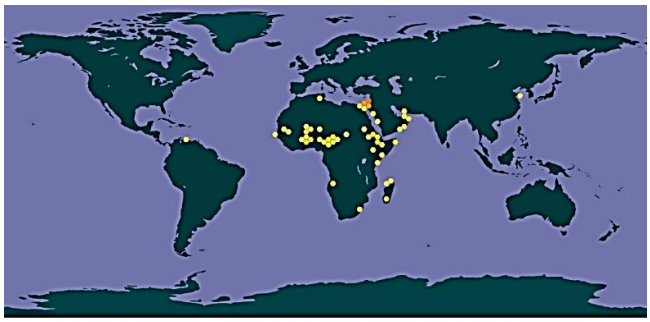

Figure 28. Distribution map of *Z. spina-christi* (Global Biodiversity Information Facility, 2017b)

1.2.8.2 Chemical compounds of *Z. spina-christi*

Z. spina-christi leaves contain several chemical constituents consisting of christinin-A (Figure 29a) (major compound), flavonoid glycosides consist of rutin and quercetin derivatives (Figure 29b and c), alkaloids (spinanine A), tannins, sterols (β sitosterol), sapogenins and saponins such as betulinic acid and triterpenoids. The whole of the chemical constituents is completely provided depending on the type of chemical organic solvents.

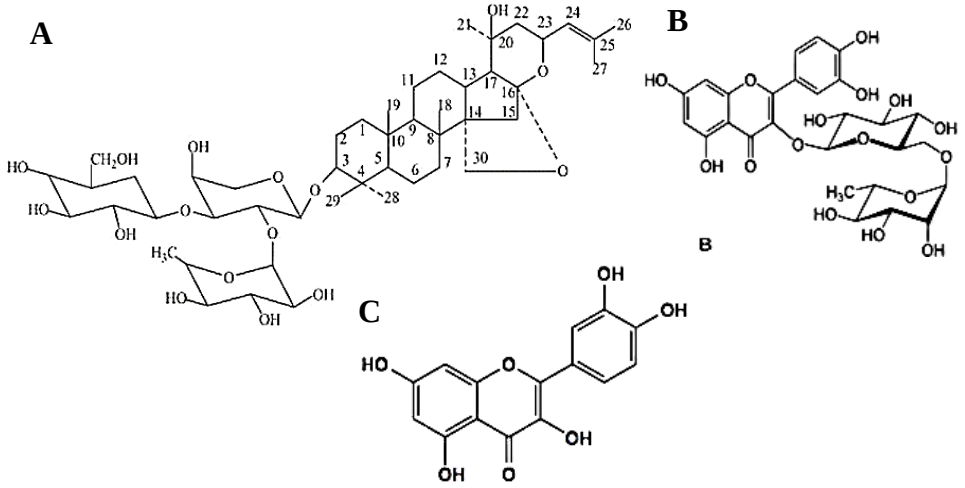

Figure 29. Chemical constituents of *Z. spina-christi*, **a)** christine-a (saponins) (Asgarpanah and Haghighat, 2012), **b)** rutin (flavonoid glycosides) (Prasad and Prasad, 2018), **c)** quercetin (flavonoid glycosides) (Chedea *et al.*, 2012)

1.2.8.3 Biological activity of *Z. spina-christi* extracts

According to the Tibb-e-Nabawi Prophet Mohammed (peace be upon him), Shamsi narrated that utilization of *Z. spina-christi* leaves for reducing abscess, furuncles, obesity, enhancing appetite, and reducing cough. Prophet Mohammed (peace be upon him) ordered someone who recently embraced Islam to perform Ghusl (Islamic manner bath) using soaked of *Z. spina-christi* leaves (Shamsi, 2016). Therefore, the reason for this activity (Ghusl) with the chemical compound of *Z. spina-christi* that possess saponins, tannins, alkaloids. Other ailments that could be cured by this *Ziziphus* genus are headache, fever, asthma, pulmonary ailment, malaria, wounds, burns, stomach discomfort, rheumatics disease from the viscera (Adzu *et al.*, 2003).

The aqueous extract of *Z. spina-christi* showed antibacterial activity against *Staphylococcus aureus*, *Bacillus subtilis*, and *Enterococcus faecalis* (Suliman and Mohammed, 2018). The substances of extract had different mechanisms according to their chemical organic solvents. A study from Shahat and colleagues suggested that *Z. spina-christi* leaves aqueous extract could give significant antiviral activity, while the chloroform extract could inhibit gram-positive microorganisms such as *Streptococcus pyogenes* and *Bacillus cereus*. Petroleum ether extract of *Z. spina-christi* exhibited antibacterial activity against *Streptococcus aureus* (Shahat *et al.*, 2001). Various bioactivities from ZSC crude extracts were nicely explored by scientists such

as antioxidants (Al-Marzooq, 2014), anti-plasmodial, and hepatoprotective (Hafiz and Mubaraki, 2016).

1.2.8.4 Anti-cancer activity of *Z. spina-christi* extracts

A review elucidated regarding the benefits of flavonoids for cancer cells, which exhibited this chemical group compound potency to induce apoptosis by causing DNA fragmentation, nuclear condensation, and also cell destructed (Reed and Pellecchia, 2005). Meanwhile, saponins can induce anti-proliferative activities such as lung cancer, esophageal carcinoma, gastric cancer, colon cancer, hepatocellular carcinoma, renal carcinoma, bladder cancer, breast cancer and ovarian cancer (Xu *et al.*, 2016).

From *Z. spina-christi* crude extract study, a study was conducted using several types of *Z. spina-christi* crude extract for anti-cancer. Jafarian and colleagues conducted a study about using variant types of *Z. spina-christi* crude extract against HeLa and MDA-MB-468. According to the study, a chloroform-methanol fraction could not significantly induce the cell lines to be apoptosis, indicated by its IC_{50} value at 100 µg/ml (Jafarian, Shirani and Zolfaghari, 2014).

Last four years, Farmani and the research team conducted a study using various types of a *Z. spina-christi* fraction such as ethanol, ethanol-aqueous, and aqueous of *Z. spina-christi* leaves to induce apoptosis and antiproliferative against MCF-7 (human mammary adenocarcinoma) (Farmani *et al.*, 2016). By the IC_{50} values showed that the ethanol fraction was the most effective indicated by its IC_{50} less than 20 µg/ml. Ethanol extract of *Z. spina-christi* could arrest the cycle cell at the G1/S phase. Subsequently, the methanol crude extract was exposed to human rhabdomyosarcoma (RD cell lines). According to the results, the methanol extract of *Z. spina-christi* exhibited low cytotoxicity towards rhabdomyosarcoma (Abu-raghif *et al.*, 2017). The anti-cancer activity of *Z. spina-christi* leaves extract was summarized in Table 12.

1.2.8.5 Anti-cancer effect of the combination *Z. spina-christi*

Several pure chemical compounds of *Z. spina-christi* leaves were discovered, such as quercetin and rutin. Quercetin and Rutin are the flavonoids group

in *Z. spina-christi* leaves. A report of treatment in quercetin together with irinotecan showed a significant cytotoxic effect on human gastric cancer. Lei and colleagues reported that the combination of quercetin and irinotecan had a tremendous and promising anti-angiogenic through down-regulating of VEGF. Therefore, this combination probably could be a potentiated anti-cancer regimen for the metastasis stage (Lei *et al.*, 2018). Another report regarding the combination of rutin and cisplatin showed no significant haematotoxicity in mice models and related to its characters such as antioxidant and oxidizable molecule (Chen *et al.*, 2013; Prasad and Prasad, 2018).

Table 12. Anti-cancer effect of *Z. spina-christi* leaves prepared with various solvents against several cancer cell lines (effective criteria less than 20 µg/ml)

Type of solvent	Cell lines	IC_{50}	Reference(s)
Hexane	HeLa	appx 500 µg/ml	Jafarian, Shirani and Zolfaghari, 2014
	MDA-MB-468 (breast carcinoma)	appx 150 µg/ml	
Chloroform	HeLa	appx 250 µg/ml	
	MDA-MB-468	appx 100 µg/ml	
Chloroform-Methanol	HeLa	100 µg/ml	
	MDA-MB-468	appx 50 µg/ml	
Butanol	HeLa	appx 250 µg/ml	
	MDA-MB-468	appx 100 µg/ml	
Methanol-Water	HeLa	appx 250 µg/ml	
	MDA-MB-468	appx 180 µg/ml	
Aqueous	HeLa	appx 550 µg/ml	
	MDA-MB-468	appx 200 µg/ml	
	MCF-7	140 µg/ml	Farmani *et al.*, 2016
Ethanol	MCF-7	20 µg/ml	
Ethanol-Aqueous	MCF-7	500 µg/ml	
Methanol	RD	> 100 µg/ml	Abu-raghif *et al*., 2017

1.2.9 *V. extensa* Wall. ex DC.

1.2.9.1 General information

Classification of *V. extensa*

Kingdom : Plantae
Division : Tracheophyta
Class : Magnoliopsida
Order : Asterales
Family : Asteraceae
Genus : Vernonia
Species : *V. extensa* Wall. ex. DC.
(Global Biodiversity Information Facility, 2017c)

V. extensa emerges in open forests or valley bushes, roads. This species forms as shrubs, or subshrubs plants with 2-3 m tall. The leaves are dark green, oblong, or oblong-lanceolate. Flower crowns are white or reddish and tubular (Figure 30). The flowers often bloom around October to March (Chen and Gilbert, 2011).

A **B**

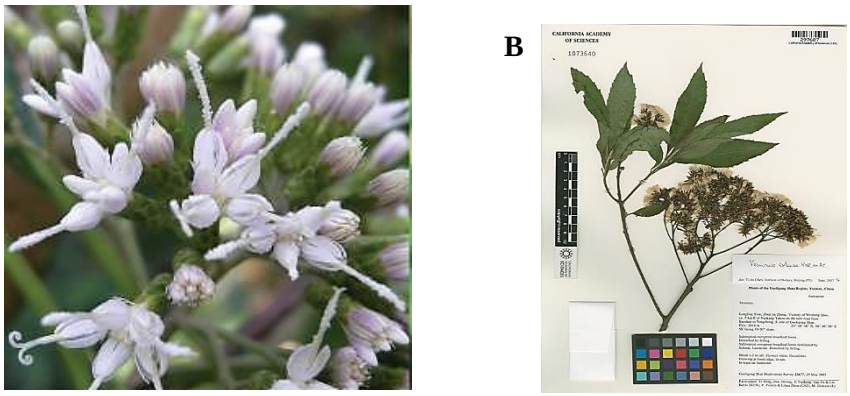

Figure 30. *V. extensa* plant, **a)** flowers (Bunwong, Chantaranothai, and Keeley, 2014), **b)** plant specimen (Global Biodiversity Information Facility, 2017c)

As shown in Figure 31, *V. extensa* has been widely distributed to the Northern Thailand (Chiang Mai and Chiang Rai Provinces), Myanmar, Cambodia and also spread to Yunnan (one of the provinces in China), India and Nepal (Global Biodiversity Information Facility, 2017c; Bunwong, Chantaranothai, and Keeley, 2014). This plant is a woody plant from Compositae (Asteraceae) family.

Figure 31. Distribution map of *V. extensa* (Global Biodiversity Information Facility, 2017c)

1.2.9.2 Chemical compounds of *V. extensa*

Several researchers reported chemical compounds from the leaves of *Vernonia. Vernonia* contains sesquiterpene lactones (Igile *et al.*, 1995), terpenoids, alkaloids (Swamy, Obey and Mutuku, 2013), vernonioside, flavonoids (such as luteolin, luteolin 7-*O*-glucosides, and luteolin 7-glucuronide) (Jisaka *et al.*, 1992; Igile *et al.*, 1994), steroidal saponins (Wang *et al.*, 2018). Additionally, *V. extensa* was reported that possessed two sterol glucosides (VE-1 and VE-2), which closely related to the bitter principles found in African *Vernonia* Genus (Ponglux *et al.*, 1992). A recent report by Thongnest and colleague revealed that aerial part of *V. extensa* extracted by dichloromethane showed several sesquiterpene lactone compounds (Fig 33) which were reported possess anti-cancer effect in human cervical cancer cells (HeLa), cholangiocarcinoma cells (HuCCA-1), lung carcinoma cells (H69AR), breast cancer cells (T47-D), and leukemic cells (HL-60) (Thongnest *et al*., 2019).

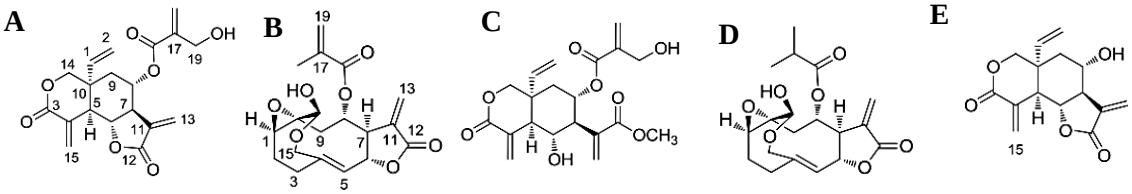

Figure 32. Several sesquiterpene lactones isolated from *V. extensa* purified by HPLC (high-performance liquid chromatography), **a)** vernodalin, **b)** vernolide, **c)** vernodalol, **(d)** vernomygdin, and **(e)** vernolepin (Thongnest *et al*., 2019)

1.2.9.3 Biological activities of *V. extensa*

The bark and stem of *V. extensa* species are used by the local people as a stimulant drink (Ponglux *et al.*, 1992). The genus *Vernonia* from Compositae (Asteraceae family) is harnessed as food, medicinal and industrial uses. *Vernonia amygdalina*, and *Vernonia colorata* as vegetables (Burkill, 1985; Iwu, 1993). Several species of *Vernonia* genus frequently used as ethnomedicine such as *Vernonia amygdalina, Vernonia condensata, Vernonia cineria, Vernonia guineensis*, and *Vernonia conferta*. Moreover, *Vernonia galamensis* is industrially to make an oil originated to its seed (Baye, Kebede, and Belete, 2001). Several genera of *Vernonia* were reported to possess several promising biological activities that were summarized in Table 13. Diverse biological activities that inflicted by Genus of *Vernonia* could lead scientists to explore more further of this promising plant species.

Table 13. Biological activities of several *Vernonia* genus

Vernonia species	**Biological activity**	**Reference(s)**
ambigua	antimalarial	Builders *et al.*, 2011
amygdalina	antidiabetic	Erasto *et al.*, 2009
	antioxidant	Anyasor *et al.*, 2010
	hepatoprotective	Adesanoye and Farombi, 2010
cinerea	immunomodulator	Pratheeshkumar and Kuttan, 2011
	anti-inflammatory	Mazumder *et al.*, 2003
	hepatoprotective	Leelaprakash, Dass and Sivajothi, 2011
cognata	antioxidant	Mota *et al.*, 2011
zeylenica	antinociceptive activity	Ratnasooriya, Deraniyagala and Peiris, 2007
urticifolia	antibacterial	Kiplimo, Everia and Koorbanally, 2011
brasiliana	anti-plasmodial	De Almeida Alves *et al.*, 1997
brasiliana	antibacterial	Kiplimo, Everia and Koorbanally, 2011
colorata	antibacterial	Rabe, Mullholland and Van Staden, 2002
	anti-plasmodial	Chukwujekwu *et al.*, 2009
	antidiabetic	Sy *et al.*, 2005
	anti-inflammatory	Cioffi *et al.*, 2004
guineensis	anti-trypanosomiasis	Tchinda *et al.*, 2002
	antifungal	Donfack *et al.*, 2012
	antimicrobial	

Table 13. Biological activities of several *Vernonia* genus (continued)

Vernonia species	Biological activity	Reference(s)
eremophila	molluscide	Alarcon, Lopes and Herz, 1990
	antibacterial	Lopes, 1991
scorpioides	antibacterial	Kreuger *et al.*, 2011
	anti-plasmodial	Buskuhl *et al.*, 2010
staehelinoides	anti-plasmodial	Pillay *et al.*, 2007
fastigiata	anti-plasmodial	Clarkson *et al.*, 2004
fastigiata	antibacterial	Roos *et al.*, 1998
cumingiana	anti-inflammatory	Liu *et al.*, 2009

1.2.9.4 Anti-cancer activity of *Vernonia* genus

Some evidences showed that the genus of *Vernonia* possibly promising as an anti-cancer such as prostate cancer cell line, PC-3 (9.894 µg/ml) (Lowe *et al.*, 2014); leukemia cell line, HL-60 (10.14 µg/ml), Reh (approximately 10 mg/ml), Nalm6 (approximately 10 mg/ml), K562 (approximately 10 mg/ml), and Molt4 (15 mg/ml) (Lowe *et al.*, 2014; Thomas *et al.*, 2016); colorectal cancer cell line, WiDr (9.902 µg/ml) (Bestari *et al.*, 2018); breast cancer cell line, MCF-7 (12.63 µg/ml), MDA-MB-231 (approximately 50 µg/ml) (Wong *et al.*, 2013; Lowe *et al.*, 2014); glioblastoma cell line, U-87 (48 µg/ml) (Rohin *et al.*, 2017), skin melanoma cell line, HT-144 (3.3 µg/ml) (Farombi and Owoeye, 2011).

1.2.9.5 Anti-cancer effect of the combination *Vernonia* genus

Vernonia genus showed its potency in the combination treatment. Wong and colleagues have explored the combination of *Vernonia amygdalina* with doxorubicin. *Vernonia amygdalina* may increase the inhibition rate of doxorubicin against breast cancer (Wong *et al.*, 2013). Moreover, this species also was investigated its potency as adjuvant treatment of cancer either *in vitro* or *in vivo* together with paclitaxel (Howard *et al.*, 2015). Moreover, a water extract of *Vernonia amygdalina* leaf extract promoted the cytotoxicity of tamoxifen, which reduced 10-fold concentration to inhibit 50% of cell growth (Izevbigie, Opata, and Bryan, 2005).

1.2.10 Anti-cancer effect of the other combination

Several previous studies revealed the capability of the combination treatment as an anti-cancer. One of the popular natural compounds, piperine, a constituent of the *Piper* genus was explored its synergistic effect along with thymoquinone (a phytocompound of *Nigella sativa*) against mice breast cancer cells. Based on the previous results, the combination decreased the proportion of VEGF proteins (Talib, 2017). Piperine also increased the cytotoxicity of paclitaxel against MCF-7 (breast cancer cell lines) (Motiwala and Rangari, 2015).

A combination of turmeric ethanol extract and bevacizumab (VEGF targeted therapy) increased the inhibition of tumor growth. On the other hand, bevacizumab works as an anti-angiogenic to remedy the metastasis cancer phase in breast cancer cell lines (Patel *et al.*, 2008). Another natural compound called by resveratrol had a synergistic effect with other chemotherapeutic drugs such as 5-fluorouracil, etoposide, mitomycin, and oxaliplatin (Redondo-Blanco *et al.*, 2017).

A study using the combination of *Rauwolfia vomitoria* and carboplatin also performed by Yu and colleagues. Combining of *Rauwolfia vomitoria* and carboplatin remarkably reduced the tumor up to 87%-90% (Yu *et al.*, 2013). A pure natural compound isolated from *Stephania tetrandra,* tetrandrine, was explored by Sun and Wink in 2014. According to the study, tetrandrine with doxorubicin showed a highly synergic effect in multidrug-resistant CACO-2 cells, which indicated by a down-regulating P-glycoprotein expression (Sun and Wink, 2014).

1.3 Objectives of the study

The main objectives of this study are as follows:

1. To investigate the anti-cancer effect of each plant crude extract on breast cancer (MCF-7 and MDA-MB-231), colorectal cancer (HT-29 and SW-620), ovarian cancer (SKOV-3 and A2780) and non-malignancy cell lines (Vero and L-929) using MTT assay.

2. To investigate an anti-cancer effect of the combination effect among selected plant crude extracts and PFPE on the selected cell lines using the MTT assay.

3. To investigate the potency of combination of selected plant crude extract with PFPE in Apoptosis and Multi-caspase activities on the selected cancer cell lines using Annexin-V/FITC and Multi-caspase assay.

CHAPTER 2
RESEARCH METHODOLOGY

2.1 Methods

Part I. Investigation of anti-cancer effect of *A. paniculata, Z. spina-christi,* and *V. extensa* leaves extracts on several cell lines

1. Plant materials and extract preparation

Two species of plants, *A. paniculata* and *Z. spina-christi* were harvested from Indonesia and identified by Assistant Professor Dr. Nurainas (chief of ANDA Herbarium, Department of Biology, Andalas University, Indonesia) with letter no. 305/K-ID/ANDA/IX/2018. Meanwhile, *V. extensa* leaves were harvested from Phatthalung Province, Thailand. *A. paniculata, Z. spina-christi,* and *V. extensa* leaves were grounded into small pieces. Thereafter, the grounded leaves were extracted by two extraction ways including of maceration and decoction.

1.1 Maceration

Maceration is an extraction process by soaking the natural sources such as leaves, stems, and barks in the organic solvent. Due to the phytocompounds are separated among their polarities. The five types of organic solvents were discriminated by the polarities such as high polarity (methanol), medium polarity (ethanol), low polarity (dichloromethane and ethyl acetate), and non-polarity (hexane). Then, the leaves were weighed and soaked in organic solvents, with grounded leaves and organic solvents weight and volume as much as 3 g and 300 ml (ratio 1:100). Subsequently, the grounds plants in organic solvent incubated within 8 h in a shaking incubator for 120 rpm at 35^{o}C and allowed in dark area within overnight. After the macerating process, the residue was filtered using a filter paper (Whatman No.1). Afterwards, the solvent was separated using a vacuum rotary evaporator at 40-45^{o}C, 1-3 mbar of vacuum pressure, and 40 rpm (rotation per min) of rotary until the residue formed. Finally, all crude extract was kept as stock. The stock was diluted by dimethyl sulfoxide (DMSO) to obtain the initial concentration (80 mg/ml). The characteristics of crude extracts were described in Table 14 below:

Table 14. Properties of used crude extracts

Plant	Extract	Textures	Colors	Percentage yield (%)
Andrographis paniculata	Methanol	Oily paste	Dark green	6.94
	Ethanol	Oily paste	Dark green	7.90
	Dichloromethane	Powder	Dark green	4.51
	Ethyl acetate	Oily paste	Dark green	4.53
	Hexane	Oily paste	Light green	0.53
Ziziphus spina-christi	Methanol	Oily paste	Dark brown	3.88
	Ethanol	Oily paste	Dark brown	4.18
	Dichloromethane	Oily paste	Dark brown	1.44
	Ethyl acetate	Oily paste	Dark brown	2.23
	Hexane	Oily paste	Yellowish	0.65
Vernonia extensa	Methanol	Oily paste	Dark green	8.50
	Ethanol	Oily paste	Dark green	9.75
	Dichloromethane	Oily paste	Dark green	5.31
	Ethyl acetate	Oily paste	Dark green	4.72
	Hexane	Oily paste	Green	1.27

1.2 Decoction and lyophilization

Decoction is an extraction process by soaking the natural sources in boiled water. Grounded leaves (3 g) were soaked in the boiled water (300 ml) within 20 min and allowed in the room temperature. The boiled water extracts have been lyophilized to obtain the certain mass of extract and mentioned as a freeze-dried extract stock. Before using, the stock was diluted by dimethyl sulfoxide (DMSO) to obtain the initial concentration (80 mg/ml).

2. Gas Chromatography-Mass Spectrometer

The Gas Chromatography-Mass Spectrometry (GC-MS) analysis was performed to determine the chemical constituents composed the extracts which showed highest cytotoxic extract. In this analysis, the dichloromethane extract of *A. paniculata*, *Z. spina-christi*, and *V. extensa* were screened in a Gas-Chromatography-Agilent 7890B combining with an Agilent 5977A triple quadrupole mass spectrometer (Agilent Technologies Inc, USA). The input temperature of 280^{o}C with the partition ratio 7:1

was harnessed, and the helium was carried out as the carrier gas at in constantly flow rate of 7 ml/min. The oven temperature was settled at 60^{o}C for 5 min at the onset, and increase at a rate of 5^{o}C/min to 315^{o}C for 15 min. Afterwards, the mass spectrometer which was using electron ionization mode in energy of 70 eV, ion source temperature of 230^{o}C, and scan mass range m/z 35-500. The chemical compounds were identified refers to its correlation of the noted fragmentation scheme of mass spectra that set up in the GC-MS system software version Wiley10 and NIST14. The analysis procedures were conducted at Scientific Equipment Center, Prince of Songkla University. The chemical structure was created by ACD ChemSketch.

3. Cell lines

Six cancer cell lines were used in this investigation, including breast cancer cell lines (MCF-7 and MDA-MB-231), colorectal cancer (HT-29 and SW-620), ovarian cancer (A2780 and SKOV-3) and non-cancerous (Vero and L-929) cell lines. The MCF-7, MDA-MB-231, SKOV-3, and Vero cell lines were purchased from American Type Culture Collection (Manassas, VA, USA) (Cat No: ATCC®HTB-22, ATCC®HTB-26, ATCC®HTB-77, and ATCC®CCL-81). A2780 cell lines were purchased from ADDEXBIO (San Diego, CA, USA) (Cat No: C0017002). The HT-29 cell lines were kindly provided by Associate Professor Dr. Ruedeekorn Wiwattanapatapee (Department of Pharmaceutical Technology, Faculty of Pharmaceutical Sciences, Prince of Songkla University). Meanwhile, the SW-620 cell lines were provided by Associate Professor Dr. Surasak Sangkhathat, M.D (Department of Surgery, Faculty of Medicine, Prince of Songkla University). L-929 cell lines were kindly provided by Associate Professor Dr. Jasadee Kaewsichan (Department of Pharmaceutical Chemistry, Faculty of Pharmaceutical Sciences, Prince of Songkla University). The characters of used cell lines were described briefly in Table 15.

3.1 Preparation of cell culture medium

Either RPMI-1640 or DMEM medium were liquefied in 800 ml of deionized water. Subsequently, $NaHCO_3$ was added, 2 g for RPMI and 3.7 g for DMEM, and adjusted pH value to 7.4 with 1N HCl. After that, deionized water was added until the final volume to 1 L. The medium was utterly supplemented with 10% fetal bovine

serum, 1% L-Glutamine (200 mM, 100X) and 1% penicillin/streptomycin (10,000 U/ml of penicillin, 10,000 µg/ml streptomycin). The medium was filtered aseptically using a 0.22 micro Millipore in a laminar flow hood. After filtration, the medium was aliquoted into a proper volume of the bottle and stored nicely at 4^{o}C. To ensure the medium is safe to be used, 5 microliters of medium were poured out and cultured in a 60 mm cell culture dish in an incubator at 37^{o}C within 5 days.

3.2 Cell culture condition

The cells were maintained in a 10 cm culture dish with either RPMI-1640 or DMEM which were supplemented with 10% fetal bovine serum, 1% penicillin/streptomycin, and 1% L-Glutamine. Vero, A2780, and SKOV-3 cell lines were grown in the RPMI-1640 culture medium. HT-29, SW-620, MDA-MB-231, and L-929 cell lines were cultured in DMEM. All cell cultures were incubated in cell incubator at 37^{o}C in 5% CO_2 and 80-90% humidity. When the cell confluence was up to approximately 80%, the cell would be propagated for the next passage and seeded for the experiment.

3.3 Cell propagating and seeding

Firstly, the culture medium was taken off from dish and cells were rinsed with 10 ml of 1X PBS. Cells were harvested with 1 ml of 0.25% (w/v) Trypsin-0.53 mM EDTA and kept in an incubator for 2-3 min to ensure the trypsin completely digested by the cells. Afterward, 9 ml of complete cell medium were poured in a new cell culture dish, and 1 ml of cell suspension was resuspended by smoothly pipetting up and down. In the end of the process, the proper cell suspension was transferred to a new cell culture dish.

4. Cell treatment

In purpose to investigate the anti-cancer effects of *A. paniculata, Z. spina-christi*, and *V. extensa* in cancer cell lines. The initial concentration of stock solutions (80 mg/ml) was diluted to be 1, 2, 4, 8, 16 mg/ml as a stock solution. Before treatment, cells were seeded with a density of 20,000 cells/well (for MCF-7, MDA-MB-231, SW-620, HT-29, and SKOV-3 cell lines) and 15,000 cells/well (for A2780,

Vero, and L-929 cell lines) in 96 well plates then allowed a night period for adhering. The cell medium was combined with plant extracts to retrieve the final concentration at 5, 10, 20, 40, and 80 µg/ml of extract concentration and incubated to the cell lines within 72 h. Additionally, to ensure DMSO (0.5%) only used as a vehicle and no induces cytotoxic effect to cancer cell lines, cell medium combined with DMSO was added in the experiment.

5. Anti-cancer effect of *A. paniculata, Z. spina-christi,* and *V. extensa* against cancer cell lines by MTT assay

The anti-cancer effect of *A. paniculata, Z. spina-christi* and *V. extensa* leaves extracts was assessed by 3-(4,5-dimethylthiazol-2-yl)-2,5-diphenyltetrazolium bromide (MTT) assay. This evaluation method was exhibited whether mitochondria succinate dehydrogenases enzymes in the living cells are active (Mosmann, 1983). After overnight sub-culture, the cells were rinsed in 1X PBS and treated by the extracts at 5, 10, 20, 40, and 80 µg/ml within 72 h. Subsequently, the treatments were removed, and the cells were rinsed with 1X PBS. After that, the cells were stained by 100 µl MTT for 30 min and then dissolved by 100 µl of DMSO to achieve the formazan salt which indicated by purple colors. Eventually, the color formation was detected using a microtiter plate reader at 570 nm and 650 nm. Concentration for all treatments was analyzed to procure the IC_{50} values by the formula below.

$$\% \text{ Survival} = \left[\frac{\text{Absorbance } 570\text{sample} - \text{Absorbance } 650\text{sample}}{\text{Absorbance } 570\text{control} - \text{Absorbance } 650\text{control}}\right]$$

6. Statistical analysis

Anti-cancer study was conducted in three independents for median inhibition concentration (IC_{50}) and the IC_{50} values were expressed as the mean ± SD.

Table 15. Summary cell lines characterization

Cell lines	Origin	Source	Histology	Type	Subtype/ Dukes stage	Reference(s)
MCF-7	Mammary gland, breast; metastatic site derivative	*Homo sapiens* (human)	Adenocarcinoma	IDC	LA	Subik *et al.*, 2010 American Type Culture Collection, 2014
MDA-MB-231	Mammary gland, breast; metastatic site derivative	*Homo sapiens* (human)	Adenocarcinoma	AC	TNB	
HT-29	Colon	*Homo sapiens* (human)	Adenocarcinoma	ND	B	American Type Culture Collection, 2014 Ehrig *et al.*, 2013
SW-620	Colon; metastatic site derivative: lymph node	*Homo sapiens* (human)	Adenocarcinoma	ND	C	
A2780	Ovary	*Homo sapiens* (human)	Adenocarcinoma	EOC	ENOCa	Anglesio *et al.*, 2013
SKOV-3	Ovary: ascites	*Homo sapiens* (human)	Adenocarcinoma	EOC	HGSC	
Vero	African green monkey kidney cells	*Cercophitecus aethiops*	Fibroblast-like	E	ND	American Type Culture Collection, 2014
L-929	Connective tissue	*Mus musculus*/Mouse C3H	Fibroblast-like	E	ND	

IDC: invasive ductal carcinoma; AC: adenocarcinoma; LA: luminal A; TNB: triple-negative B; B: dukes stage b; C: dukes stage c; ENOCa: endometrioid carcinoma; HGSC: high-grade serous carcinoma; ND: not determined; E: epithelial-like

Part II. Investigation of anti-cancer effect of combination among selected extract with PFPE on selected cancer cell lines

1. PFPE extraction

Black peppercorns *Piper nigrum* were gathered from Songkhla province, Thailand. The plant specimen with voucher specimen number as SKP 146161401. This plant specimen was deposited in the Southern Centre of Thai Traditional Medicine, Department of Pharmacognosy and Pharmaceutical Botany, Prince of Songkla University, Thailand. The preparation of PFPE was constructed by maceration process, continued by soaked and shaken gently the 250 g peppercorns in 300 mL of dichloromethane at 35^{o}C within 3 h. Thereafter, the peppercorns were filtered by Whatman filter paper No.1. The solvent was separated by using rotary evaporator. The oily residue (dark brown color) was obtained and recrystallized with cold diethyl ether and the yellow crystals mentioned as piperine. Eventually, the stock was diluted by dimethyl sulfoxide (DMSO) to obtain the initial concentration (80 mg/ml).

2. Anti-cancer effect of combination dichloromethane extract of *A. paniculata*/*Z. spina-christi*/*V. extensa* and PFPE against cancer cell lines by MTT assay

After determining IC_{50}, a further analysis was conducted using IC_{50} of the highest cytotoxic extract of each plant and combined with IC_{50} of PFPE on the certain cell lines. This experiment was conducted out to investigate the anti-cancer effects of the combination among selected extracts with PFPE. This study was designed as in four ratios, including IC_{50} extract : IC_{50} PFPE, 0.5 IC_{50} extract : IC_{50} PFPE, IC_{50} extract : 0.5 IC_{50} PFPE, and 0.5 IC_{50} extract : 0.5 IC_{50} PFPE.

3. Calculation of the combination index (CI)

The CI was appraised from dose-effect data, both single and combined drug treatments. Chou and Talalay described the synergistic effect by the value of CI, CI less than 1 is synergism (CI < 1); CI = 1 indicates additive effect; and CI > 1 indicates antagonism (Chou, 2010). The CI values were computerized by *CompuSyn* software (downloaded from www.combosyn.com). The combination index of combined drug treatment is defined as the equation below:

$$CI = DRI_1 + DRI_2 \qquad \text{[Eq 1]}$$

$$CI = \frac{D1}{Dx1} + \frac{D2}{Dx2} \qquad \text{[Eq 2]}$$

DRI_1 and *DRI_2* are the doses reduction of compound 1 and compound 2, respectively. *D1* and *D2* are the combination of doses among treatment *1* and treatment *2*. *Dx1* and *Dx2* each is the dose of treatment with only treatment 1 and treatment 2 that will give the same effect as the combination, respectively. The dose of *Dx1* and *Dx2* require to be estimated from the dose-effect data of single-drug treatments (Chou, 2010).

Part III. Investigation potency of selected plant extract with PFPE in apoptosis and multi-caspase on the selected cancer cell lines

1. Annexin V/PI apoptosis assay

This study was performed to investigate whether the extracts induce apoptosis towards breast cancer cells. Due to the combination of dichloromethane extract of *V. extensa* and PFPE showed considerable anti-cancer activity, hence this combination was observed its apoptotic effect against MCF-7 cell lines. The MCF-7 cell lines were seeded into 12-well plates at a density of $2x10^5$ cells/well within overnight. After that, the cells were treated by the combination of dichloromethane extract of *V. extensa* and PFPE (ratio IC_{50}:IC_{50}) for 0, 24, 48, 72, and 96 h. The cells were collected and resuspended in 1X PBS. The cell pellets were harvested, 100 µl of Annexin V-FITC and 100 µl of PI (Catalog No. MCH100105) dry were added to the cell pellets and incubated at room temperature for 30 min. The fluorescent signals of Annexin V-FITC and PI were analyzed promptly using the Muse® Cell Analyzer (Merck Millipore, Germany).

2. Multi-caspase assay

This study was performed to investigate whether the extracts could be triggering the caspases proteins in breast cancer cells. Due to the combination of dichloromethane extract of *V. extensa* leaves and PFPE showed considerable anti-cancer activity, hence this combination was observed its effect of caspase inducing by multi-caspase assay in MCF-7 cell lines. The MCF-7 cell lines were seeded into 12-

well plates at a density of $2x10^5$ cells/well within overnight. Then the cells were incubated by the combination of dichloromethane extract of *V. extensa* leaves and PFPE (ratio IC_{50}:IC_{50}) within 0, 24, 48, 72, and 96 h, separately. Then, treated cells were harvested entirely and resuspended in 1X PBS. The cell pellets were harvested and incubated in 5 µl of Muse® Multi-caspase assay within 30 min and 150 µl of 7-AAD (Catalog No. MCH100109) for 15 min. The fluorescent signals of Multi-caspase and 7-AAD were completely determined by the Muse® Cell Analyzer (Merck Millipore, Germany).

3. Statistical analysis

The apoptosis and multi-caspase assay study were established at least two independents to obtain the average and standard deviation (SD). A $P < 0.05$ was considered as statistically significant. All results were represented as the mean ± standard deviation (SD).

2.2 Materials

2.2.1 Chemicals, reagents, and equipments

This study was using chemical substances and reagents, which were purchased from an assured and standardized company, as described in Table 16. Furthermore, the chemical substances and equipment utilized in this study were displayed in Table 17.

Table 16. The chemical substances, reagents, and materials used in the study

Specific Items	Manufactory	Cat. No.
Chemical Reagent		
Sodium chloride (NaCl)	Omnipur®	7710-500gm
Sodium Phosphate Dibasic Anhydrous (Na_2HPO_4)	Amresco®	0404-1KGS
Potassium Chloride (KCl)		0395-500G
Potassium Phosphate (KH_2PO_4)		0781-500G
Dimethyl Sulfoxide (C_2H_6OS)		0231-500ML
Ethanol (C_2H_5OH)	J. T. Baker®	8006-32-2.5L
Methanol (CH_3OH)		9070-03-4L
Methylene Chloride (CH_2Cl_2)		9324-03-4L
Ethyl Acetate ($C_4H_8O_2$)		9280-03-4L
Acetone (C_3H_6O)		9006-03-4L
Hexane (C_6H_{14})	RCI Lab scan Ltd	AR10904L
RPMI-1640 complete medium powder	Gibco™	31800022
DMEM complete medium powder		12100046
Trypsin		25200056
Antibiotic (Penicillin-Streptomycin 5,000 U/ml)		15070063
L-Glutamine 200 mM		LS25030081
Fetal Bovine Serum		16000036
MTT reagent	GibThai	M6494
Multi-caspase reagent	Muse®	MCH100109
Apoptosis reagent		MCH100105
Materials		
Filter paper 3mm	Whatman®	1001-090
pH indicator test strip	Merck	1095350001
Cellulose acetate membrane filter	Sartorius®	1107

Table 17. The used equipments in the study

Specific Items	Manufactory
ESCO class II biosafety cabinet	Esco
Olympus CKX53 inverted microscope	Olympus
Spectra Emax® Plus microplate reader	Molecular Devices
Olympus microscope digital camera (DPT2 IX71)	Olympus
CO_2 incubator	Shel Lab
Vortex-2 Genie	Scientific Industries
Vacuum-Rotavapor set	Buchi Rotary Evaporators
Auto pipette 10 µL, 100 µL, 200 µL, and 1,000 µL	Gilson
Auto pipette 5,000 µL	Eppendorf
Centrifuge 5420	
Muse® Cell analyzer	Merck Millipore
Liquid Nitrogen Tank	Thermo scientific
Autoclave HVE-50	Hirayama

CHAPTER 3
RESULTS

Part I. Anti-cancer effect of *A. paniculata*, *Z. spina-christi*, and *V. extensa* leaves extracts on several cell lines

1. Cytotoxic activity of different plant extracts on several cell lines by MTT assay

A study about the cytotoxic activity was carried out to investigate the anti-cancer effect of *A. paniculata*, *Z. spina-christi* and *V. extensa* leaves on several cancerous cell lines, through MTT assay. Theoretically, the MTT assay measures the viability cells through the mitochondrial dehydrogenase. Cells were incubated by various concentration (5-80 µg/ml) of crude extracts within 72 h. The IC_{50} values of each extract was highlighted as the anti-cancer activity of the extract (Fig 33-35). The highest cytotoxic extracts were indicated by IC_{50} less than 20 µg/ml (Sriwiriyajan *et al*., 2014) and used in the further analysis including of the combination treatment.

1.1 Cytotoxic activity of *A. paniculata* leaves different extracts on several cell lines by MTT assay

A. paniculata leaves were found possess cytotoxicity to cancer cell lines. According to Figure 33, the dichloromethane extract of *A. paniculata* leaves (abbreviated as DEAP) indicated the strongest cytotoxic effect against HT-29 and SW-620 cells indicated at an IC_{50} of 8.93 ± 0.52 µg/ml and 7.49 ± 0.04 µg/ml, respectively. Moreover, the ovarian cancer cell lines (A2780) gave a high respond when exposed by DEAP. As a representative of normal cells, L929 and Vero cells were used in this investigation. Moreover, DEAP indicated less cytotoxicity in Vero and L-929 cell lines. Other extracts, methanolic and ethyl acetic extracts of *A. paniculata* leaves (abbreviated as MEAP and EAAP) indicated high cytotoxicity on SKOV-3 and SW-620 cells proven by an IC_{50} 7.60 ± 0.72 µg/ml and 10.31 ± 0.32 µg/ml, respectively. On the other hand, hexane extract of *A. paniculata* (HEAP) showed low cytotoxicity to MCF-7, SW-620, and A2780, at an IC_{50} of 47.46 ± 0.93 µg/ml, 39.40 ± 0.42 µg/ml, and 34.27 ± 2.31 µg/ml, respectively. However, freeze dried extract of *A. paniculata* (FDAP) did not show any cytotoxic activity to all cell lines.

1.2 Cytotoxic activity of *Z. spina-christi* leaves different extracts on several cell lines by MTT assay

The cytotoxic screening of different extracts of *Z. spina-christi* or Sedr leaves was conducted against cancer cell lines. According to Figure 34, the dichloromethane extract of *Z. spina-christi* leaves (abbreviated as DEZSC) demonstrated a highly cytotoxic effect toward MCF-7 and A2780 cell lines, indicated by an IC_{50} of 13.35 ± 0.30 µg/ml and 14.64 ± 1.51 µg/ml, respectively. Surprisingly, DEZSC showed less cytotoxicity towards Vero and L929 cell lines at IC_{50} values of 21.05 ± 0.18 µg/ml and 47.03 ± 2.91 µg/ml, respectively. Another result showed that the methanol extract of *Z. spina-christi* leaves (abbreviated as MEZSC) indicated a high cytotoxicity to A2780 cells at an IC_{50} of 18.54 ± 2.33 µg/ml. Meanwhile, freeze dried and hexane extracts did not show any cytotoxicity to cancer cell lines.

1.3 Cytotoxic activity of *V. extensa* leaves different extracts on several cell lines by MTT assay

A bitter leaf tree, taxonomically named as *V. extensa* is an endemic *Vernonia* species widely grown in Northern Thailand. The dichloromethane extract of *V. extensa* leaves (DEVE) showed remarkable cytotoxicity against A2780 and MCF-7 cell lines at an IC_{50} values of 10.08 ± 0.04 µg/ml and 15.58 ± 1.81 µg/ml, respectively. Other extracts including ethyl acetic and ethanolic extracts of *V. extensa* leaves (abbreviated as EAVE and EEVE) gave significant cytotoxic activity to A2780 and SW-620 with IC_{50} values at 15.22 ± 0.58 µg/ml and 17.03 ± 0.09 µg/ml, respectively (Figure 35). Meanwhile, freeze dried and hexane extracts did not show any cytotoxicity to cancer cell lines. As a positive reference drug, doxorubicin showed strong cytotoxicity to all cancerous cell lines and normal cell lines.

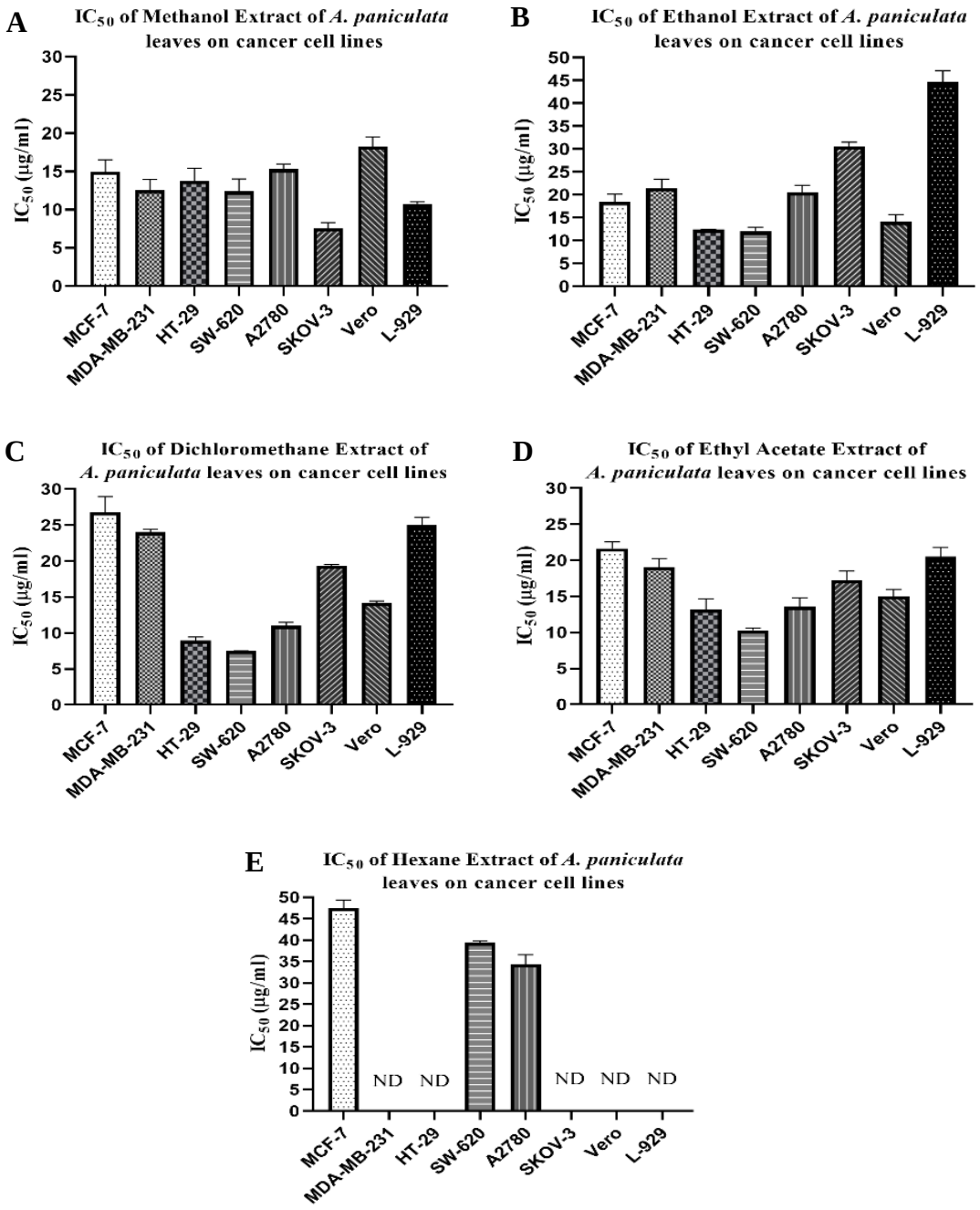

Figure 33. Inhibitory concentration to inhibit behalf population of cell lines (IC_{50}) (µg/ml) mean ± SD of *A. paniculata* leaves extract against several cancer cell lines including **a)** methanol extract, **b)** ethanol extract, **c)** dichloromethane extract, **d)** ethyl acetate extract, and **e)** hexane extract. ND: not inhibited

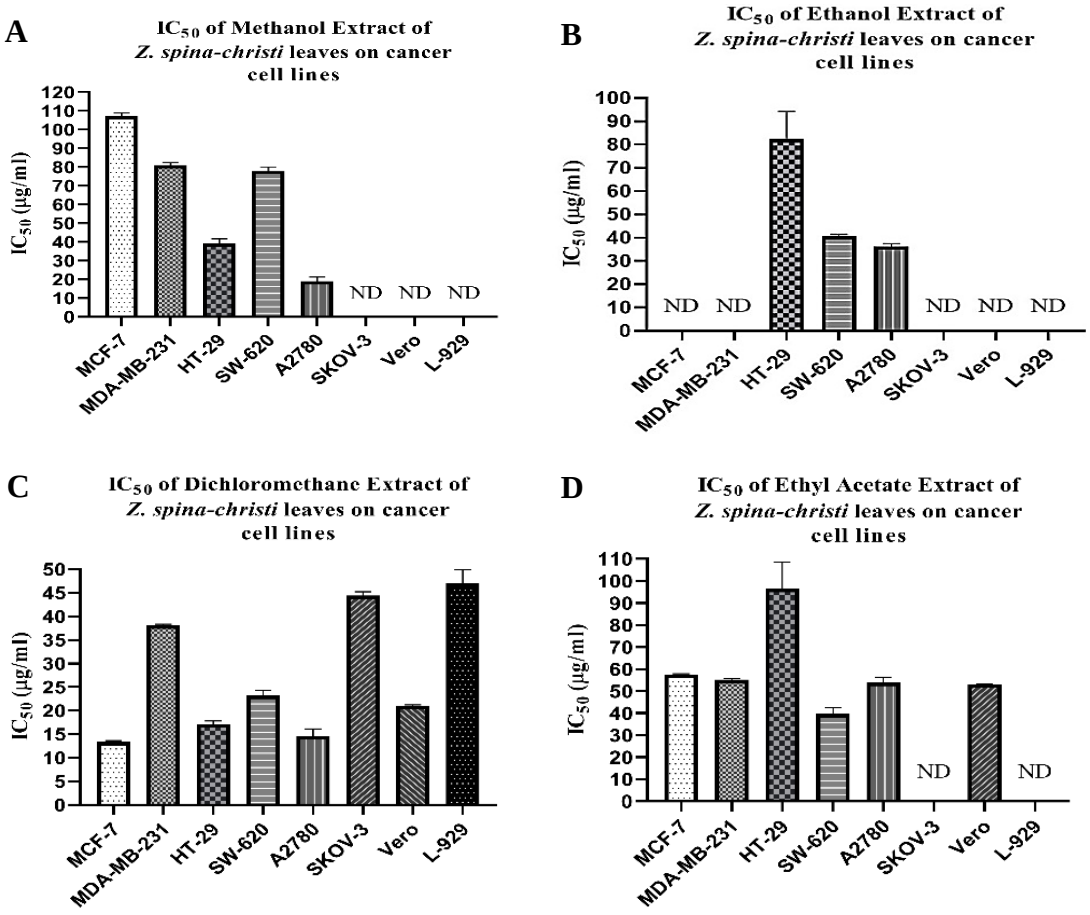

Figure 34. Inhibitory concentration to inhibit behalf population of cell lines (IC_{50}) (µg/ml) mean ± SD of *Z. spina-christi* leaves extract against several cancer cell lines including **a)** methanol extract, **b)** ethanol extract, **c)** dichloromethane extract, and **d)** ethyl acetate extract. ND: not inhibited

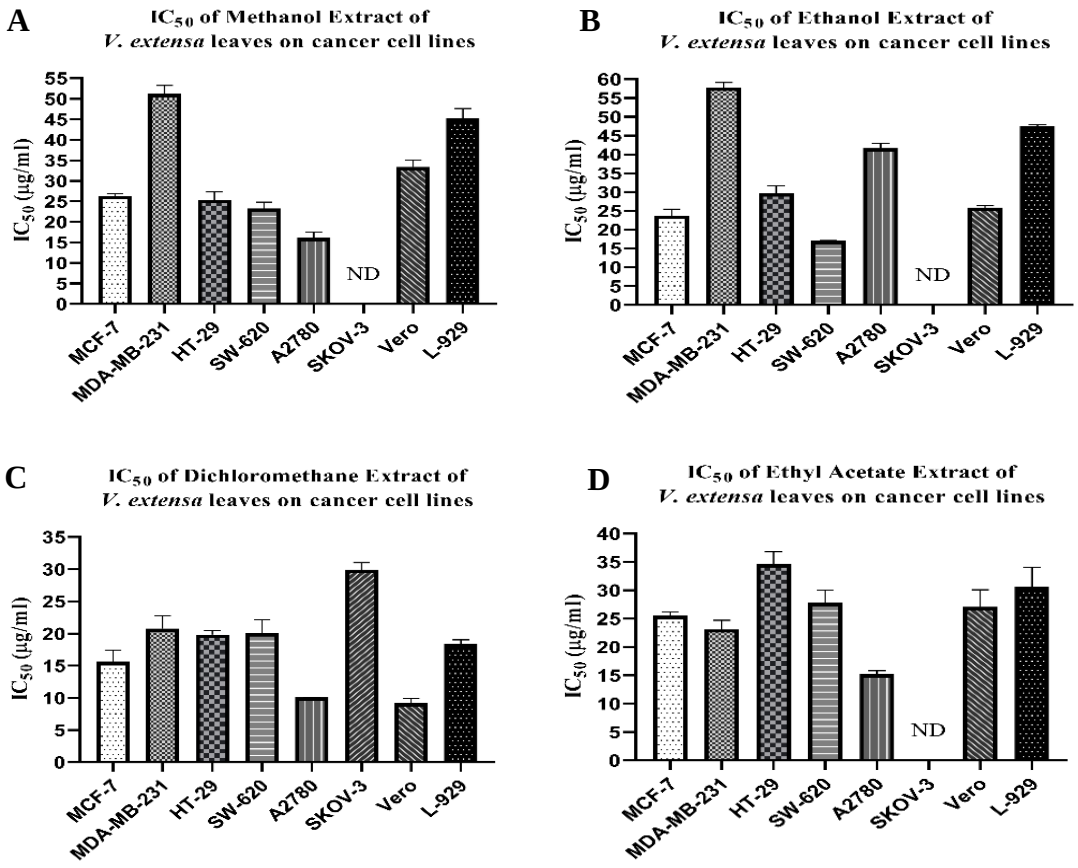

Figure 35. Inhibitory concentration to inhibit behalf population of cell lines (IC_{50}) (µg/ml) mean ± SD of *V. extensa* leaves extract against several cancer cell lines including **a)** methanol extract, **b)** ethanol extract, **c)** dichloromethane extract, and **d)** ethyl acetate extract. ND: not inhibited

2. Phytocompounds screening by GC-MS analysis

Gas Chromatography-Mass Spectrometry (GC-MS) analysis was performed qualitatively to investigate the present bioactive compounds of extracts. This investigation was harnessing the dichloromethane extract of *A. paniculata*, *Z. spina-christi,* and *V. extensa* leaves extracts due to these extracts included to the category which showed IC_{50} less than 20 μg/ml and less toxic to non-cancerous cell lines. Hence, the GC-MS analysis was carried out to determine which compounds contained in the strongest cytotoxic activity in cancerous cell lines. All phytocompounds were briefly classified and then reviewed based on their biological activities and mechanisms as shown in Table 18-23. Moreover, Table 24 describes the comparison among phytochemical compounds of each plant extracts to distinguish the expected mechanisms exerted by each extract.

2.1 Phytocompounds of dichloromethane extract of *A. paniculata* leaves

GC-MS technique was exploited to reveal the phytocompounds of dichloromethane extract of *A. paniculata* leaves. DEAP was observed and compounds were separated to ten groups such as steroids (four compounds), hydrocarbons (three compounds), alcohols (two compounds), aldehydes (two compounds), fatty acids (one compound), terpenes (two compounds), phthalates (one compound), tocopherols (one compound), and carboxylic acids ester (one compound). Majorly, the dichloromethane extract of *A. paniculata* leaves contains 1-heptatriacotanol (60.29%, alcohol group) and androsta-1,4-dien-3-one,6,17-dihydroxy-,(6β,17β) (32.27%, steroid group) (Figure 36, Table 18, and Table 21).

2.2 Phytocompounds of dichloromethane extract of *Z. spina-christi* leaves

GC-MS technique was exploited to reveal the phytocompounds of dichloromethane extract of *Z. spina-christi* leaves. DEZSC was observed and compounds were separated to nine groups such as fatty acids (five compounds), terpenes (five compounds), steroids (five compounds), tocopherols (four compounds), fatty alcohols (two compounds), phthalates (one compound), and furan alkanes (one compound). The dichloromethane extract of *Z. spina-christi* leaves majorly contains palmitic acid (26.92%, fatty acids group), linolenic acid (11.22%, fatty acids group),

neophytadiene (7.91%, terpenes), linoleic acid (6.76%, fatty acids group), n-tetracosanol-1 (6.07%, fatty alcohols group), octacosanol (5.25%, fatty alcohols group), and stigmast-5-en-3-ol (5.24%, steroids group) (Figure 37, Table 19, and Table 22).

2.3 Phytocompounds of dichloromethane extract of *V. extensa* leaves

GC-MS technique was exploited to reveal the phytocompounds of dichloromethane extract of *V. extensa* leaves. DEVE was observed and compounds were separated to 16 groups such as hydrocarbons (six compounds), terpenes (five compounds), fatty acids (three compounds), benzofurans (two compounds), steroids (one compound), tocopherols (one compound), benzoic acid esters (one compound), benzenoids (one compound), phenylpropanes (one compound), fatty alcohols (one compound), ketones (one compound), aldehydes (one compound), alkaloids (one compound), fatty acids ester (one compound), and carboxylic acid (one compound). The dichloromethane extract of *V. extensa* leaves majorly contains palmitic acid (21.40%, fatty acids group), neophytadiene (19.36%, terpenes group), phytol (13.36%, terpenes group), linolenic acid (12.08%, fatty acids group), linoleic acid (6.70%, fatty acids group), hentriacontane (5.41%, alkanes group), and stigmasterol (5.34%, steroids group) (Figure 38, Table 20, and Table 23).

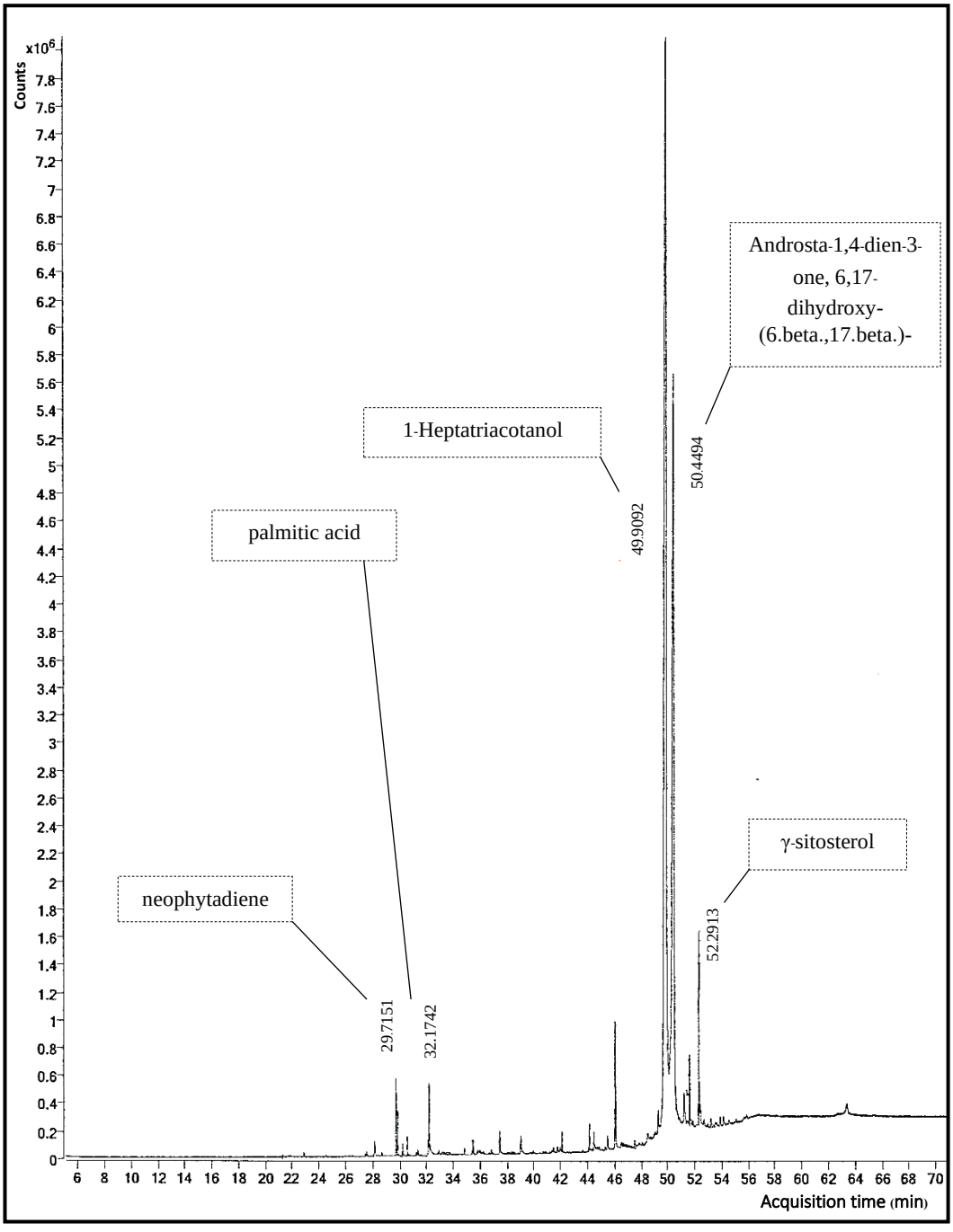

Figure 36. GC-MS chromatogram of DEAP

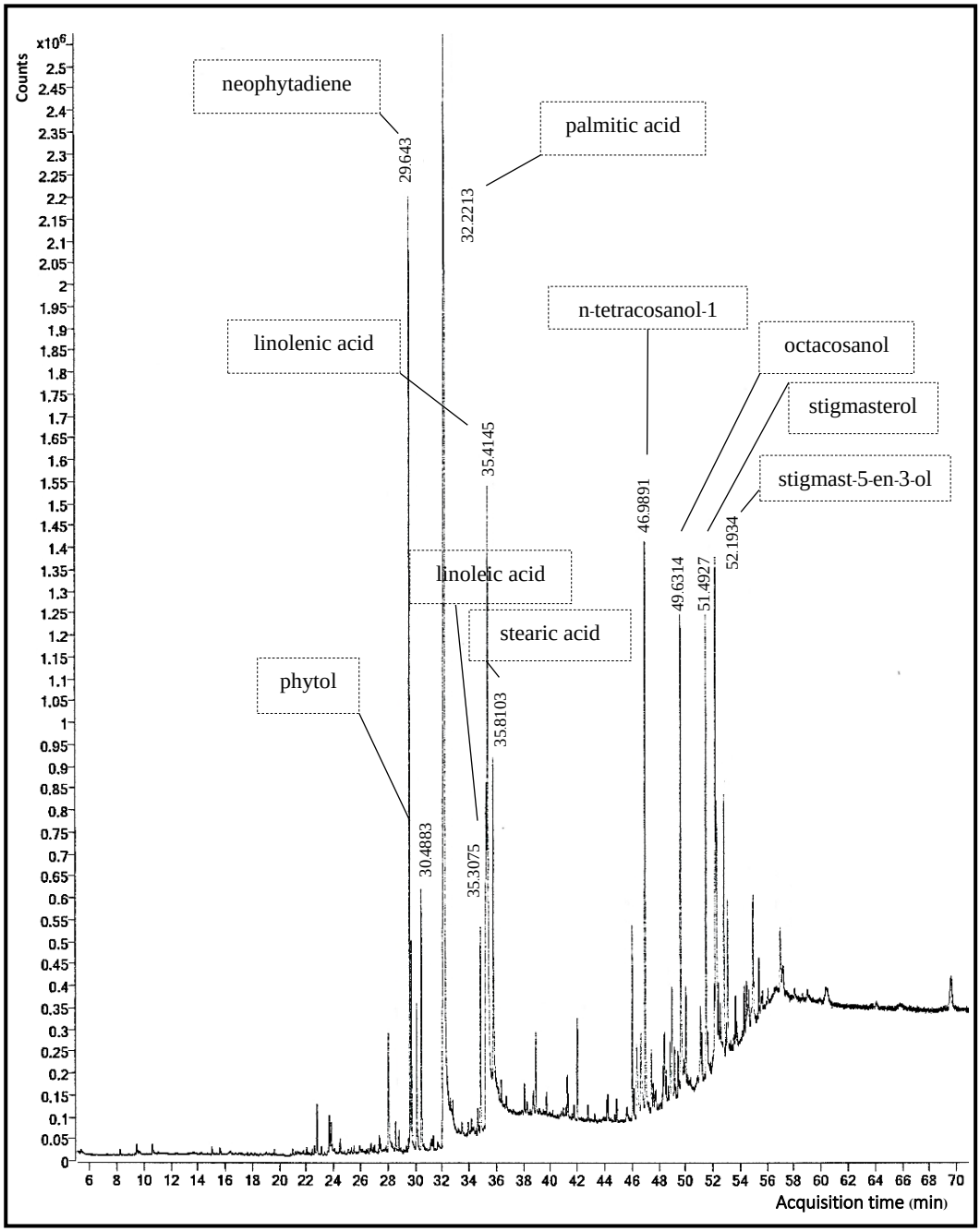

Figure 37. GC-MS chromatogram of DEZSC

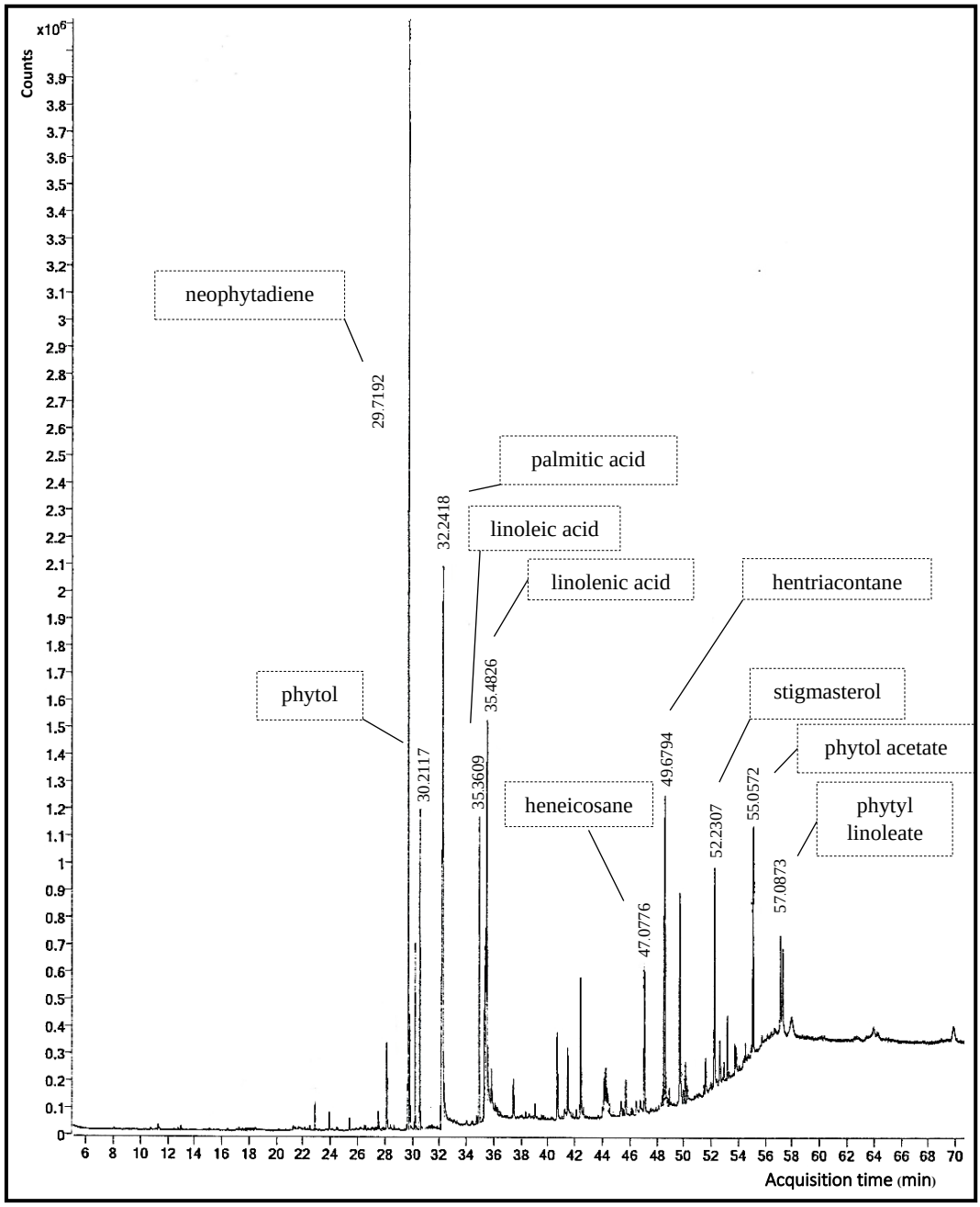

Figure 38. GC-MS chromatogram of DEVE

Table 18. Phytochemical compounds contained in DEAP using GC-MS analysis according to the retention time

S/No.	RT	Compound Name	Structure	Formula	MW (g/mol)	Component Area	Total peak area	Estimated Conc. (%)	Activity
1	17.34	Furfuryl alcohol	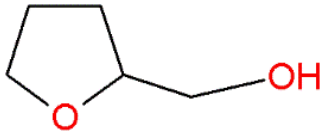	$C_5H_{10}O_2$	102.13	12134.3	147043139.1	0.01	Antioxidant (Wei *et al.*, 2010), Antimicrobial on *Salmonella typhimurium* (Monien *et al.*, 2011)
2	21.27	Octadecane	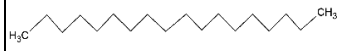	$C_{18}H_{38}$	254.5	27454	147043139.1	0.02	Antioxidant (Morah and Uduagwu, 2017), Anti-cancer on PC-3 cells (Ryu *et al.*, 2012)
3	29.71	Neophytadiene	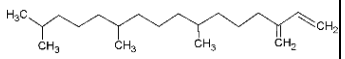	$C_{20}H_{38}$	278.5	1765632	147043139.1	1.20	Anti-cancer on MCF-7 and HeLa cells (Eswaraiah *et al.*, 2019), Anti-inflammatory (Carretero *et al.*, 2008), Antioxidant , Antimicrobial on *E. Coli, S. Aureus, C. Albicans, and A. Niger* (Mendiola *et al.*, 2008)
4	29.83	6,10,14-trimethyl pentadecane-2-one	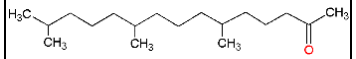	$C_{18}H_{36}O$	268.5	781103.2	147043139.1	0.53	Antimicrobial on *Y. Pseudotuberculosis, E. Faecalis* and *S. Aureus* (Yayli *et al.*, 2006)
5	31.23	2-Methyltetradecanal	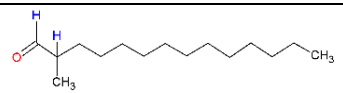	$C_{15}H_{30}O$	226.4	46180.7	147043139.1	0.03	No activity reported

Table 18. Phytochemical compounds contained in DEAP using GC-MS analysis according to the retention time (continued)

S/No.	RT	Compound Name	Structure	Formula	MW (g/mol)	Component Area	Total peak area	Estimated Conc. (%)	Activity
6	32.17	Palmitic acid		$C_{16}H_{32}O_2$	256.42	1825402.4	147043139.1	1.24	Anti-cancer on HCT-116 cells and showed high affinity interaction on DNA topoisomerase-I (Ravi and Krishnan, 2016), Antifungal on *B. Cereus* (Idowu and Ojo, 2017), Antioxidant on increasing DPPH free radical scavenging (Shah and Iqbal, 2018)
7	33.30	2-octylacolein	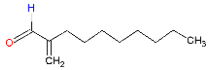	$C_{11}H_{20}O$	168.28	17227.5	147043139.1	0.01	No activity reported
8	34.74	3,7-Dimethyl-2,3-epoxyoctanal	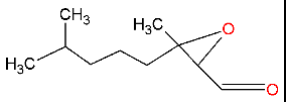	$C_{10}H_{18}O_2$	170.25	20863.2	147043139.1	0.01	No activity reported
9	38.15	Tricosane		$C_{23}H_{48}$	324.6	45075.5	147043139.1	0.03	Anti-cancer on HepG2 and MDA-MB-231 cells (Poma *et al.*, 2018), Antimicrobial on *S. Aureus*, *M. Lysodeikticus*, *K. Pneumoniae*, *B. Subtilis* and *C. Albicans* (Mihailović *et al.*, 2011)

Table 18. Phytochemical compounds contained in DEAP using GC-MS analysis according to the retention time (continued)

S/No.	RT	Compound Name	Structure	Formula	MW (g/mol)	Component Area	Total peak area	Estimated Conc. (%)	Activity
10	42.08	1,2-Benzenedicarboxylic acid, bis(2-ethylhexyl) ester	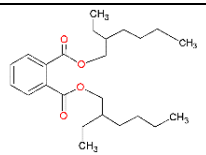	$C_{24}H_{38}O_4$	390.6	363356.2	147043139.1	0.25	Antioxidant by increasing free radical scavenging with DPPH assay (Al-Huqail, Elgaaly and Ibrahim, 2018),
11	47.08	2-oxobutanoic acid neopentyl ester	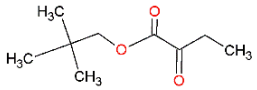	$C_9H_{16}O_3$	172.22	20773.3	147043139.1	0.01	No activity reported
12	49.90	1-Heptatriacotanol		$C_{37}H_{76}O$	537	88645295	147043139.1	60.29	Anti-cancer activity (Hameed *et al*., 2016), Highly antimicrobial on *P. Aeruginosa* (Olajuyigbe *et al.*, 2018)
13	50.13	α-Tocopherol	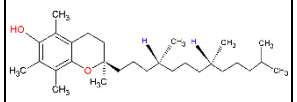	$C_{29}H_{50}O_2$	430.7	80509.6	147043139.1	0.05	Antiproliferative and cell cycle arrest on HeLa cells (Pédeboscq *et al.*, 2012)
14	50.44	Androsta-1,4-dien-3-one, 6,17-dihydroxy-, (6β,17β)	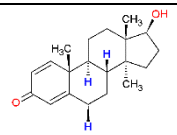	$C_{19}H_{26}O_3$	302.4	47451933	147043139.1	32.27	No activity reported

Table 18. Phytochemical compounds contained in DEAP using GC-MS analysis according to the retention time (continued)

S/No.	RT	Compound Name	Structure	Formula	MW (g/mol)	Component Area	Total peak area	Estimated Conc. (%)	Activity
15	51.58	Stigmasterol	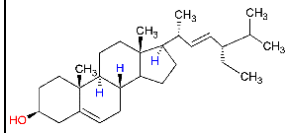	$C_{29}H_{48}O$	412.7	1440675.9	147043139.1	0.98	Anti-angiogenesis on HUVECs cells (Kangsamaksin *et al.*, 2017), Anti-inflammatory in counteracting the IL-1β (Gabay *et al.*, 2010), Antioxidant and Antigenotoxic by reducing DNA damage (Ali *et al.*, 2015)
16	52.29	γ-Sitosterol	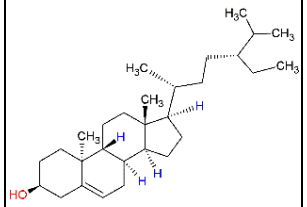	$C_{29}H_{50}O$	414.7	4469568.1	147043139.1	3.04	Anti-cancer by cell cycle arrest in G2/M and apoptosis through *c-myc* suppression in MCF-7 and A-549 (Sundarraj *et al.*, 2012), Antimicrobial on *S. Aureus*, *S. Typhimurium* and *C.* Albicans, Anti-inflammatory by increasing free radical scavenging by DPPH assay (Abu-lafi *et al.*, 2019)
17	52.64	β-Amyrin	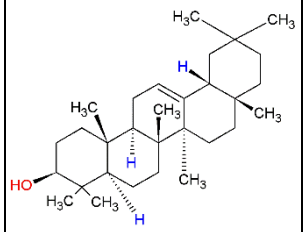	$C_{30}H_{50}O$	426.7	29955.2	147043139.1	0.02	Anti-cancer on Hep-G2 cells indicated by cell cycle arrest and apoptosis with increasing of Bax and decreasing Bcl-2 (Wen, Gu and Zeng, 2018), Anti-inflammatory (Holanda Pinto *et al.*, 2008)

Table 19. Phytochemical compounds contained in DEZSC leaves using GC-MS analysis according to the retention time

S/No.	RT	Compound Name	Structure	Formula	MW (g/mol)	Component Area	Total peak area	Estimated Conc. (%)	Activity
1	28.06	Myristic acid	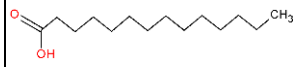	$C_{14}H_{28}O_2$	228.37	933665.7	70377764	1.33	No activity reported
2	29.64	Neophytadiene	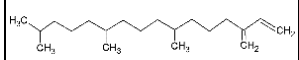	$C_{20}H_{38}$	278.52	5569752.2	70377764	7.91	Anti-cancer on MCF-7 and HeLa cells (Eswaraiah *et al.*, 2019), Anti-inflammatory (Carretero *et al.*, 2008), Antioxidant , Antimicrobial on *E. Coli*, *S. Aureus*, *C. Albicans*, *and A. Niger* (Mendiola *et al.*, 2008)
3	29.75	6,10,14-trimethyl pentadecane-2-one	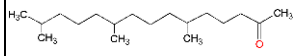	$C_{18}H_{36}O$	268.48	1258285.7	70377764	1.79	Antimicrobial on *Y. Pseudotuberculosis*, *E. Faecalis* and *S. Aureus* (Yayli *et al.*, 2006)
4	30.14	Phytol, acetate	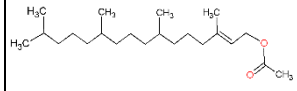	$C_{22}H_{42}O_2$	338.57	898958.7	70377764	1.28	Antimicrobial on *Aspergillus terreus*, Anti-cancer on MCF-7 and HepG2 cells (Farid *et al.*, 2015)

Table 19. Phytochemical compounds contained in DEZSC using GC-MS analysis according to the retention time (continued)

S/No.	RT	Compound Name	Structure	Formula	MW (g/mol)	Component Area	Total peak area	Estimated Conc. (%)	Activity
5	30.48	Phytol	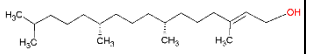	$C_{20}H_{40}O$	296.53	2863580.8	70377764	4.07	Anti-cancer on A549 by depolarizing the mitochondrial membrane potential and upregulating BAX and downregulating BCL-2 and promoting cas-9 and -3, Antiangiogenic on chick embryo *chorioallantoic* membrane (Sakthivel, Malar and Devi, 2018), Antioxidant by showing free radical decreasing and Antinociception on central and peripheral nerve system (Santos *et al.*, 2013), Antimicrobial on *Pseudomonas aeruginosa*, *Staphylococcus aureus*, *Escherichia coli*, *Salmonella typhi* (Nithya, Ragavendran and Natarajan, 2018)
6	32.22	Palmitic acid	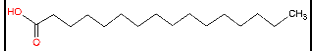	$C_{16}H_{32}O_2$	256.42	18942470.1	70377764	26.92	Anti-cancer on HCT-116 cells and showed high affinity interaction on DNA

Table 19. Phytochemical compounds contained in DEZSC using GC-MS analysis according to the retention time (continued)

S/No.	RT	Compound Name	Structure	Formula	MW (g/mol)	Component Area	Total peak area	Estimated Conc. (%)	Activity
									topoisomerase-I (Ravi and Krishnan, 2016), Antifungal on *B. Cereus* (Idowu and Ojo, 2017), Antioxidant on increasing DPPH free radical scavenging (Shah and Iqbal, 2018)
7	35.30	Linoleic acid	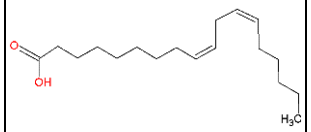	$C_{18}H_{32}O_2$	280.46	4760405.4	70377764	6.76	Anti-cancer on LoVo and RKO cells by increasing *cas-3* and *-9* (Lu *et al.*, 2010), Antimicrobial on *S. Aureus* and *S. Pyogenes* (Zheng *et al.*, 2005)
8	35.41	Linolenic acid	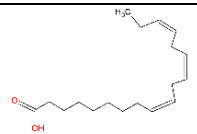	$C_{18}H_{30}O_2$	278.43	7894118.3	70377764	11.22	Antimicrobial on *Staphylococcus aureus* and *B. Cereus* (Lee, Kim and Shin, 2002)
9	35.81	Stearic acid	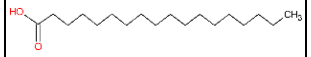	$C_{18}H_{36}O_2$	284.48	2671328.9	70377764	3.80	Anti-cancer on human breast cancer cells induced mouse model (Fermor *et al.*, 1992), Antioxidant on reducing neurons damage of H_2O_2 (Wang *et al.*, 2007)

Table 19. Phytochemical compounds contained in DEZSC using GC-MS analysis according to the retention time (continued)

S/No.	RT	Compound Name	Structure	Formula	MW (g/mol)	Component Area	Total peak area	Estimated Conc. (%)	Activity
10	38.92	4,8,12,16-Tetramethylheptadecane-4-olide	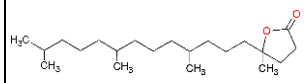	$C_{21}H_{40}O_2$	324.54	496771.6	70377764	0.71	Anti-cancer on HeLa cells (Swantara *et al.*, 2019)
11	41.99	Bis(2-ethylhexyl) phthalate	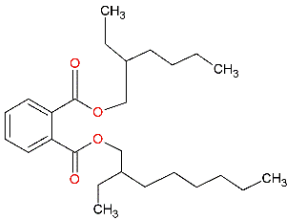	$C_{24}H_{38}O_4$	390.56	622269.6	70377764	0.88	Anti-cancer on K562 and showed apoptosis by upregulating BAX, promoting casp-3, -9 and -8 and downregulating BCL-2 (Moushumi Priya and Jayachandran, 2012), Antimicrobial on *B. Subtilis*, *S. Lutea*, *E. Coli*, *S. Sonnei* and *S. Shiga* (Habib and Karim, 2009)
12	46.04	Squalene	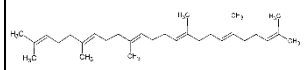	$C_{30}H_{50}$	410.72	1183900.6	70377764	1.68	Anti-cancer on A431 (skin cancer cell lines) (Mohansrinivasan *et al.*, 2015), chemoprotection on cisplatin and carboplatin (Das *et al.*, 2008)
13	46.37	α-Tocospiro A	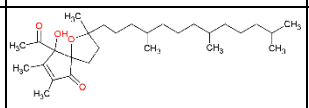	$C_{29}H_{50}O_4$	462.70	941127.8	70377764	1.34	No activity reported
14	46.67	α-Tocospiro B	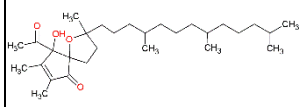	$C_{29}H_{50}O_4$	462.70	1014104.6	70377764	1.44	No activity reported

Table 19. Phytochemical compounds contained in DEZSC using GC-MS analysis according to the retention time (continued)

S/No.	RT	Compound Name	Structure	Formula	MW (g/mol)	Component Area	Total peak area	Estimated Conc. (%)	Activity
15	46.98	n-Tetracosanol-1	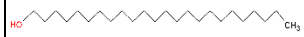	$C_{24}H_{50}O$	354.65	4270594.2	70377764	6.07	Anti-cancer on melanoma cells (Vergara *et al*., 2015), Antimutagenic on *S. Typhimurium* (Makhafola *et al.*, 2017), Antibacterial on *S. Aureus*, *P. Aeruginosa*, *K. Pneumonia* and *P. Vulgaris* (Kumari, Menghani and Mithal, 2019)
19	48.96	γ-Tocopherol	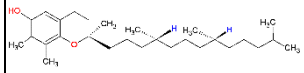	$C_{28}H_{48}O_2$	416.68	780983.8	70377764	1.11	Antioxidant by retarding the oxidation of RO TAG (Lampi *et al.*, 1999)

Table 19. Phytochemical compounds contained in DEZSC using GC-MS analysis according to the retention time (continued)

S/No.	RT	Compound Name	Structure	Formula	MW (g/mol)	Component Area	Total peak area	Estimated Conc. (%)	Activity
20	49.63	Octacosanol		$C_{28}H_{58}O$	410.76	3702492.7	70377764	5.26	Anti-cancer on A549 cells, Antibacterial on *Pseudomonas aeruginosa*, *Bordetella bronchiseptica*, *Escherichia coli*, *Burkholderia cenocepacia*, *Acinetobacter iwoffii*, *Acinetobacter baumannii*, *Moraxella catarrhalis*, *Bacillus subtilis* and *Staphylococcus aureus* (Coccimiglio *et al.*, 2016)
21	50.01	Vitamin E	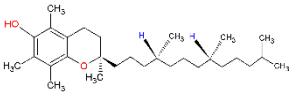	$C_{29}H_{50}O_2$	430.71	539595.8	70377764	0.77	Anti-cancer on ORL-48 cells (Zulkapli, Abdul Razak and Zain, 2017), Antioxidant by decreasing free radical scavenger (Duval and Poelman, 1995), Immunomodulator effect on CD4+CD- T cells (Erf *et al.*, 1998)

Table 19. Phytochemical compounds contained in DEZSC using GC-MS analysis according to the retention time (continued)

S/No.	RT	Compound Name	Structure	Formula	MW (g/mol)	Component Area	Total peak area	Estimated Conc. (%)	Activity
22	51.08	Campesterol	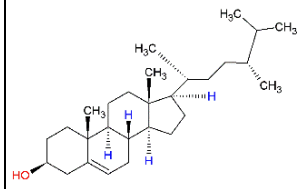	$C_{28}H_{48}O$	400.68	730757.8	70377764	1.04	Anti-angiogenic on HUVECs cells and *in vivo chorio allantoic membrane* (Choi *et al.*, 2007), Antioxidant by decreasing lipid peroxidation (Yoshida and Niki, 2003)
23	51.49	Stigmasterol	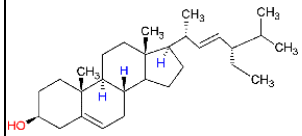	$C_{29}H_{48}O$	412.69	3458486.4	70377764	4.91	Anti-angiogenesis on HUVECs cells (Kangsamaksin *et al.*, 2017), Anti-inflammatory in counteracting the IL-1β (Gabay *et al.*, 2010), Antioxidant and Antigenotoxic by reducing DNA damage (Ali *et al.*, 2015)
25	52.19	Stigmast-5-en-3-ol	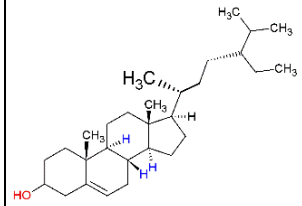	$C_{29}H_{50}O$	414.7	3684884.3	70377764	5.24	Anti-cancer on HL-60 and MCF-7 cells (Fernando *et al.*, 2018), Immunomodulator by increasing hemagglutinating antibody titre (Parihar and Balekar, 2017)

Table 19. Phytochemical compounds contained in DEZSC leaves using GC-MS analysis according to the retention time (continued)

S/No.	RT	Compound Name	Structure	Formula	MW (g/mol)	Component Area	Total peak area	Estimated Conc. (%)	Activity
26	52.82	Lupenone	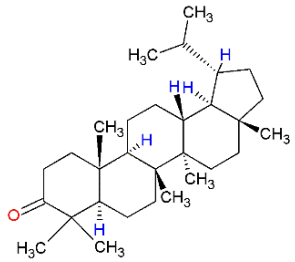	$C_{30}H_{48}O$	424.70	2051422.2	70377764	2.91	Anti-inflammatory by inhibiting oedema in mice and reducing NO production on RAW 264.7 macrophages (Romero-Estrada *et al.*, 2016), Anti-cancer on MCF-7 cells (Suwito *et al.*, 2016)
27	53.08	Lupeol	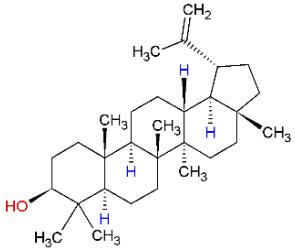	$C_{30}H_{50}O$	426.72	1107807	70377764	1.91	Anti-angiogenesis in HUVECs (Kangsamaksin *et al.*, 2017), Anti-cancer on MCF-7 cells (Pitchai, Roy and Ignatius, 2014), Antioxidant (Tchimene *et al.*, 2016), Anti-inflammatory by reducing prostaglandin E2 (PGE2) (Fernández *et al.*, 2001)

Table 20. Phytochemical compounds contained in DEVE using GC-MS analysis according to the retention time

S/No.	RT	Compound Name	Structure	Formula	MW (g/mol)	Component Area	Total peak area	Estimated Conc. (%)	Activity
1	15.68	1,2-Di-tert-butylbenzene	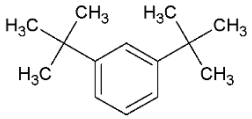	$C_{14}H_{22}$	190.32	40972.4	54027295	0.08	No activity reported
2	17.91	2-Chlorohexylacet-ate	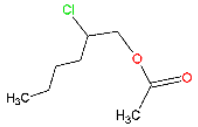	$C_8H_{15}ClO_2$	178.66	9316.1	54027295	0.02	No activity reported
3	22.10	Pentadecane	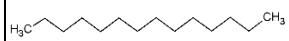	$C_{15}H_{32}$	212.41	13166	54027295	0.02	Antibacterial on *B. subtilis*, *S. aureus*, *E. coli*, *P. aeruginosa*, *E. faecalis* and *P. vulgaris* (Uma and Parvathavarthini, 2010), Antimicrobial on *S. aureus*, *B. subtilis*, *E. coli*, *P. aeruginosa* (Chuah *et al.*, 2018)
4	22.49	5-Isopropyl-4-(trifluoromethyl)-1H-pyrimidin-2-one	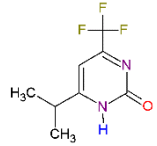	$C_8H_9F_3N_2O$	206.17	19979.9	54027295	0.04	No activity reported
5	22.85	Dihydroactinidiolide	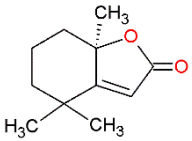	$C_{11}H_{16}O_2$	180.24	254098.7	54027295	0.47	Anti-cancer on KB and HCT-116 cells (Malek *et al.*, 2009)

Table 20. Phytochemical compounds contained in DEVE using GC-MS analysis according to the retention time (continued)

S/No.	RT	Compound Name	Structure	Formula	MW (g/mol)	Component Area	Total peak area	Estimated Conc. (%)	Activity
6	27.44	Heptanoic acid, tridecafluoro-, heptyl ester	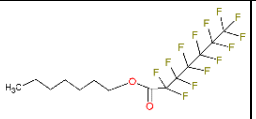	$C_{14}H_{15}F_{13}O_2$	462.25	12327.2	54027295	0.02	No activity reported
7	28.13	Loliolide	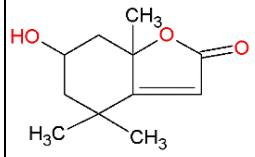	$C_{11}H_{16}O_3$	196.24	888511.4	54027295	1.64	Anti-inflammation by reducing ROS and upregulating IL-1a, IL-17, IL-22 and p-PI3K and p-AKT on keratinocytes (Park *et al.*, 2019), Antimicrobial on *C. albicans* (Ragasa, De Luna and Hofilena, 2005)
8	29.61	1-dodecanol		$C_{12}H_{26}O$	186.33	28139.6	54027295	0.05	No activity reported
9	29.71	Neophytadiene	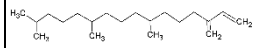	$C_{20}H_{38}$	278.5	10458579.3	54027295	19.36	Anti-cancer on MCF-7 and HeLa cells (Eswaraiah *et al.*, 2019), Anti-inflammatory (Carretero *et al.*, 2008), Antioxidant (Raman *et al.*, 2012), Antimicrobial on *E. coli*, *S. aureus*, *C. albicans, and A. niger* (Mendiola *et al.*, 2008)

Table 20. Phytochemical compounds contained in DEVE using GC-MS analysis according to the retention time (continued)

S/No.	RT	Compound Name	Structure	Formula	MW (g/mol)	Component Area	Total peak area	Estimated Conc. (%)	Activity
10	29.82	6,10,14-trimethyl pentadecane-2-one	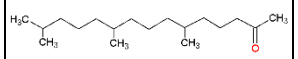	$C_{18}H_{36}O$	268.5	1040334.7	54027295	1.93	Antimicrobial on *Y. pseudotuberculosis*, *E. faecalis* and *S. aureus* (Yayli *et al.*, 2006)
11	30.21	Phytol	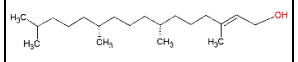	$C_{20}H_{40}O$	296.5	7217201.3	54027295	13.36	Anti-cancer on A549 by depolarizing the mitochondrial membrane potential and upregulating BAX and downregulating BCL-2 and promoting cas-9 and -3, Antiangiogenic on chick embryo *chorioallantoic* membrane (Sakthivel *et al.*, 2018), Antioxidant by showing free radical decreasing and Antinociception on central and peripheral nerve system (Santos *et al.*, 2013), Antimicrobial on *Pseudomonas aeruginosa*, *Staphylococcus aureus*, *Escherichia coli*, *Salmonella typhi* (Nithya *et al.* , 2018)

Table 20. Phytochemical compounds contained in DEVE using GC-MS analysis according to the retention time (continued)

S/No.	RT	Compound Name	Structure	Formula	MW (g/mol)	Component Area	Total peak area	Estimated Conc. (%)	Activity
12	31.22	2-Methyloctanal	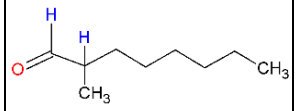	$C_9H_{18}O$	142.24	20078.5	54027295	0.04	No activity reported
13	32.12	1,2-Benzenedicarboxy-lic acid, dibutyl ester	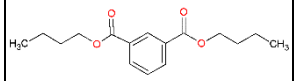	$C_{16}H_{22}O_4$	278.34	104176.4	54027295	0.19	Anti-cancer by binding with *k-ras* protein in COLO 320 cells (Gunalan *et al.*, 2016),Antimicrobial on *S. aureus* and *E. coli* (Elgorban *et al.*, 2019)
14	32.24	Palmitic acid	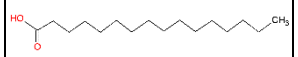	$C_{16}H_{32}O_2$	256.42	11562122.4	54027295	21.40	Anti-cancer on HCT-116 cells and showed high affinity interaction on DNA topoisomerase-I (Ravi and Krishnan, 2016), Antifungal on *B. cereus* (Idowu and Ojo, 2017), Antioxidant on increasing DPPH free radical scavenging (Shah and Iqbal, 2018)
15	34.41	Pentatriacontane		$C_{35}H_{72}$	492.9	181984.5	54027295	0.34	Antimicrobial on *S. aureus* (Pasdaran *et al.*, 2018)

Table 20. Phytochemical compounds contained in DEVE leaves using GC-MS analysis according to the retention time (continued)

S/No.	RT	Compound Name	Structure	Formula	MW (g/mol)	Component Area	Total peak area	Estimated Conc. (%)	Activity
16	35.36	Linoleic acid	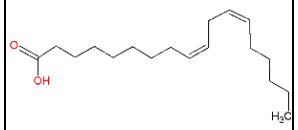	$C_{18}H_{32}O_2$	280.4	3619345	54027295	6.70	Anti-cancer on LoVo and RKO cells by increasing *cas-3* and *-9* (Lu *et al.*, 2010), Antimicrobial on *S. aureus* and *S. pyogenes* (Zheng *et al.*, 2005)
17	35.48	Linolenic acid	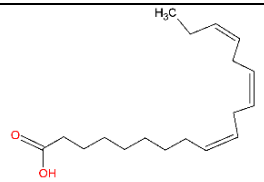	$C_{18}H_{30}O_2$	278.4	6527253.8	54027295	12.08	Antimicrobial on *Staphylococcus aureus* and *B. cereus* (Lee *et al*., 2002)
18	36.52	4-Tridecen-2-ynal, (Z)-	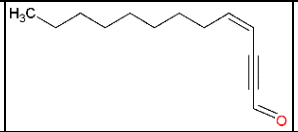	$C_{13}H_{20}O$	192.3	32308.7	54027295	0.06	No activity reported
19	43.99	3-Penten-2-one	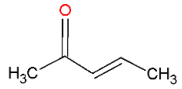	C_5H_8O	84.12	26559.6	54027295	0.05	No activity reported
20	44.30	Tricosane		$C_{23}H_{48}$	324.6	177168.8	54027295	0.33	Anti-cancer on HepG2 and MDA-MB-231 cells (Poma *et al.*, 2018), Antimicrobial on *S. aureus*, *M. lysodeikticus*, *K. pneumoniae*, *B. subtilis* and *C. albicans* (Mihailović *et al.*, 2011)

Table 20. Phytochemical compounds contained in DEVE using GC-MS analysis according to the retention time (continued)

S/No.	RT	Compound Name	Structure	Formula	MW (g/mol)	Component Area	Total peak area	Estimated Conc. (%)	Activity
21	45.72	Phenol, 2-(1-phenylethyl)-	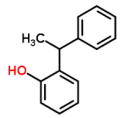	$C_{14}H_{14}O$	198.26	51594	54027295	0.10	No activity reported
22	47.07	Heneicosane		$C_{21}H_{44}$	296.6	1687797.1	54027295	3.12	Anti-cancer on HCT-116 and HepG2 (Alkhalf *et al.*, 2019), Antioxidant on *S. aureus*, *E. faecium*, *S. agalactiae*, *B. subtilus* (Albouchi *et al.*, 2013)
23	49.67	Hentriacontane		$C_{31}H_{64}$	436.8	2924496	54027295	5.41	Antiinflammatory by suppressing TNF-alpha, IL-6, PGE_2 and COX-2 (Kim *et al.*, 2011)
24	50.09	dl-α-Tocopherol	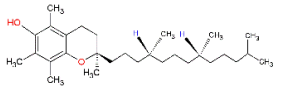	$C_{29}H_{50}O_2$	430.7	322648.7	54027295	0.60	Anti-cancer on ORL-48 cells (Zulkapli *et al.*, 2017), Antioxidant by decreasing free radical scavenger (Duval and Poelman, 1995), Immunomodulator effect on CD4+CD- T cells (Erf *et al.*, 1998)

Table 20. Phytochemical compounds contained in DEVE leaves using GC-MS analysis according to the retention time (continued)

S/No.	RT	Compound Name	Structure	Formula	MW (g/mol)	Component Area	Total peak area	Estimated Conc. (%)	Activity
25	52.23	Stigmasterol	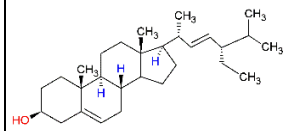	$C_{29}H_{48}O$	412.7	2886417	54027295	5.34	Anti-angiogenesis on HUVECs cells (Kangsamaksin *et al.*, 2017), Anti-inflammatory in counteracting the IL-1β (Gabay *et al.*, 2010), Antioxidant and Antigenotoxic by reducing DNA damage (Ali *et al.*, 2015)
26	55.05	Phytol, acetate	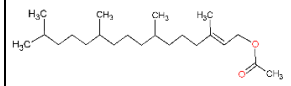	$C_{22}H_{42}O_2$	338.6	2522205.6	54027295	4.67	Antimicrobial on *Aspergillus terreus*, Anti-cancer on MCF-7 and HepG2 cells (Farid *et al.*, 2015)
27	57.08	Phytyl linoleate	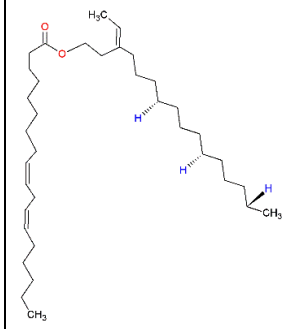	$C_{38}H_{70}O_2$	558.92	1398512	54027295	2.59	No activity reported

Table 21. The abundance of phytoconstituents contained in DEAP separated by the chemical group

Chemical group	Nature of compound	Structure	Formula	MW (g/mol)	Estimated Conc. (%)	Activity
Alcohols	1-Heptatriacotanol		$C_{37}H_{76}O$	537	60.29	Anti-cancer activity (Hameed *et al*., 2016), Highly antimicrobial on *P. aeruginosa* (Olajuyigbe *et al.*, 2018)
	Furfuryl alcohol	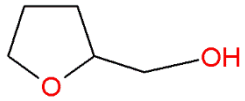	$C_5H_{10}O_2$	102.13	0.01	Antioxidant (Wei *et al.*, 2010), Antimicrobial on *Salmonella typhimurium* (Monien *et al.*, 2011)
Steroids	Androsta-1,4-dien-3-one, 6,17-dihydroxy-, (6β,17 β)	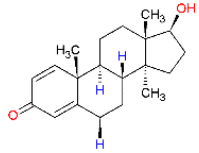	$C_{19}H_{26}O_3$	302.4	32.27	No activity reported
	Stigmasterol	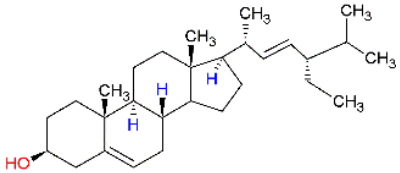	$C_{29}H_{48}O$	412.7	0.98	Anti-angiogenesis on HUVECs cells (Kangsamaksin *et al.*, 2017), Anti-inflammatory in counteracting the IL-1β (Gabay *et al.*, 2010), Antioxidant and Antigenotoxic by reducing DNA damage (Ali *et al.*, 2015)
	γ-Sitosterol	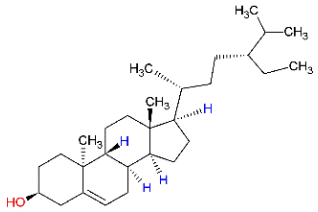	$C_{29}H_{50}O$	414.7	3.04	Anti-cancer by cell cycle arrest in G2/M and apoptosis through *c-myc* suppression in MCF-7 and A-549 (Sundarraj *et al.*, 2012), Antimicrobial on *S. aureus*, *S. typhimurium* and *C.* albicans, Anti-inflammatory by increasing free radical scavenging by DPPH assay (Abu-lafi *et al.*, 2019)

Table 21. The abundance of phytoconstituents contained in DEAP separated by the chemical group (continued)

Chemical group	Nature of compound	Structure	Formula	MW (g/mol)	Estimated Conc. (%)	Activity
Steroids	β-Amyrin	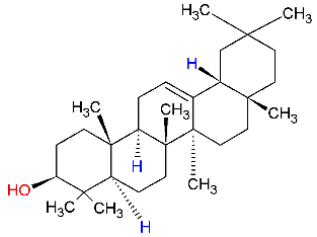	$C_{30}H_{50}O$	426.7	0.02	Anti-cancer on Hep-G2 cells indicated by cell cycle arrest and apoptosis with increasing of Bax and decreasing Bcl-2 (Wen *et al.*, 2018), Anti-inflammatory by increasing TNF-α and the gingival MPO and TBARS (Holanda Pinto *et al.*, 2008), Antimicrobial on *S. aureus*, *B. subtilis*, *S. typhi*, *E. coli*, *P. aeruginosa* (Abdel-raouf *et al.*, 2015)
Fatty acids	Palmitic acid	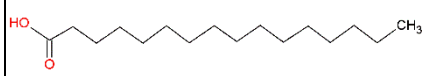	$C_{16}H_{32}O_2$	256.42	1.28	Anti-cancer on HCT-116 cells and showed high-affinity interaction on DNA topoisomerase-I (Ravi and Krishnan, 2016), Antifungal on *B. cereus* (Idowu and Ojo, 2017), Antioxidant on increasing DPPH free radical scavenging (Shah and Iqbal, 2018)
Terpenes	Neophytadiene	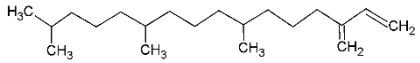	$C_{20}H_{38}$	278.5	1.20	Anti-cancer on MCF-7 and HeLa cells (Eswaraiah *et al.*, 2019), Anti-inflammatory (Carretero *et al.*, 2008), Antioxidant (Raman *et al.*, 2012), Antimicrobial on *E. coli*, *S. aureus*, *C. albicans, and A. niger* (Mendiola *et al.*, 2008)
	6,10,14-trimethyl pentadecane-2-one	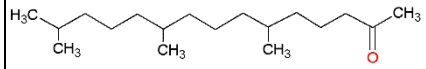	$C_{18}H_{36}O$	268.5	0.53	Antimicrobial on *Y. pseudotuberculosis*, *E. faecalis* and *S. aureus* (Yayli *et al.*, 2006)
Phthalates	1,2-Benzenedicarboxylic acid, bis(2-ethylhexyl) ester	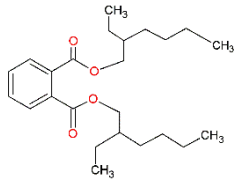	$C_{24}H_{38}O_4$	390.6	0.25	Antioxidant by increasing free radical scavenging with DPPH assay (Al-Huqail, Elgaaly, and Ibrahim, 2018)

Table 21. The abundance of phytoconstituents contained in DEAP separated by the chemical group (continued)

Chemical group	Nature of compound	Structure	Formula	MW (g/mol)	Estimated Conc. (%)	Activity
Tocopherols	α-Tocopherol	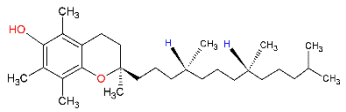	$C_{29}H_{50}O_2$	430.7	0.05	Antiproliferative and cell cycle arrest on HeLa cells (Pédeboscq *et al.*, 2012)
Aldehydes	2-Methyltetradecanal	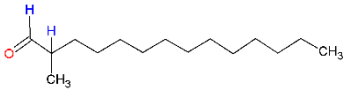	$C_{15}H_{30}O$	226.4	0.03	No activity reported
	3,7-Dimethyl-2,3-epoxyoctanal	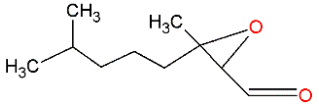	$C_{10}H_{18}O_2$	170.25	0.01	No activity reported
Hydrocarbons	Tricosane		$C_{23}H_{48}$	324.6	0.03	Anti-cancer on HepG2 and MDA-MB-231 cells (Poma *et al.*, 2018), Antimicrobial on *S. aureus*, *M. lysodeikticus*, *K. pneumoniae*, *B. subtilis* and *C. albicans* (Mihailović *et al.*, 2011)
	2-octylacolein	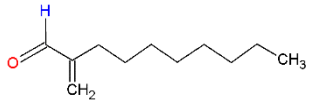	$C_{11}H_{20}O$	168.28	0.01	No activity reported
	Octadecane	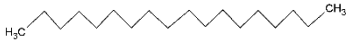	$C_{18}H_{38}$	254.5	0.02	Antioxidant (Morah *et al.*, 2017), Anti-cancer on PC-3 cells (Ryu *et al.*, 2012)
Carboxylic acids ester	2-oxobutanoic acid neopentyl ester	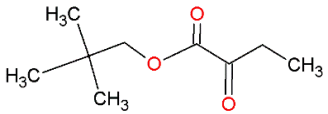	$C_9H_{16}O_3$	172.22	0.01	No activity reported

Table 22. The abundance of phytoconstituents contained in DEZSC separated by the chemical group

Chemical group	Nature of compound	Structure	Formula	MW (g/mol)	Estimated Conc. (%)	Activity
Fatty acids	Palmitic acid	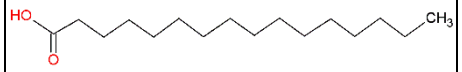	$C_{16}H_{32}O_2$	256.42	26.92	Anti-cancer on HCT-116 cells and showed high affinity interaction on DNA topoisomerase-I (Ravi and Krishnan, 2016), Antifungal on *B. cereus* (Idowu and Ojo, 2017), Antioxidant on increasing DPPH free radical scavenging (Shah and Iqbal, 2018)
	Linolenic acid	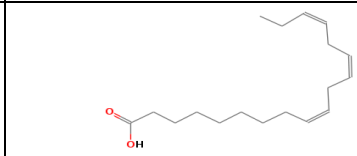	$C_{18}H_{30}O_2$	278.43	11.22	Antimicrobial on *Staphylococcus aureus* and *B. cereus* (Lee *et al*., 2002)
	Linoleic acid	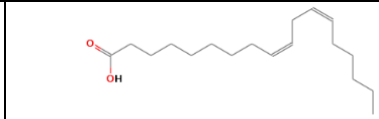	$C_{18}H_{32}O_2$	280.46	6.76	Anti-cancer on LoVo and RKO cells by increasing *cas-3* and *-9* (Lu *et al.*, 2010), Antimicrobial on *S. aureus* and *S. pyogenes* (Zheng *et al.*, 2005)
	Stearic acid	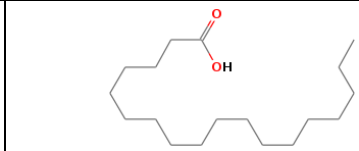	$C_{18}H_{36}O_2$	284.48	3.80	Anti-cancer on human breast cancer cells induced mouse model (Fermor *et al.*, 1992), Antioxidant on reducing neurons damage of H_2O_2 (Wang *et al.*, 2007)
	Myristic acid	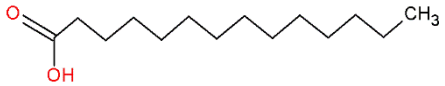	$C_{14}H_{28}O_2$	228.37	1.33	No activity reported

Table 22. The abundance of phytoconstituents contained in DEZSC separated by the chemical group (continued)

Chemical group	Nature of compound	Structure	Formula	MW (g/mol)	Estimated Conc. (%)	Activity
Terpenes	Neophytadiene	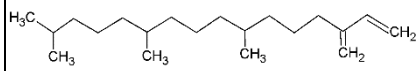	$C_{20}H_{38}$	278.5	7.91	Anti-cancer on MCF-7 and HeLa cells (Eswaraiah *et al.*, 2019), Anti-inflammatory (Carretero *et al.*, 2008), Antioxidant (Raman *et al.*, 2012), Antimicrobial on *E. coli*, *S. aureus*, *C. albicans, and A. niger* (Mendiola *et al.*, 2008)
	Phytol	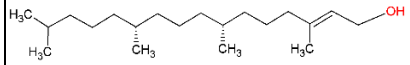	$C_{20}H_{40}O$	296.53	4.07	Anti-cancer on A549 by depolarizing the mitochondrial membrane potential and upregulating BAX and downregulating BCL-2 and promoting cas-9 and -3, Antiangiogenic on chick embryo *chorioallantoic* membrane (Sakthivel *et al.*, 2018), Antioxidant by showing free radical decreasing and Antinociception on central and peripheral nerve system (Santos *et al.*, 2013), Antimicrobial on *Pseudomonas aeruginosa*, *Staphylococcus aureus*, *Escherichia coli*, *Salmonella typhi* (Nithya *et al.*, 2018)
	6,10,14-trimethyl pentadecane-2-one	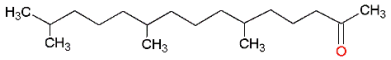	$C_{18}H_{36}O$	268.48	1.79	Antimicrobial on *Y. pseudotuberculosis*, *E. faecalis*, and *S. aureus* (Yayli *et al.*, 2006)

Table 22. The abundance of phytoconstituents contained in DEZSC separated by the chemical group (continued)

Chemical group	Nature of compound	Structure	Formula	MW (g/mol)	Estimated Conc. (%)	Activity
Terpenes	Squalene	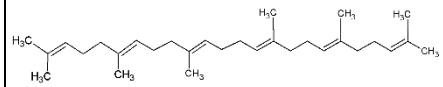	$C_{30}H_{50}$	410.72	1.68	Anti-cancer on A431 (skin cancer cell lines) (Mohansrinivasan *et al.*, 2015), chemoprotection on cisplatin and carboplatin (Das *et al.*, 2008)
	Phytol, acetate	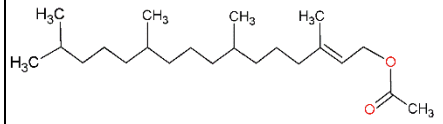	$C_{22}H_{42}O_2$	338.57	1.28	Antimicrobial on *Aspergillus terreus*, Anti-cancer on MCF-7 and HepG2 cells (Farid *et al.*, 2015)
Fatty alcohols	n-Tetracosanol-1	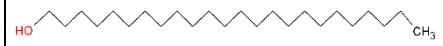	$C_{24}H_{50}O$	354.65	6.07	Anti-cancer on melanoma cells (Vergara *et al*., 2015), Antimutagenic on *S. typhimurium* (Makhafola *et al.*, 2017), Antibacterial on *S. aureus*, *P. aeruginosa*, *K. pneumonia* and *P. vulgaris* (Kumari, Menghani and Mithal, 2019)
	Octacosanol		$C_{28}H_{58}O$	410.76	5.26	Anti-cancer on A549 cells, Antibacterial on *Pseudomonas aeruginosa*, *Bordetella bronchiseptica*, *Escherichia coli*, *Burkholderia cenocepacia*, *Acinetobacter iwoffii*, *Acinetobacter baumannii*, *Moraxella catarrhalis*, *Bacillus subtilis* and *Staphylococcus aureus* (Coccimiglio *et al.*, 2016)

Table 22. The abundance of phytoconstituents contained in DEZSC separated by the chemical group (continued)

Chemical group	Nature of compound	Structure	Formula	MW (g/mol)	Estimated Conc. (%)	Activity
Steroids	Lupeol	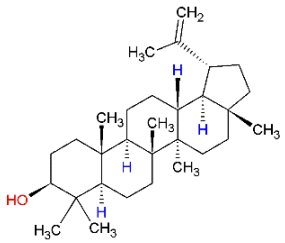	$C_{30}H_{50}O$	426.72	1.91	Anti-angiogenesis in HUVECs (Kangsamaksin *et al.*, 2017), Anti-cancer on MCF-7 cells (Pitchai *et al.*, 2014), Antioxidant (Tchimene *et al.*, 2016), Anti-inflammatory by reducing prostaglandin E2 (PGE2) (Fernández *et al.*, 2001)
Steroids	Stigmast-5-en-3-ol	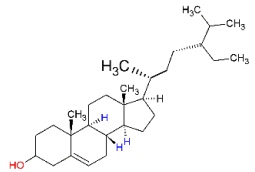	$C_{29}H_{50}O$	414.7	5.24	Anti-cancer on HL-60 and MCF-7 cells (Fernando *et al.*, 2018), Immunomodulator by increasing hemagglutinating antibody titer (Parihar *et al.*, 2017)
	Stigmasterol	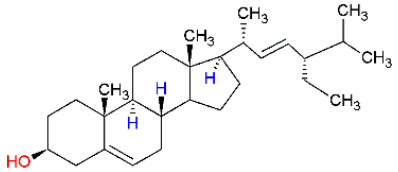	$C_{29}H_{48}O$	412.69	4.91	Anti-angiogenesis on HUVECs cells (Kangsamaksin *et al.*, 2017), Anti-inflammatory in counteracting the IL-1β (Gabay *et al.*, 2010), Antioxidant and Antigenotoxic by reducing DNA damage (Ali *et al.*, 2015)
	Campesterol	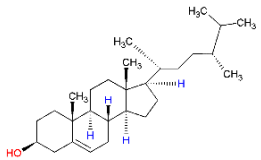	$C_{28}H_{48}O$	400.68	1.04	Anti-angiogenic on HUVECs cells and *in vivo chorioallantoic membrane* (Choi *et al.*, 2007), Antioxidant by decreasing lipid peroxidation (Yoshida *et al.*, 2003)

Table 22. The abundance of phytoconstituents contained in DEZSC separated by the chemical group (continued)

Chemical group	Nature of compound	Structure	Formula	MW (g/mol)	Estimated Conc. (%)	Activity
Steroids	Lupenone	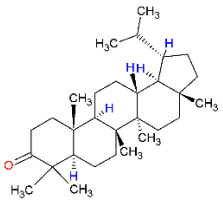	$C_{30}H_{48}O$	424.70	2.91	Anti-inflammatory by inhibiting edema in mice and reducing NO production on RAW 264.7 macrophages (Romero-Estrada *et al.*, 2016), Anti-cancer on MCF-7 cells (Suwito *et al.*, 2016)
Tocopherols	α -Tocospiro B	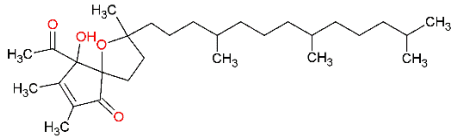	$C_{29}H_{50}O_4$	462.70	1.44	No activity reported
	α-Tocospiro A	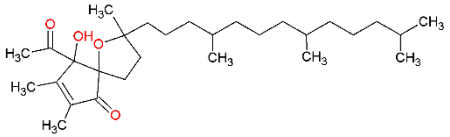	$C_{29}H_{50}O_4$	462.70	1.34	No activity reported
	γ-Tocopherol	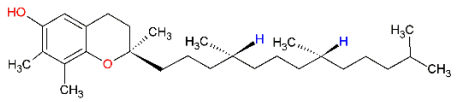	$C_{28}H_{48}O_2$	416.68	1.11	Antioxidant by retarding the oxidation of RO TAG (Lampi *et al.*, 1999)
	Vitamin E	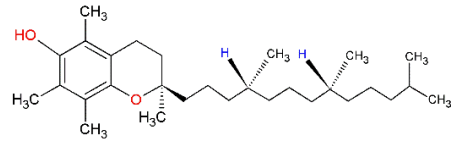	$C_{29}H_{50}O_2$	430.71	0.77	Anti-cancer on ORL-48 cells (Zulkapli *et al*., 2017), Antioxidant by decreasing free radical scavenger (Duval and Poelman, 1995), Immunomodulator effect on CD4+CD- T cells (Erf *et al.*, 1998)

Table 22. The abundance of phytoconstituents contained in DEZSC separated by the chemical group (continued)

Chemical group	Nature of compound	Structure	Formula	MW (g/mol)	Estimated Conc. (%)	Activity
Phthalates	Bis(2-ethylhexyl) phthalate	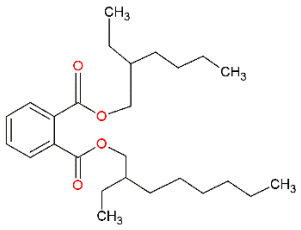	$C_{24}H_{38}O_4$	390.56	0.88	Anti-cancer on K562 and showed apoptosis by upregulating BAX, promoting casp-3, -9 and -8 and downregulating BCL-2 (Moushumi Priya and Jayachandran, 2012), Antimicrobial on *B. subtilis*, *S. lutea*, *E. coli*, *S. sonnei* and *S. shiga* (Habib *et al.*, 2009)
Furan Alkanes	4,8,12,16-Tetramethylheptadecane-4-olide	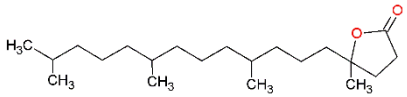	$C_{21}H_{40}O_2$	324.54	0.71	Anti-cancer on HeLa cells (Swantara *et al.*, 2019)

Table 23. The abundance of phytoconstituents contained in DEVE separated by the chemical group

Chemical group	Nature of compound	Structure	Formula	MW (g/mol)	Estimated Conc. (%)	Activity
Fatty acids	Palmitic acid	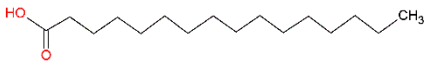	$C_{16}H_{32}O_2$	256.42	21.40	Anti-cancer on HCT-116 cells and showed high-affinity interaction on DNA topoisomerase-I (Ravi and Krishnan, 2016), Antifungal on *B. cereus* (Idowu and Ojo, 2017), Antioxidant on increasing DPPH free radical scavenging (Shah and Iqbal, 2018)
	Linolenic acid	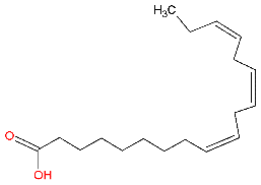	$C_{18}H_{30}O_2$	278.4	12.08	Antimicrobial on *Staphylococcus aureus* and *B. cereus* (Lee *et al*., 2002)
	Linoleic acid	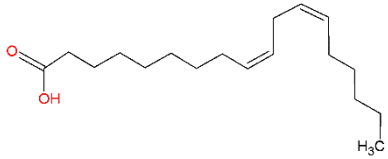	$C_{18}H_{32}O_2$	280.4	6.70	Anti-cancer on LoVo and RKO cells by increasing *cas-3* and *-9* (Lu *et al.*, 2010), Antimicrobial on *S. aureus* and *S. pyogenes* (Zheng *et al.*, 2005)
Terpenes	Neophytadiene	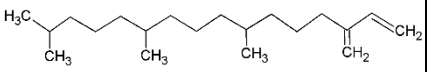	$C_{20}H_{38}$	278.5	19.36	Anti-cancer on MCF-7 and HeLa cells (Eswaraiah *et al.*, 2019), Anti-inflammatory (Carretero *et al.*, 2008), Antioxidant (Raman *et al.*, 2012), Antimicrobial on *E. coli*, *S. aureus*, *C. albicans, and A. niger* (Mendiola *et al.*, 2008)

Table 23. The abundance of phytoconstituents contained in DEVE separated by the chemical group (continued)

Chemical group	Nature of compound	Structure	Formula	MW (g/mol)	Estimated Conc. (%)	Activity
Terpenes	Phytol	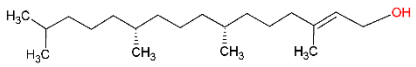	$C_{20}H_{40}O$	296.5	13.36	Anti-cancer on A549 by depolarizing the mitochondrial membrane potential and upregulating BAX and downregulating BCL-2 and promoting *cas-9* and -3, Antiangiogenic on chick embryo *chorioallantoic* membrane (Sakthivel *et al*., 2018), Antioxidant by showing free radical decreasing and Antinociception on central and peripheral nerve system (Santos *et al.*, 2013), Antimicrobial on *Pseudomonas aeruginosa*, *Staphylococcus aureus*, *Escherichia coli*, *Salmonella typhi* (Nithya *et al.*, 2018)
	Phytol, acetate	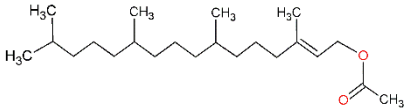	$C_{22}H_{42}O_2$	338.6	4.67	Antimicrobial on *Aspergillus terreus*, Anti-cancer on MCF-7 and HepG2 cells (Farid *et al.*, 2015)
	Phytyl linoleate	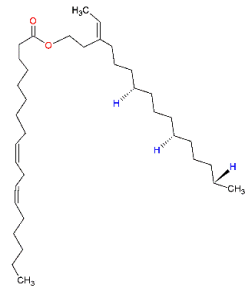	$C_{38}H_{70}O_2$	558.92	2.59	No activity reported

Table 23. The abundance of phytoconstituents contained in DEVE separated by the chemical group (continued)

Chemical group	Nature of compound	Structure	Formula	MW (g/mol)	Estimated Conc. (%)	Activity
Terpenes	6,10,14-trimethyl pentadecane-2-one	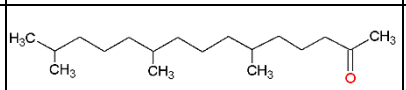	$C_{18}H_{36}O$	268.5	1.93	Antimicrobial on *Y. pseudotuberculosis*, *E. faecalis*, and *S. aureus* (Yayli *et al.*, 2006)
Steroids	Stigmasterol	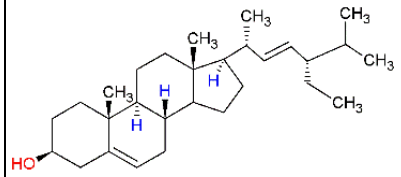	$C_{29}H_{48}O$	412.69	5.34	Anti-angiogenesis on HUVECs cells (Kangsamaksin *et al.*, 2017), Anti-inflammatory in counteracting the IL-1β (Gabay *et al.*, 2010), Antioxidant and Antigenotoxic by reducing DNA damage (Ali *et al.*, 2015)
Hydrocarbons	Hentriacontane		$C_{31}H_{64}$	436.8	5.41	Antiinflammatory by suppressing TNF-alpha, IL-6, PGE_2, and COX-2 (Kim *et al.*, 2011)
	Heneicosane		$C_{21}H_{44}$	296.6	3.12	Anti-cancer on HCT-116 and HepG2 (Alkhalf *et al.*, 2019), Antioxidant on *S. aureus*, *E. faecium*, *S. agalactiae*, *B. subtilus* (Albouchi *et al.*, 2013)
	Pentatriacontane		$C_{35}H_{72}$	492.9	0.34	Antimicrobial on *S. aureus* (Pasdaran *et al.*, 2018)
	Tricosane		$C_{23}H_{48}$	324.6	0.33	Anti-cancer on HepG2 and MDA-MB-231 cells (Poma *et al.*, 2018), Antimicrobial on *S. aureus*, *M. lysodeikticus*, *K. pneumoniae*, *B. subtilis* and *C. albicans* (Mihailović *et al.*, 2011)

Table 23. The abundance of phytoconstituents contained in DEVE separated by the chemical group (continued)

Chemical group	Nature of compound	Structure	Formula	MW (g/mol)	Estimated Conc. (%)	Activity
Hydrocarbons	4-Tridecen-2-ynal, (Z)-	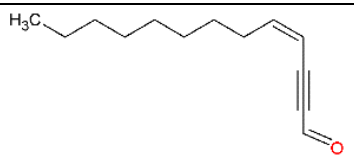	$C_{13}H_{20}O$	192.3	0.06	No activity reported
	Pentadecane	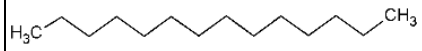	$C_{15}H_{32}$	212.41	0.02	Antibacterial on *B. subtilis*, *S. aureus*, *E. coli*, *P. aeruginosa*, *E. faecalis* and *P. vulgaris* (Uma *et al*., 2010), Antimicrobial on *S. aureus*, *B. subtilis*, *E. coli*, *P. aeruginosa* (Chuah *et al.*, 2018)
Benzofurans	Loliolide	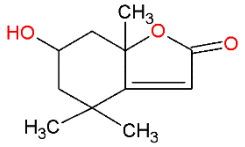	$C_{11}H_{16}O_3$	196.24	1.64	Anti-inflammation by reducing ROS and upregulating IL-1a, IL-17, IL-22 and p-PI3K and p-AKT on keratinocytes (Park *et al.*, 2019), Antimicrobial on *C. albicans* (Ragasa *et al*., 2005)
	Dihydroactinidiolide	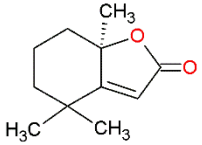	$C_{11}H_{16}O_2$	180.24	0.47	Anti-cancer on KB and HCT-116 cells (Malek *et al.*, 2009)
Tocopherols	dl-α-Tocopherol	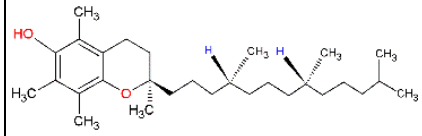	$C_{29}H_{50}O_2$	430.7	0.60	Anti-cancer on ORL-48 cells (Zulkapli *et al*., 2017), Antioxidant by decreasing free radical scavenger (Duval and Poelman, 1995), Immunomodulator effect on CD4+CD- T cells (Erf *et al.*, 1998)

Table 23. The abundance of phytoconstituents contained in DEVE separated by the chemical group (continued)

Chemical group	Nature of compound	Structure	Formula	MW (g/mol)	Estimated Conc. (%)	Activity
Benzoic acid esters	1,2-Benzenedicarboxylic acid, dibutyl ester	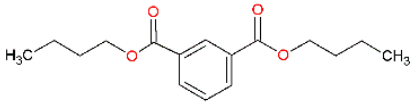	$C_{16}H_{22}O_4$	278.34	0.19	Anti-cancer by binding with *k-ras* protein in COLO 320 cells (Gunalan *et al.*, 2016), Antimicrobial on *S. aureus* and *E. coli* (Elgorban *et al.*, 2019)
Benzenoids	Phenol, 2-(1-phenylethyl)-	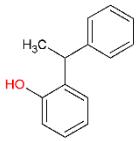	$C_{14}H_{14}O$	198.26	0.10	No activity reported
Aromatic hydrocarbons	1,2-Di-tert-butylbenzene	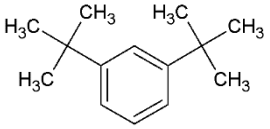	$C_{14}H_{22}$	190.32	0.08	No activity reported
Fatty alcohols	1-dodecanol		$C_{12}H_{26}O$	186.33	0.05	No activity reported
Ketones	3-Penten-2-one	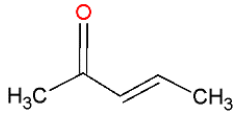	C_5H_8O	84.12	0.05	No activity reported
Aldehydes	2-Methyloctanal	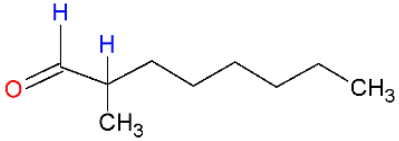	$C_9H_{18}O$	142.24	0.04	No activity reported

Table 23. The abundance of phytoconstituents contained in DEVE separated by the chemical group (continued)

Chemical group	Nature of compound	Structure	Formula	MW (g/mol)	Estimated Conc. (%)	Activity
Alkaloids	5-Isopropyl-4-(trifluoromethyl)-1H-pyrimidin-2-one	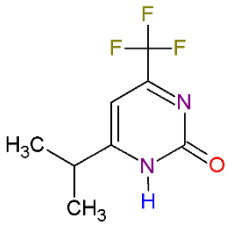	$C_8H_9F_3N_2O$	206.17	0.04	No activity reported
Fatty acids ester	Heptanoic acid, tridecafluoro-, heptyl ester	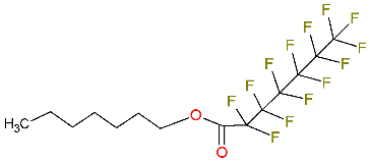	$C_{14}H_{15}F_{13}O_2$	462.25	0.02	No activity reported
Carboxylic acid	2-Chlorohexylacetate	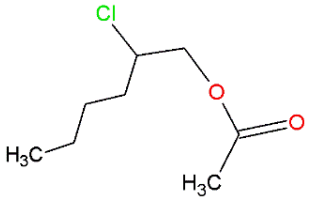	$C_8H_{15}ClO_2$	178.66	0.02	No activity reported

Table 24. Comparison of phytocompounds among DEAP, DEZSC, and DEVE using GC-MS analysis

No	Compound name	DEAP (%)	DEZSC (%)	DEVE (%)	Activity
1	1-Heptatriacotanol	60.29	-	-	Anti-cancer activity (Hameed *et al*., 2016), Highly antimicrobial on *P. aeruginosa* (Olajuyigbe *et al.*, 2018)
2	Androsta-1,4-dien-3-one, 6,17-dihydroxy-, (6β,17 β)	32.27	-	-	No activity reported
3	Palmitic acid	1.28	26.92	21.40	Anti-cancer on HCT-116 cells and showed high-affinity interaction on DNA topoisomerase-I (Ravi and Krishnan, 2016), Antifungal on *B. cereus* (Idowu and Ojo, 2017), Antioxidant on increasing DPPH free radical scavenging (Shah and Iqbal, 2018)
4	Linolenic acid	-	11.22	12.08	Antimicrobial on *Staphylococcus aureus* and *B. cereus* (Lee *et al*., 2002)
5	Neophytadiene	1.20	7.91	19.36	Anti-cancer on MCF-7 and HeLa cells (Eswaraiah *et al.*, 2019), Anti-inflammatory (Carretero *et al.*, 2008), Antioxidant (Raman *et al.*, 2012), Antimicrobial on *E. coli*, *S. aureus*, *C. albicans*, *and A. niger* (Mendiola *et al.*, 2008)
6	Linoleic acid	-	6.32	6.70	Anti-cancer on LoVo and RKO cells by increasing *cas-3* and *-9* (Lu *et al.*, 2010), Antimicrobial on *S. aureus* and *S. pyogenes* (Zheng *et al.*, 2005)
7	γ-sitosterol	3.04	-	-	Anti-cancer by cell cycle arrest in G2/M and apoptosis through *c-myc* suppression in MCF-7 and A-549 (Sundarraj *et al.*, 2012), Antimicrobial on *S. aureus*, *S. typhimurium* and *C.* albicans, Anti-inflammatory by increasing free radical scavenging by DPPH assay (Abu-lafi *et al.*, 2019)
8	n-Tetracosanol-1	-	6.07	-	Anti-cancer on melanoma cells (Vergara *et al*., 2015), Antimutagenic on *S. typhimurium* (Makhafola *et al.*, 2017), Antibacterial on *S. aureus*, *P. aeruginosa*, *K. pneumonia* and *P. vulgaris* (Kumari, Menghani and Mithal, 2019)

Table 24. Comparison of phytocompounds among DEAP, DEZSC, and DEVE using GC-MS (continued)

No	Compound name	DEAP (%)	DEZSC (%)	DEVE (%)	Activity
9	Octacosanol	-	5.26	-	Anti-cancer on A549 cells, Antibacterial on *Pseudomonas aeruginosa*, *Bordetella bronchiseptica*, *Escherichia coli*, *Burkholderia cenocepacia*, *Acinetobacter iwoffii*, *Acinetobacter baumannii*, *Moraxella catarrhalis*, *Bacillus subtilis* and *Staphylococcus aureus* (Coccimiglio *et al.*, 2016)
10	Stigmast-5-en-3-ol	-	5.24	-	Anti-cancer on HL-60 and MCF-7 cells (Fernando *et al.*, 2018), Immunomodulator by increasing hemagglutinating antibody titer (Parihar *et al.*, 2017)
11	Stigmasterol	0.98	4.91	5.34	Anti-angiogenesis on HUVECs cells (Kangsamaksin *et al.*, 2017), Anti-inflammatory in counteracting the IL-1β (Gabay *et al.*, 2010), Antioxidant and Antigenotoxic by reducing DNA damage (Ali *et al.*, 2015)
12	Stearic acid	-	3.80	-	Anti-cancer on human breast cancer cells induced mouse model (Fermor *et al.*, 1992), Antioxidant on reducing neurons damage of H_2O_2 (Wang *et al.*, 2007)
13	Phytol	-	4.07	13.36	Anti-cancer on A549 by depolarizing the mitochondrial membrane potential and upregulating BAX and downregulating BCL-2 and promoting cas-9 and -3, Antiangiogenic on chick embryo *chorioallantoic* membrane (Sakthivel *et al*., 2018), Antioxidant by showing free radical decreasing and Antinociception on central and peripheral nerve system (Santos *et al.*, 2013), Antimicrobial on *Pseudomonas aeruginosa*, *Staphylococcus aureus*, *Escherichia coli*, *Salmonella typhi* (Nithya *et al.*, 2018)
14	Hentriacontane	-	-	5.41	Antiinflammatory by suppressing TNF-alpha, IL-6, PGE_2, and COX-2 (Kim *et al.*, 2011)
15	Heneicosane	-	-	3.12	Anti-cancer on HCT-116 and HepG2 (Alkhalf *et al.*, 2019), antimicrobial (Albouchi *et al.*, 2013)

Table 24. Comparison of phytocompounds among DEAP, DEZSC, and DEVE using GC-MS (continued)

No	Compound name	DEAP (%)	DEZSC (%)	DEVE (%)	Activity
16	Phytyl linoleate	-	-	2.59	No activity reported
17	Lupenone	-	2.91	-	Anti-inflammatory by inhibiting edema in mice and reducing NO production on RAW 264.7 macrophages (Romero-Estrada *et al*., 2016), Anti-cancer on MCF-7 cells (Suwito *et al*., 2016)
18	Loliolide	-	-	1.64	Anti-inflammation by reducing ROS and upregulating IL-1a, IL-17, IL-22 and p-PI3K and p-AKT on keratinocytes (Park *et al.*, 2019), Antimicrobial on *C. albicans* (Ragasa *et al*., 2005)
19	Squalene	-	1.68	-	Anti-cancer on A431 (skin cancer cell lines) (Mohansrinivasan *et al.*, 2015), chemoprotection on cisplatin and carboplatin (Das *et al.*, 2008)
20	Lupeol	-	1.91	-	Anti-angiogenesis in HUVECs (Kangsamaksin *et al.*, 2017), Anti-cancer on MCF-7 cells (Pitchai, Roy and Ignatius, 2014), Antioxidant (Tchimene *et al.*, 2016), Anti-inflammatory by reducing prostaglandin E2 (PGE2) (Fernández *et al.*, 2001)
21	Phytol, acetate	-	1.28	4.67	Antimicrobial on *Aspergillus terreus*, Anti-cancer on MCF-7 and HepG2 cells (Farid *et al.*, 2015)
22	α-Tocospiro B	-	1.44	-	No activity reported
23	α-Tocospiro A	-	1.34	-	No activity reported
24	γ-Tocopherol	-	1.11	-	Antioxidant by retarding the oxidation of RO TAG (Lampi *et al.*, 1999)
25	Campesterol	-	1.04	-	Anti-angiogenic on HUVECs cells and *in vivo chorioallantoic membrane* (Choi *et al.*, 2007), Antioxidant by decreasing lipid peroxidation (Yoshida *et al*., 2003)
26	6,10,14-trimethyl pentadecane-2-one	0.53	1.79	1.93	Antimicrobial on *Y. pseudotuberculosis*, *E. faecalis*, and *S. aureus* (Yayli *et al.*, 2006)
27	Myristic acid	-	1.33	-	No activity reported

Part II. Anti-cancer effect of combination among the selected extract with PFPE on the selected cancer cell lines

As the dichloromethane extract of all plants leaves gave the strongest cytotoxic activity and included to the criteria of *in vitro* cytotoxicity which IC_{50} less than 20 µg/ml and less toxic to non-cancerous cell lines, the dichloromethane extract of all plant leaves were combined with PFPE against highly respond cell lines. This study was performed by harnessing the IC_{50} values of each extract as a baseline and utterly done with four ratios (IC_{50}:IC_{50}, $0.5IC_{50}$:IC_{50}, IC_{50}:$0.5IC_{50}$ and $0.5IC_{50}$:$0.5IC_{50}$). The CI values were computerized by *Compusyn* software to determine the interaction of the extracts and PFPE.

All ratios of combination among DEAP and PFPE showed an antagonistic effect to HT-29 and SW-620 cells with the CI values of 1.12 ± 0.04 to 1.86 ± 0.05 and 1.14 ± 0.01 to 1.33 ± 0.04, respectively. Combination among DEZSC combined with PFPE showed an antagonistic effect, while exposed to the A2780 cell line with the CI values of 1.39 ± 0.07 to 8.05 ± 5.49. Surprisingly, the reduction of PFPE dose (final dose 0.5 x IC_{50}) was giving a synergistic effect when combined with IC_{50} of DEZSC against MCF-7 cells indicated with the CI values of 0.72 ± 0.77. Moreover, combination among DEVE and PFPE showed an antagonistic effect against A2780 cell line with the CI values of 1.23 ± 0.08 to 6.70 ± 1.61. A noteworthy finding revealed that DEVE indicated the greatest synergistic interaction along with PFPE against MCF-7 cell line with the CI values of 0.34 ± 0.06 to 0.44 ± 0.14. Surprisingly, the ratio IC_{50}:IC_{50} showed the highest cell inhibition at 97.29 ± 0.33%. This finding encourages to use this regimen in apoptosis and multi-caspase activity experiments. Alternatively, behalf the doses of combination (0.5 IC_{50}:0.5 IC_{50}) indicated the antagonistic effect against MCF-7 cell line with the CI values of 1.42 ± 0.06 (Table 25). Therefore, in further investigation this combination at ratio IC_{50}:IC_{50} was used as a regimen in apoptosis and multi-caspase activity.

Table 25. Combination Index (CI) value of the combination among DEAP, DEZSC, and DEVE with PFPE at different four ratios against selected cell line

Combination	Cell Line	Ratio	Dose (µg/ml)		%inhibition ± SD	CI ± SD	Remark
			Extract	PFPE			
DEAP+PFPE	HT-29	IC_{50}:IC_{50}	8.93	17.63	82.35 ± 1.13	1.12 ± 0.04	Antagonism
		$0.5IC_{50}$:IC_{50}	4.46	17.63	54.89 ± 1.34	1.86 ± 0.05	Antagonism
		IC_{50}:$0.5IC_{50}$	8.93	8.82	47.37 ± 2.45	1.74 ± 0.08	Antagonism
		$0.5IC_{50}$: $0.5IC_{50}$	4.46	8.82	34.21 ± 0.24	1.73 ± 0.01	Antagonism
	SW-620	IC_{50}:IC_{50}	7.49	11.30	81.20 ± 1.55	1.09 ± 0.06	Antagonism
		$0.5IC_{50}$:IC_{50}	3.74	11.30	67.68 ± 1.25	1.29 ± 0.04	Antagonism
		IC_{50}:$0.5IC_{50}$	7.49	5.65	65.58 ± 0.77	1.14 ± 0.01	Antagonism
		$0.5IC_{50}$: $0.5IC_{50}$	3.74	5.65	43.00 ± 1.20	1.33 ± 0.04	Antagonism
DEZSC+PFPE	MCF-7	IC_{50}:IC_{50}	13.35	21.06	78.65 ± 4.33	1.19 ± 0.16	Antagonism
		$0.5IC_{50}$:IC_{50}	6.675	21.06	50.4 ± 2.65	1.86 ± 0.11	Antagonism
		IC_{50}:$0.5IC_{50}$	13.35	10.53	82.66 ± 2.65	0.72 ± 0.07	Synergism
		$0.5IC_{50}$: $0.5IC_{50}$	6.675	10.53	37.07 ± 1.05	1.52 ± 0.04	Antagonism
	A2780	IC_{50}:IC_{50}	14.64	21.12	72.46 ± 5.09	1.39 ± 0.07	Antagonism
		$0.5IC_{50}$:IC_{50}	7.32	21.12	13.59 ± 4.36	8.05 ± 5.49	Antagonism
		IC_{50}:$0.5IC_{50}$	14.64	10.56	48.7 ± 8.73	1.66 ± 0.30	Antagonism
		$0.5IC_{50}$: $0.5IC_{50}$	7.32	10.56	3.7 ± 5.09	4.77 ± 0.91	Antagonism
DEVE+PFPE	MCF-7	IC_{50}:IC_{50}	15.58	21.06	97.29 ± 0.33	0.36 ± 0.03	Synergism
		$0.5IC_{50}$:IC_{50}	7.79	21.06	93.65 ± 3.72	0.44 ± 0.14	Synergism
		IC_{50}:$0.5IC_{50}$	15.58	10.53	95.32 ± 1.50	0.34 ± 0.06	Synergism
		$0.5IC_{50}$: $0.5IC_{50}$	7.79	10.53	37.69 ± 4.12	1.42 ± 0.06	Antagonism
	A2780	IC_{50}:IC_{50}	10.08	21.12	80.41 ± 1.97	1.23 ± 0.08	Antagonism
		$0.5IC_{50}$:IC_{50}	5.04	21.12	10.11 ± 4.19	6.70 ± 1.61	Antagonism
		IC_{50}:$0.5IC_{50}$	10.08	10.56	51.22 ± 4.84	1.63 ± 0.16	Antagonism
		$0.5IC_{50}$: $0.5IC_{50}$	5.04	10.56	5.54 ± 2.14	5.55 ± 1.18	Antagonism

Part III. The potency of selected plant extract with PFPE in apoptosis and multi-caspases activity on the selected cancer cell lines

1. Apoptosis activity

Previously, the ratio IC_{50}:IC_{50} of combination amongst dichloromethane extract of *V. extensa* leaves (DEVE) and PFPE showed the greatest cytotoxic activity and synergistic effect towards MCF-7 cell line. The apoptosis activity was evaluated by carrying the combination of DEVE and PFPE in ratio IC_{50} extract : IC_{50} PFPE as a treatment and stained with Annexin V/PI. The MCF-7 cell line was incubated at time varying (24, 48, 72 and 96 h) and 0 h as a control. Figure 39 displays live, early apoptosis, late apoptosis, and dead cells. Surprisingly, the total apoptosis rate was increased significantly at 72 and 96 h for 33.37 ± 4.00%, and 47.95 ± 10.42%, respectively (*p*-value less than 0.05). Briefly, annexin V/PI assay revealed that the rate of apoptosis increased in response to the combination of DEVE and PFPE with a time-dependent manner.

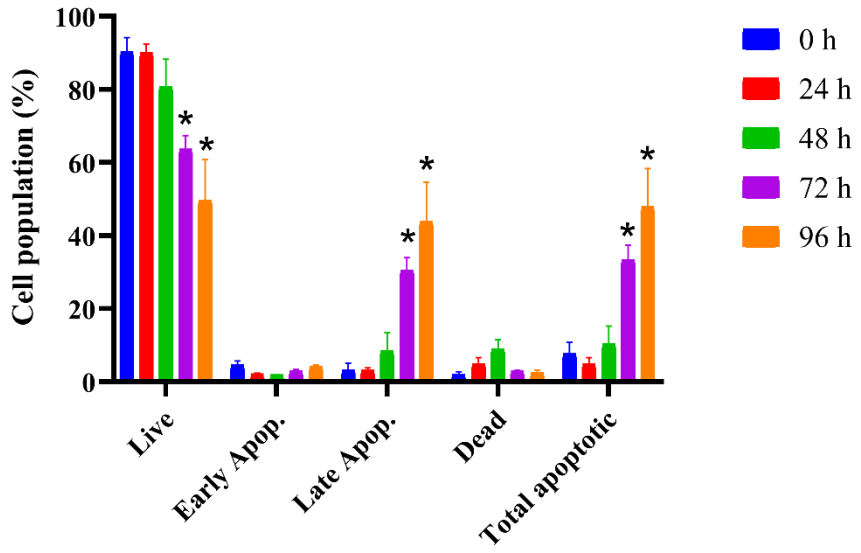

Figure 39. Live, early apoptosis, late apoptosis, dead and total apoptotic cells percentage treated with the combination of DEVE and PFPE at ratio IC_{50}:IC_{50} in MCF-7 cell lines within 24, 48, 72, and 96 h. Data exhibited as mean ± SD with at least two independent experiments. $P < 0.05$ was concluded as significant difference compared to control group (0 h)

2. Multi-caspase activity

After the apoptotic activity was evaluated by annexin V/PI, multi-caspase activity was assessed to determine whether combination of DEVE and PFPE at ratio IC_{50}:IC_{50} could be associated with caspases using multi-caspase. After treatment, the treated cell was stained in multi-caspase and 7-AAD assays. As the results described in Figure 40, caspases+ cells were initially observed at 28.25 ± 1.20%. Intriguingly, the total caspases were increased significantly at 72 h compared to control with 67.93 ± 6.19% (*p*-value less than 0.05). Therefore, the results revealed that the combination among DEVE and PFPE at ratio IC_{50}:IC_{50} increased the multi-caspase activity in the time-dependent manner.

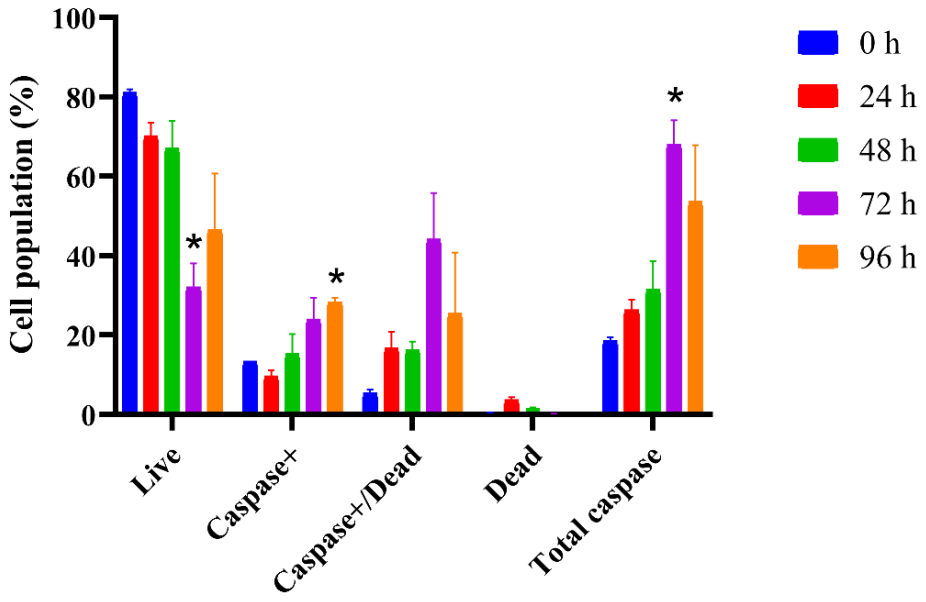

Figure 40. Relative cell caspases treated with the combination of DEVE and PFPE at ratio IC_{50}:IC_{50} in MCF-7 cell lines within 24, 48, 72, and 96 h as determined by Multi-caspase and 7-AminoActinomycin D (7-AAD). Data represented mean ± SD of at least two independent experiments. $P < 0.05$ was concluded as significant difference compared to control group (0 h)

CHAPTER 4
DISCUSSION

Part I. Anti-cancer effect of different plant extracts on several cell lines

Cancer is a non-communicable disease (NCD) causing around 9.6 million death cases and the second position under heart diseases in 2018 (WHO, 2018). Breast, colorectal, and ovarian cancers are the menacing issue for the human race since many free radicals and carcinogens expand massively and severely caused devastation in DNA (Barnes *et al.*, 2018; Santos-Sánchez *et al.*, 2019). Many studies have been performed about to the potency of natural products in both cancer treatment and prevention *in vitro* based research. This study was done in cell lines (*in vitro*) to find out underlying mechanisms of the natural products. The study was wholly initiated with crude extracts.

The evaluation of the cytotoxic effect focused on the median inhibitory concentration (IC_{50}) of all extracts. *A. paniculata*, a species possessing a versatile phytoconstituent, namely andrographolide. The dichloromethane extract of *A. paniculata* was reported contained andrographolide and its derivatives (Kumar *et al.*, 2004). That report indicated a significant inhibitory of proliferation in SW-620 and HT-29 cell lines. Other previous studies were concerning in the cytotoxic activity of the dichloromethane extract of *A. paniculata* towards colorectal cancer cells, which had been done before by Kumar and Tan colleagues (2004 and 2016). Dichloromethane extract of *A. paniculata* leaves significantly inhibited the proliferation of HT-29 cell lines, indicated by an IC_{50} less than 10 µg/ml (Kumar *et al.*, 2004; Tan *et al.*, 2016). Several studies denoted that whole parts of *A. paniculata* possessed a remarkable anti-cancer activity towards several cell lines (Ponglux *et al.*, 1992; Kumar *et al.*, 2004; Cheung *et al.*, 2005; Sukardiman *et al.*, 2014).

Sedr or Christ's thorn jujube (scientific name: Z. *spina-christi*) is widely distributed and well-known in the Middle East and has been introduced to Southeast Asia countries such as Indonesia, Thailand, Malaysia, Brunei, etc. Present study results indicated that the dichloromethane extract of *Z. spina-christi* leaves possessed the most significant anti-cancer effect against A2780 and MCF-7 cell lines. Accordantly, the same genus, *Ziziphus mauritiana* barks, were extracted and fractionated into

dichloromethane. This fraction indicated very high cytotoxicity in NCI-H460 and MCF-7 cells (Tagne *et al.*, 2015).

Another notable result was found in this study. Taxonomically, bitter leaves (English) or *phim pai lin* (Thai) are identified as *V. extensa*, which belong to the Asteraceae family. The bitter leaf extracts were tested and revealed that the dichloromethane extract of *V. extensa* leaves showed the highest inhibitory effect in MCF-7 and A2780 cell lines. A study was conducted by Thongnest and colleagues revealed a noteworthy anti-cancer effect induced by this extract toward HepG2 (human liver carcinoma cell lines), HuCCA-1 (human cholangiocarcinoma cell lines), A549 (human non-small cell lung cancer cell lines), and MOLT-3 (human leukemic cell lines) (Thongnest *et al.*, 2019).

Phytochemical analysis was carried out to find out the major bioactive compounds of the most cytotoxic crude extracts. Due to the DEAP, DEZSC, and DEVE have texture apparently like oily paste, the expectation that these extracts contain active volatile compounds then the GC-MS analysis was conducted. The phytocompounds of DEAP, DEZSC, and DEVE were selected in which match factor more than 85%. The chromatogram of GC-MS analysis clearly described some significant peaks, which are described by Figure 36-38. According to Table 21, DEAP contained 5 major peaks separated in several chemical groups such as alcohols, steroids, fatty acids, and terpenes. Palmitic acid and neophytadiene extracted from *Kigelia pinnata* and *Avicennia alba*, respectively, showed an anti-cancer activity (Ravi and Krishnan, 2016; Eswaraiah *et al.*, 2019). A recent report revealed that palmitic acid and neophytadiene were respectively observed in hexane fraction of *Commelina nudiflora* as well as the aqueous and methanolic fraction of *Eupatorium odoratum*. The fractions showed low antioxidant activity (Shah and Iqbal, 2018). Two major compounds, 1-heptatriacotanol and androsta-1,4-dien,3-one, 6,17-dihydroxy-(6β,17β) have not been reported to their anti-cancer activity. Thus, a study either *in vivo* or molecular signaling pathways is required to evaluate of the potency of the compounds in the future.

The GC-MS analysis of DEZSC was concisely illustrated in Figure 37 and Table 22. Several phytocompounds of DEZSC were reported in their anti-cancer property. Neophytadiene extracted from aqueous and methanolic extract of *E. odoratum* exhibited its anti-cancer property in human breast cancer cells (Eswaraiah *et*

al., 2019) as well as palmitic acid from *K. pinnata* and pure linoleic acid had a cytotoxic effect in human colorectal cancer cells (Lu *et al.*, 2010; Ravi and Krishnan, 2016). Furthermore, fatty alcohols such as n-tetracosanol-1 and octacosanol were denoted their anti-cancer activity in melanoma and non-small cell lung cancer cells, respectively (Vergara *et al.*, 2015; Coccimiglio *et al.*, 2016). Other chemical compounds that presence in DEZSC leaves, stigmast-5-en-3-ol, and stigmasterol belong to the steroids group. Stigmast-5-en-3-ol was reported as a potential anti-cancer phytoconstituent against HL-60 and MCF-7 cell lines (Fernando *et al.*, 2018) as well as stigmasterol could induce anti-angiogenic in HUVEC cells (Kangsamaksin *et al.*, 2017).

Besides its high cytotoxicity to cancerous cells, DEZSC leaves exhibited slight cytotoxicity to Vero and L929 cell lines. The determined phytoconstituents were reported possessed of antioxidant and anti-inflammatory features (Wang *et al.*, 2007; Carretero *et al.*, 2008; Gabay *et al.*, 2010). The results are concordance to previous a finding that a butanol extract of *Ziziphus spina-christi* leaves did not show any manifestation of hepatotoxicity and nephrotoxicity (Abdel-zaher *et al.*, 2005). The antioxidant substance such flavonoids would become an active anti-cancer agent while it is collaborating with another chemical group such as sesquiterpenes (Sghaier *et al.*, 2011). Antioxidants are determined as the chemical compounds that can attenuate the damaging effects of reactive oxygen species (ROS) (Kooti and Daraei, 2017). The reactive oxygen species would devastate various biomolecules consists of proteins, lipids, and lipoproteins and bring to many diseases such as cancers (Sharma *et al.*, 2012). Therefore, the findings could emphasize that DEZSC leaves might be a potential candidate for cancer prevention and treatment.

Figure 38 and Table 23 were provided to describe phytocompounds of DEVE leaves. Numerous natural compounds were investigated and employed for cancer treatment. The study results imply the most considerable cytotoxicity of DEVE leaves and confirm the bioactive phytocompounds contained in DEVE. Palmitic acid and heneicosane showed an anti-cancer property towards colorectal cancer cell lines such as HCT-116 cells (Ravi and Krishnan, 2016; Alkhalf *et al.*, 2019), LoVo and RKO were significantly inhibited by linoleic acid (Lu *et al.*, 2010). Neophytadiene exhibited an anti-cancer effect against MCF-7 and HeLa cell lines (Eswaraiah *et al.*, 2019).

Ponglux and colleagues revealed that two sterol glucosides extracted from the methanolic extract of *V. extensa.* The methanolic extract had similar properties to the bitter compound found in the African *Vernonia* genus (Ponglux *et al.*, 1992). Similarly, *Vernonia* genus was studied in several cancer cell lines including prostate cancer cell lines PC-3, human leukemic cell lines HL-60, colorectal cancer cell lines WiDr, breast cancer cell lines MCF-7, and human melanoma cell lines HT-144 (Farombi and Owoeye, 2011; Wong *et al.*, 2013; Lowe *et al.*, 2014; Bestari *et al.*, 2018). The study results suggest that DEAP, DEZSC, and DEVE leaves might be considered as potential alternative medicines to suppress the cancerous cells by either reducing the free radical or directly suppressing the cancer proliferation.

Part II. Anti-cancer effect of combination among the selected extract with PFPE on the selected cancer cell lines

Previously, the study revealed that the dichloromethane extract of *A. paniculata, Z. spina-christi,* and *V. extensa* showed the strongest cytotoxicity which is included to have *in vitro* cytotoxicity, indicated as IC_{50} < 20 µg/ml (Sriwiriyajan *et al.*, 2014). A study to compare the cytotoxicity piperine and PFPE reported that piperine had more than 20 µg/ml which was less than PFPE 7.45 ± 1.59 µg/ml (Sriwiriyajan *et al*., 2014). These reports emphasized that PFPE is more potent than piperine and might be high potency as a combination with plant extracts.

The investigation using DEAP, DEZSC, and DEVE conducted in four ratios in which IC_{50} as a baseline. The combination study demonstrated that DEAP and DEZSC showed antagonistic effect with PFPE. Alternatively, DEVE and PFPE showed a synergistic effect. According to Table 24, DEVE have several volatile promising phytocompounds, which are greater than DEAP and DEZSC, such as neophytadiene, phytol, hentriacontane, heneicosane, and phytol acetate which previously reported in anti-cancer activity. Thus, DEVE phytocompounds might collaborate together with PFPE active compounds.

The results highlighted a synergistic effect (CI < 1) in both DEVE with PFPE against the MCF-7 cell line. Neophytadiene (19.36%, in DEVE) and phytol acetate (4.67% in DEVE) showed cytotoxicity against breast cancer cell lines (MCF-7) (IC_{50}= 57.02 µg/ml and 3.53 µg/ml, respectively) (Farid *et al.*, 2015; Eswaraiah *et al.*,

2019). Moreover, beta-selinene (0.60% in PFPE), piperyline (2.58% in PFPE), pellitorine (2.28% in PFPE), piperlonguminine (4.77% in PFPE), and kusunokinin (1.28% in PFPE) showed cytotoxic activity against breast cancer cell lines (MCF-7) (IC_{50} = 19.69 µg/ml, 27.1 µg/ml, 1.8 µg/ml, 1.63 µg/ml, and 1.18 µg/ml, respectively) (Kaewsa-ard *et al.*, 2012; Ku *et al.*, 2014; De Souza Grinevicius *et al.*, 2016; Sriwiriyajan *et al.*, 2017).

Another phytocompounds showed cytotoxicity towards cancer cell lines. Palmitic acid (21.40% in DEVE), linoleic acid (6.70% in DEVE), dihydroactinidiolide (0.47% in DEVE), and 1,2-benzenedicarboxylic acid, dibutyl ester (0.19% in DEVE) showed cytotoxicity in human colorectal cancer cell lines (HCT-116, LoVo, RKO, and COLO 320) (Malek *et al.*, 2009; Lu *et al.*, 2010; Gunalan *et al.*, 2016; Ravi and Krishnan, 2016; Alkhalf *et al.*, 2019). Phytol acetate (4.67% in DEVE), heneicosane (3.12% in DEVE) and tricosane (0.33% in DEVE) showed anti-cancer effect against HepG2 (human liver carcinoma) (Farid *et al.*, 2015; Poma *et al.*, 2018; Alkhalf *et al.*, 2019). While the phytocompounds of PFPE including pipersintenamide (5.65% in PFPE) and beta-elemene (2.93% in PFPE) showed anti-cancer effect towards human cancerous cell lines (Chen *et al.*, 2002; Li *et al.*, 2017). This regimen might be an enormous anti-cancer drug due to its anti-cancer activity in cancer cells.

Interestingly, the most major compound of DEVE, palmitic acid (21.40% in DEVE) strongly intercalated to DNA topoisomerase-I as well as kusunokinin (1.28% in PFPE) intercalated to DNA topoisomerase-II expression (Ravi and Krishnan, 2016; Sriwiriyajan *et al.*, 2017). DNA topoisomerases have been targeted as anti-cancer drugs such as irinotecan, camptothecin, and topotecan (DNA topoisomerase-I inhibitor), and etoposide, amsacrine, and teniposide (DNA topoisomerase-II inhibitor) (Kathiravan *et al.*, 2013). Double topoisomerase inhibitions are a strategy in the anti-cancer treatment to prevent multi-drug resistance (MDR) (Bielawski *et al.*, 2006).

Hentriacontane (5.41% in DEVE) could suppress TNF-α protein (Kim *et al.*, 2011). TNF-α is a protein promoter of the inflammatory and immune system which enable to modulate the metabolism of cell by regulating gene expression which plays roles as cell proliferation and survival modulator (Miscia *et al.*, 2002). The TNF-α proteins could enhance signal transducer and activator of transcription 3 (STAT3)

phosphorylation *via* NF-κB, which promotes breast cancer progression (Cai *et al.*, 2017). STAT3 is a transcription factor that regulates cell proliferation, apoptosis, angiogenesis, immune responses, and inflammation. Excessive STAT3 expression could trigger tumor development through oncogenic gene expression in various human cancers, by leading to promote tumor malignancy. On the other hand, STAT3 expression could suppress the immune system (Lee, Jeong, and Ye, 2019). Interestingly, caryophyllene oxide (0.42% in PFPE) was reported as a STAT3 inhibitor (Kim *et al.*, 2013). Another phytocompound namely 1,2-benzenedicarboxylic acid, dibutyl ester (0.19% in DEVE) showed high binding to KRAS protein (Gunalan *et al.*, 2016). The KRAS protein expression was reported increasing phosphatidylinositol-3-kinase (PI3K)/3-phosphoinositide-dependent kinase-1 (Pdk1) protein level. PI3K/Pdk1 activates AKT signaling pathway and leads to NF-κB. As previously mentioned, NF-κB phosphorylates and promotes breast cancer progression (Eser *et al.*, 2014; Cai *et al.*, 2017). Due to the ratio IC_{50}:IC_{50} of DEVE and PFPE showed the highest percentage of inhibition compared to the others (see Table 25), the combination of DEVE and PFPE at ratio IC_{50}:IC_{50} was used in is expected in targeting of multiple signaling pathways which would be a potential target for cancer treatment. In the final part of this study, the combination of DEVE and PFPE ratio at IC_{50}:IC_{50} was considerably used in apoptosis and multi-caspase activities.

Part III. The potency of selected plant extract with PFPE in apoptosis and multi-caspases on the selected cancer cell lines

Due to the combination study among DEVE and PFPE at ratio IC_{50}:IC_{50} inhibited synergistically towards MCF-7 cell lines, then the further experiments were conducted to evaluate the apoptotic and multi-caspase activities induced by the combination which related to the anti-cancer feature. Apoptosis is known as programmed cell death which is targeting cell suicide orchestrated by several cellular signaling pathways (Alberts *et al.*, 2008). Several characteristics of apoptosis consist of cell shrinkage, DNA fragmentation, and chromatin condensation (Wlodkowic *et al.*, 2011). The activation of apoptosis is initiated by the movement of phosphatidylserine (PS) from the inner side of the cell to the surface of membrane cell in the early apoptosis

event (Koopman *et al.*, 1994). The study highlighted that the combination of DEVE and PFPE induces apoptosis with time-dependent (see Figure 39 and 40).

Previous western blot analysis elucidated the mechanisms of other phytocompounds. Palmitic acid (21.40% in DEVE), phytol (13.36% in DEVE), linoleic acid (6.70% in DEVE), stigmasterol (5.34% in DEVE), and α-tocopherol (0.60% in DEVE) enhance apoptosis cells as well as apoptotic and anti-apoptotic associated proteins (Lu *et al.*, 2010; Zulkapli *et al.*, 2017; Li *et al.*, 2018a; Sakthivel, Malar and Devi, 2018; Zafaryab *et al.*, 2019). Moreover, phytol and linoleic acid induced caspase-dependent apoptosis. Not only phytocompounds of DEVE, but also phytocompounds of PFPE such as beta-elemene (2.93% in PFPE), piperyline (2.58% in PFPE), delta-cadinene (0.60% in PFPE), and cubebin (0.28% in PFPE) induced caspase-dependent apoptosis towards leukemic, ovarian, and breast cancer cell line, respectively (Medina *et al.*, 1997; Li *et al.*, 2014; Hui *et al.*, 2015; Niwa *et al.*, 2016). Apoptosis is indicated by losing of mitochondrial membrane potential and cyt-c normally followed by the activating of caspases (Li *et al.*, 2018b). These findings revealed that the combination among DEVE and PFPE at ratio IC_{50}:IC_{50} induces caspase-dependent apoptosis in MCF-7 cells with time-dependent.

CHAPTER 5
CONCLUSIONS

Part I. Anti-cancer effect of different plant extracts on several cell lines

1. Cytotoxic activity of *A. paniculata, Z. spina-christi,* and *V. extensa* leaves extracts on several cell lines by MTT assay

The results from the anti-cancer effect of different extracts of *A. paniculata, Z. spina-christi,* and *V. extensa* towards several cell lines suggest that:

1. Dichloromethane extract of *A. paniculata* leaves showed the strongest anti-cancer effect on HT-29 and SW-620 cell lines with IC_{50} at 8.93 ± 0.52 μg/ml and 7.49 ± 0.04 μg/ml, respectively.

2. Dichloromethane extract of *Z. spina-christi* showed the strongest anti-cancer effect on MCF-7 and A2780 cell lines with IC_{50} at 13.35 ± 0.30 μg/ml and 14.64 ± 1.51 μg/ml, respectively.

3. Dichloromethane extract of *V. extensa* showed the strongest anti-cancer effect on MCF-7 and A2780 cell lines with IC_{50} at 15.58 ± 1.81 μg/ml and 10.08 ± 0.04 μg/ml, respectively.

2. Phytocompounds screening by GC-MS analysis

The GC-MS technique results of dichloromethane extract of *A. paniculata, Z. spina-christi,* and *V. extensa* leaves suggest that:

1. Dichloromethane extract of *A. paniculata* leaves contains 17 compounds with 2 major volatile compounds, 1-heptatriacotanol (60.29%, alcohols group) and androsta-1,4-dien-3-one, 6,17-dihydroxy-,(6β,17β) (32.27%, steroids group).

2. Dichloromethane extract of *Z. spina-christi* leaves contains 23 compounds with seven major volatile compounds such as palmitic acid (26.92%, fatty acids group), linolenic acid (11.22%, fatty acids group), neophytadiene (7.91%, terpenes group), linoleic acid (6.76%, fatty acids group), n-tetracosanol-1 (6.07%, fatty alcohols group), octacosanol (5.25%, fatty alcohols group), and stigmast-5-en-3-ol (5.24%, steroids group).

3. Dichloromethane extract of *V. extensa* leaves contains 27 compounds with seven major volatile compounds such as palmitic acid (21.40%, fatty acids group), neophytadiene (19.36%, terpenes group), phytol (13.36%, terpenes group), linolenic acid (12.08%, fatty acids group), linoleic acid (6.70%, fatty acids group), hentriacontane (5.41%, alkanes group), and stigmasterol (5.34%, steroids group).

Part II. Anti-cancer effect of combination among the selected extract with PFPE on the selected cancer cell lines

According to the study results, the combination among dichloromethane extract of *A. paniculata* (DEAP), *Z. spina-christi* (DEZSC), and *V. extensa* (DEVE) with PFPE on the chosen cell lines suggest that:

1. A combination of DEAP and PFPE at all ratio showed an antagonistic effect in HT-29 and SW-620 cell lines within 72 h treatment.

2. A combination of DEZSC and PFPE at all ratio showed an antagonistic effect in MCF-7 and A2780 cell lines except at ratio IC_{50}:0.5IC_{50} showed a synergistic interaction in MCF-7 cell line within 72 h treatment.

3. A combination of DEVE and PFPE at ratio IC_{50}:IC_{50}, 0.5IC_{50}:IC_{50}, and IC_{50}:0.5IC_{50} showed a synergistic effect in MCF-7 cells with CI value at 0.36 ± 0.03, 0.44 ± 0.14, and 0.34 ± 0.06 in MCF-7 cell line, and all ratio showed antagonistic interaction in A2780 cell line within 72 h treatment.

Part III. The potency of selected plant extract with PFPE in apoptosis and multi-caspases on the selected cancer cell lines

According to the study results, the combination among dichloromethane extract of *V. extensa* leaves and PFPE at ratio IC_{50}:IC_{50} induced apoptosis and leading to multi-caspase activity with time-dependent 24 to 96 h compared to control (0 h incubation) in MCF-7 cell line.

Future works

After investigating the promising phytocompounds contained in dichloromethane extract of *V. extensa* leaf, several phytocompounds of extract and collaborated with PFPE compounds were presumably involved as working via multiple signaling pathways such as TNF-α, STAT3, and DNA topoisomerase-I and II as well as caspases-mediated apoptosis. Therefore, it is necessary to conduct the western blot analysis to determine the protein expression of TNF-α, STAT3 and DNA topoisomerase-I and II and also apoptotic and anti-apoptotic proteins such as bax and bcl-2 which are involved as cancer target therapy.

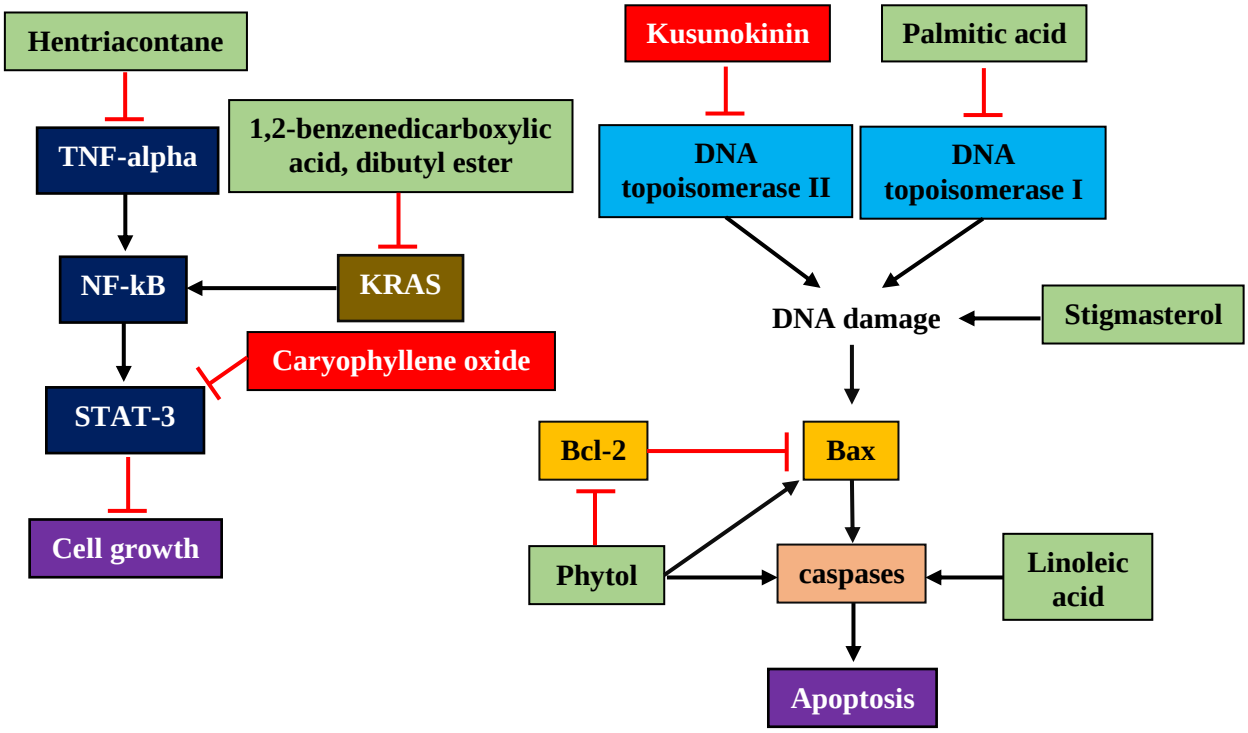

Figure 41. Expected pathway induced by the combination of DEVE and PFPE

REFERENCES

Aati H, El-Gamal A, Shaheen H, Kayser O. Traditional use of ethnomedicinal native plants in the Kingdom of Saudi Arabia. J Ethnobiol Ethnomed. 2019;15(2):1-9.

Abdel-raouf N, Al-Enazy NM, Al-Homaidan AA, Ibraheem IBM, Al-Othman MR, Hatamleh AA. Antibacterial β-amyrin isolated from *Laurencia microcladia.* Arab J Chem. 2015;8(1):32–37.

Abdel-zaher AO, Salim SY, Assaf MH, Abdel-Hady RH. Antidiabetic activity and toxicity of *Zizyphus spina-christi* leaves. J Ethnopharmacol. 2005;101(1–3):129–138.

Abosi AO, Raseroka BH. *In vivo* antimalarial activity of *Vernonia amygdalina*. Br J Biomed Sci. 2003;60(2):89–91.

Abud HE. Shaping developing tissues by apoptosis. Cell Death Differ. 2004;11:797–799.

Abu-lafi S, Rayan M, Masalha M, Abu-Farich B, Al-Jaas H, et al. Phytochemical composition and biological Activities of Wild *Scolymus maculatus* L. Medicines. 2019;6(2):53.

Abu-Raghif AR, Jasim GA, Hanoon MM. Anti-proliferative Activity of *Zizyphus spina-christi* leaves methanol extract against Rhabdomyosarcoma (Rd) cell line. Int J Pharm Pharm Sci. 2017;9(2):279–282.

Adesanoye OA, Farombi EO. 2010. Hepatoprotective effects of *Vernonia amygdalina* (astereaceae) in rats treated with carbon tetrachloride. Exp Toxicol Pathol. 2010;62(2):197–206.

Adriance MC, Inman JL, Petersen OW, Bissell MJ. Myoepithelial cells: good fences make good neighbors. Breast Cancer Res. 2005;7(5):190–197.

Adzu B, Amos S, Amizan MB, Gamaniel K. Evaluation of the antidiarrhoeal effects of *Zizyphus spina-christi* stem bark in rats. Acta Trop. 2003;87(2):245–250.

Agarwal D. 2015. Research paper a new anticancer flavonoid from the leaves of *Andrographis paniculata*. J Global Biosci. 2015;4(5):2355–2360.

Akinpelu DA. 1999. Antimicrobial activity of *Vernonia amygdalina* leaves. Fitoterapia. 1999;70(4):432–434.

Akkoca AN, Yanik S, Özdemir ZT, Cihan FG, Sayar S, Cincin TG, et al. TNM and modified Dukes staging along with the demographic characteristics of patients with colorectal carcinoma. Int J Clin Exp Med. 2014;7(9):2828–2835.

Alarcon MCBV, Lopes JLC, Herz W. Glaucolide B, a molluscicidal sesquiterpene lactone, and other constituents of *Vernonia eremophila*. Planta Med. 1990;56:271–273.

Alberts B, Johnson A, Lewis J, Raff M, Keith R, Walter P. Chapter 17: Programmed Cell Death (Apoptosis). In: Molecular Biology of the Cell. 5th edition. 2008. p.1115.

Albouchi F, Hassen I, Casabianca H, Hosni K. Phytochemicals, antioxidant, antimicrobial and phytotoxic activities of *Ailanthus altissima* (Mill.) Swingle leaves. S Afr J Bot. 2013;87(2013):164–174.

Al-Huqail AA, Elgaaly GA, Ibrahim MM. Identification of bioactive phytochemical from two Punica species using GC–MS and estimation of antioxidant activity of seed extracts. Saudi J Biol. Sci. 2018;25(7):1420–1428.

Ali H, Dixit S, Ali D, Alqahtani SM, Alarifi S, Alkahtani S. Isolation and evaluation of anticancer efficacy of stigmasterol in a mouse model of DMBA-induced skin carcinoma. Drug Des Devel Ther. 2015;9:2793–2800.

Alkhalf MI, Alansari WS, Ibrahim EA, Elhalwagy MEA. Anti-oxidant, anti-inflammatory and anti-cancer activities of avocado (*Persea americana*) fruit and seed extract. J King Saud Univ Sci. 2019;31(4):1358–1362.

Al-Marzooq MA. Phenolic compounds of Napek leave (*Zizyphus spina-christi* L.) as natural antioxidants. J Food Nutr Sci. 2014;2(5):207.

American Cancer Society, Breast cancer risk factors you cannot change [internet] 2017a [cited 2019 Jan 22]. Available from: https://www.cancer.org/cancer/breast-cancer/risk-and-prevention/breast-cancer-risk-factors-you-cannot-change.html.

American Cancer Society, Invasive Breast Cancer (IDC/ILC) [internet] 2017b [cited 2019 Jan 22]. Available from: https://www.cancer.org/cancer/breast-cancer/understanding-a-breast-cancer-diagnosis/types-of-breast cancer/invasive-breast-cancer.html.

American Cancer Society, Treating breast cancer [internet] 2017c [cited 2019 Jan 22]. Available from: https://www.cancer.org/content/dam/CRC/PDF/Public/8581.00.pdf.

American Cancer Society, Hormone therapy for breast cancer [internet] 2017d [cited 2019 Jan 22]. Available from: https://www.cancer.org/cancer/breast-cancer/treatment/hormone-therapy-for-breast-cancer.html.

American Cancer Society, How chemotherapy drugs work [internet] 2019c [cited 2020 May 15]. Available from: https://www.cancer.org/treatment/treatments-and-side-effects/treatment-types/chemotherapy/how-chemotherapy-drugs-work.html

American Cancer Society, Chemotherapy for breast cancer [internet] 2017e [cited 2019 Jan 22]. Available from: https://www.cancer.org/cancer/breast-cancer/treatment/chemotherapy-for-breast-cancer.html.

American Cancer Society, How is chemotherapy used to treat cancer [internet] 2019d [cited 2020 May 24]. Available from: https://www.cancer.org/treatment/treatments-and-side-effects/treatment-types/chemotherapy/how-is-chemotherapy-used-to-treat-cancer.html.

American Cancer Society, Targeted therapy for breast cancer [internet] 2018a [cited 2019 Jan 22]. Available from: https://www.cancer.org/cancer/breast-cancer/treatment/targeted-therapy-for-breast-cancer.html.

American Cancer Society, Colorectal cancer risk factors [internet] 2018b [cited 2019 Jan 22]. Available from: https://www.cancer.org/content/dam/CRC/PDF/Public/8605.00.pdf.

American Cancer Society, Treatment of colon cancer, by stage [internet] 2018c [cited 2019 Jan 22]. Available from: https://www.cancer.org/cancer/colon-rectal-cancer/treating/by-stage-colon.html.

American Cancer Society, Ovarian cancer risk factors [internet] 2018d [cited 2019 Jan 22]. Available from: https://www.cancer.org/cancer/ovarian-cancer/causes-risks-prevention/risk-factors.html.

American Cancer Society, Targeted therapy for breast cancer [internet] 2018e [cited 2019 Jan 22]. Available from: https://www.cancer.org/cancer/breast-cancer/treatment/targeted-therapy-for-breast-cancer.html.

American Cancer Society, Surgery for ovarian cancer [internet] 2018f [cited 2019 Jan 22]. Available from: https://www.cancer.org/cancer/ovarian-cancer/treating/surgery.html.

American Cancer Society, Known and Probable Human Carcinogens [internet] 2019a [cited 2019 Jan 22]. Available from: https://www.cancer.org/cancer/cancer-causes/general-info/known-and-probable-human-carcinogens.html.

American Cancer Society, Key Statistics for Ovarian Cancer [internet] 2019b [cited 2019 Jan 28]. Available from: https://www.cancer.org/cancer/ovarian-cancer/about/key-statistics.html.

American Joint Committee on Cancer (AJCC), AJCC Cancer staging form supplement [internet] 2018 [cited 2019 Jan 28]. Available from: https://cancerstaging.org/references-tools/deskreferences/Documents/AJCC%20Cancer%20Staging%20Form%20upplement.pdf.

American Type Culture Collection, ATCC® cell lines by gene mutation [internet] 2014 [cited 2019 Jan 24]. Available from: https://www.atcc.org/~/media/pdfs/culture%20guides/cell_lines_by_gene_mutation.ashx.

Anglesio MS, Wiegand KC, Melynk N, Chow C, Salamanca C, Prentice LM, et al. Type-specific cell line models for type-specific ovarian cancer research. PLoS ONE. 2013;8(9).

Anju D, Jugnu G, Kavita S, Arun N, Sandeep D. A review on medicinal prospectives of *Andrographis Paniculata* Nees', J Pharm Sci Innov. 2012;1(1):1–4.

Anyasor GN, Ogunwenmo KO, Oyelana OA, Akpofunure BE. Phytochemical constituents and antioxidant activities of aqueous and methanol stem extracts of Costus afer Ker Gawl. (Costaceae). Afr J Biotechnol. 2010;9(31):4880–4884.

Asgarpanah J, Haghighat E. Phytochemistry and pharmacologic properties of *Ziziphus spina-christi* (L.) Willd. Afr J Pharm Pharmacol. 2012;6(31).

Banerjee S, Kaye SB. New strategies in the treatment of ovarian cancer: Current clinical perspectives and future potential. Clin Cancer Res. 2013;19(5):961–968.

Barnes JL, Zubair M, John K, Poirier MC, Martin FL. Carcinogens and DNA damage. Biochem Soc Trans. 2018;46(5):1213–1224.

Baye T, Kebede H, Belete K. Agronomic evaluation of *Vernonia galamensis* germplasm collected from eastern Ethiopia. Ind Crop Prod. 2001;14(3):179–190.

BC Cancer Agency Cancer Drug Manual, Drug name: Leucovorin [internet] 2006 [cited 2019 Jan 22]. Available from: http://www.bccancer.bc.ca/drug-database-site/drug%20index/leucovorin_monograph_1apr2013_formatted.pdf.

Bestari R, Ichwan M, Mustofa, Satria D. Anticancer Activity of *Vernonia amygdalina* Del. Extract on WiDr Colon Cancer Cell Line. In 2nd Public Health International Conference. Atlantis Press. 2018. p.172–176.

Bou-assaly W, Mukherji S. Cetuximab (Erbitux). Am J Neuroradiol. 2010;31(4):626–627.

Bray F, Ferlay J, Soerjomataram I, Siegel RL, Torre LA, Jemal A. Global cancer statistics 2018: GLOBOCAN estimates of incidence and mortality worldwide for 36 cancers in 185 countries. CA Cancer J Clin. 2018;68(6):394–424.

Breast Screen Victoria, Lobular carcinoma in situ, atypical lobular hyperplasia and atypical ductal hyperplasia of the breast [internet] 2018 [cited 2019 Feb 14]. Available from: https://clara.breastscreen.org.au/intranet/documents/21/355/BSV_LCISALHADH_fact_sheet.pdf.

Bresalier RS, Raper SE, Hujanen ES, Kim YS. A new animal model for human colon cancer metastasis. Int J Cancer. 1987;39(5):625–630.

Builders MI, Wannang NN, Ajoku GA, Builders PF, Orisadipe A, Aguiyi JC. Evaluation of the antimalarial potential of *Vernonia ambigua* Kotschy and Peyr (Asteraceae). Int J Pharmacol. 2011;7(2):238–247.

Bunwong S, Chantaranothai P, Keeley SC. Revisions and key to the Vernonieae (Compositae) of Thailand. PhytoKeys. 2014;37:25–101.

Burkill HM. The useful plants of west tropical African. 2nd ed. 2018. Kew.

Buskuhl H, de Oliveira FL, Blind LZ, de Freitas RA, Barison A, Campos FR, et al. Sesquiterpene lactones from *Vernonia scorpioides* and their in vitro cytotoxicity. Phytochem. 2010;71(13):1539–1544.

Cai X, Cao C, Li J, Chen F, Zhang S, Liu B, et al. Inflammatory factor TNF-α promotes the growth of breast cancer via the positive feedback loop of TNFR1/NF-κB (and/or p38)/p-STAT3/HBXIP/TNFR1. Oncotarget. 2017;1–15.

Calabrese C, Berman SH, Babish JG, Ma X, Shinto L, Dorr M, et al. A phase I trial of andrographolide in HIV positive patients and normal volunteers. Phytother Res. 2000;14(5):333–338.

Canadian Cancer Society, Stages of breast cancer [internet] 2019 [cited 2019 Jan 22]. Available from: http://www.cancer.ca/en/cancer-information/cancer-type/breast/staging/?region=on.

Cancer Quest, Colon and Rectal Cancer [internet] 2018 [cited 2019 Feb 01]. Available from: https://www.cancerquest.org/patients/cancer-type/colon-and-rectal-cancer.

Carretero ME, López-Pérez JL, Abad MJ, Bermejo P, Tillet S, Israel A, et al. Preliminary study of the anti-inflammatory activity of hexane extract and fractions from *Bursera simaruba* (Linneo) Sarg. (Burseraceae) leaves. J Ethnopharmacol. 2008;116(1):11–15.

Chedea VS, Vicas SI, Socaciu C, Nagaya T, Ogola HJO, Yokota K, et al. Lipoxygenase-Quercetin interaction: a kinetic study through biochemical and spectroscopy approaches. In Biochemical testing. InTech, 2012. p. 151–178.

Chen JJ, Huang YC, Chen YC, Wang SH, Peng CY, Chen IS. Cytotoxic Amides from Piper sintenense', Planta Medica. 2002;68:980–985.

Chen H, Miao Q, Geng M, Liu J, Hu Y, Tian L. Anti-tumor effect of rutin on human neuroblastoma cell lines through inducing G2/M cell cycle arrest and promoting apoptosis. The Sci World J. 2013;2013.

Chen W, Feng L, Nie H, Zheng X. Andrographolide induces autophagic cell death in human liver cancer cells through cyclophilin D-mediated mitochondrial permeability transition pore. Carcinog. 2012;33(11):2190–2198.

Chen X, Zhang J, Yuan L, Lay Y, Wong YK, Lim TK, et al. Andrographolide suppresses MV4-11 cell proliferation through the inhibition of FLT3 signaling, fatty acid synthesis and cellular iron uptake. Molecules. 2017;22(9):1–18.

Chen X, He Y, Lu F. Review article autophagy in stem cell biology: A perspective on stem cell self-renewal and differentiation. Stem Cells Int. 2018;2018:1–11.

Chen YL, Gilbert MG, Vernonieae [internet] 2011 [cited 2020 Mar 25]. Available from: http://flora.huh.harvard.edu/china/mss/volume20/Flora_of_China_Volume_20_21_Vernonieae.pdf.

Cheng L, Lai, MD. Aberrant crypt foci as microscopic precursors of colorectal cancer. World J Gastroenterol. 2003;9(12):2642–2649.

Cheung HY, Cheung SH, Li J, Cheung CS, Lai WP, Fong WF, et al. Andrographolide isolated from *Andrographis paniculata* induces cell cycle arrest and mitochondrial-mediated apoptosis in human leukemic HL-60 cells. Planta Med. 2005;71(12):1106–1111.

Choi JM, Lee EO, Lee HJ, Kim KH, Ahm KS, Shim BS, et al. Identification of campesterol from *Chrysanthemum coronarium* L. and its antiangiogenic activities. Phytother Res. 2007;21(10):954–959.

Chou TC. Drug combination studies and their synergy quantification using the chou-talalay method. Cancer Res. 2010;70(2):440-446.

Chuah XQ, Okechukwu PN, Amini F, Teo SS. Eicosane, pentadecane and palmitic acid: The effects in in vitro wound healing studies. Asian Pac J Trop Biomed. 2018;8(10):490–499.

Chukwujekwu JC, Lategan CA, Smith PJ, Van Heerden FR, Van Staden J. Antiplasmodial and cytotoxic activity of isolated sesquiterpene lactones from the acetone leaf extract of *Vernonia colorata*. S Afr J Bot. 2009;75(1):176–179.

Cioffi G, Sanogo R, Diallo D, Romussi G, De Tommasi N. New compounds from an extract of *Vernonia colorata* leaves with anti-inflammatory activity. J Nat Prod. 2004;67(3):389–394.

Clarkson C, Maharaj VJ, Crouch NR, Grace OM, Pillay P, Matsabisa MG, et al. In vitro antiplasmodial activity of medicinal plants native to or naturalised in South Africa. J Ethnopharmacol. 2004;92:177–191.

Clement PB. 1987. Anatomy and histology of the ovary. In Kurman, R. J. (ed.) Blaustein's Pathology of the female genital tract. New York: Springer, 1987. p. 438–470.

Coccimiglio J, Alipour M, Jiang ZH, Gottardo C, Suntres Z. Antioxidant, antibacterial, and cytotoxic activities of the ethanolic *Origanum vulgare* extract and its major constituents. Oxid Med Cell Longev. Hindawi Publishing Corporation. 2016;2016.

Cortes BJE, Pazdur R. Docetaxel. Journal of Clinical Oncology. 1995;13(10):2643–2655.

Cox DG, Kraft P, Hankinson SE, Hunter DJ. Haplotype analysis of common variants in the BRCA1 gene and risk of sporadic breast cancer. Breast Cancer Res. 2005;7(2):171–175.

Cramer P, Bushnell DA, Fu J, Gnatt AJ, Maier-Davis B, Thompson NE. Architecture of RNA polymerase II and implications for the transcription mechanism. Science. 2000;288(5466):640–649.

Croce CM. Oncogenes and cancer. N Engl J Med. 2008;358(5):502–511.

Crown J, O'Leary M. The taxanes: An update. The Lancet. 2000;355(9210):1176–1178.

Dafni A, Levy S, Lev E. The ethnobotany of Christ's Thorn Jujube (*Ziziphus spina-christi*) in Israel. J Ethnobiol Ethnomed. 2005;1:1–11.

Dai L, Wang G, Pan W. Andrographolide inhibits proliferation and metastasis of SGC7901 gastric cancer cells. Hindawi BioMed Res Int. 2017b. p.1–11.

Dai X, Cheng H, Bai Z, Li J. Breast cancer cell line classification and Its relevance with breast tumor subtyping. J Cancer. 2017a;8(16):3131–3141.

Dang CV. MYC on the path to cancer. Cell. 2012;149(1):22–35.

Das B, Antoon R, Tsuchida R, Lotfi S, Morozova O, Farhat W, et al. Squalene selectively protects mouse bone marrow progenitors against cisplatin and carboplatin-induced cytotoxicity *in vivo* without protecting tumor growth. Neoplasia. 2008;10(10):1105–1119.

Dasari S, Tchounwou PB. Cisplatin in cancer therapy: Molecular mechanisms of action. Eur J Pharmacol. 2014;740:364–378.

Davis KM. *Andrographis paniculata specimen*. In: Global Biodiversity Information Facility Secretariat, *Andrographis paniculata* Nees [Internet] 2017 [cited 2019 Jan 29]. Available from: https://www.gbif.org/occurrence/1585965249.

De Almeida Alves TM, Nagem TJ, De Carvalho LH, Krettli AU, Zani CL. Antiplasmodial triterpene from *Vernonia brasiliana*. Planta Med. 1997;63(6):554–555.

De Menezes Patricio Santos CC, Salvadori MS, Mota VG, Costa LM, de Almeida AAC, de Oliveira GAL, et al. 2013. Antinociceptive and antioxidant activities of phytol *in vivo* and *in vitro* models. Neurosci J. 2013;2013:1–9.

De Sousa GF, Wlodarczyk SR, Monteiro G. Carboplatin: Molecular mechanisms of action associated with chemoresistance. Br J Pharm Sci. 2014;50(4):693–702.

De Souza Grinevicius VMA, Kviecinski MR, Mota NSRS, Ourique F, Castro LSEPW, Andreguetti RR, et al. Piper nigrum ethanolic extract rich in piperamides causes ROS overproduction, oxidative damage in DNA leading to cell cycle arrest and apoptosis in cancer cells. J Ethnopharmacol. 2016;189:139–147.

Deng WL. Outline of current clinical and pharmacological research on *Andrographis paniculata* in China. Newslett Chin. 1978;10:27-31.

Deugnier MA, Teulière J, Faraldo MM, Thiery JP, Glukhova MA, et al. The importance of being a myoepithelial cell. Breast Cancer Res 2002;4(6):224–230.

Doi H, Matsui T, Ohye T, Saito K, Katsuda I, Hidehiko A. Andrographolide from the herb *Andrographis paniculata* induces apoptosis on cultured human leukemic cells. Fujita Med J. 2017;3(3):48–54.

Donfack ARN, Toyang NJ, Wabo HK, Tane P, Awouafack MD, Kikuchi H, et al. Stigmastane derivatives from the roots of *Vernonia guineensis* and their antimicrobial activity. Phytochem Lett. Phytochemical Society of Europe. 2012;5(3):596–599.

Duval C, Poelman MC. Scavenger effect of Vitamin E and derivatives on free radicals generated by photoirradiated pheomelanin. J Pharm Sci. 1995;84(1):107–110.

Earnshaw WC, Heck MMS. Localization of topoisomerase II in mitotic chromosomes. J Cell Biol. 1985;100(5):1716–1725.

Easton DF, Pooley KA, Dunning AM, Pharoah PDP, Thompson D, Ballinger DG, et al. 2007. Genome-wide association study identifies novel breast cancer susceptibility loci. Nature. 2007;447(7148):1087–1093.

Ehrig K, Kilinc MO, Chen NG, Stritzker J, Buckel L, Zhang Q, et al. Growth inhibition of different human colorectal cancer xenografts after a single intravenous injection of oncolytic vaccinia virus GLV-1h68. J Transl Med. 2013;11:79.

Elgorban AM, Bahkali AH, Abdel-Wahab MA, et al. 2019. Natural products of *Alternaria* sp., an endophytic fungus isolated from *Salvadora persica* from Saudi Arabia. Saudi J Biol Sci. King Saud University. 2019;26(5):1068–1077.

Ellis LM. Mechanisms of action of Bevacizumab as a component of therapy for metastatic colorectal cancer. Semin Oncol. 2006;33(5):S1-S7.

Erasto P, De Venter V, Roux S, Grierson DS, Afolayan AJ. Effect of leaf extracts of *Vernonia amygdalina* on glucose utilization in chang-liver, C2C12 muscle and 3T3-L1 cells. Pharm Biol. 2009;47(2):175–181.

Erf GF, Bottje WG, Bersi TK, Headrick MD, Fritts CA. Effects of dietary Vitamin E on the immune system in broilers: altered proportions of CD4 T cells in the thymus and spleen. Poult Sci. 1998;77(4):529–537.

Eser, S, Schnieke A, Schneider G, Saur D. Oncogenic KRAS signalling in pancreatic cancer', British Journal of Cancer. Nature Publishing Group. 2014;111:817–822.

Eswaraiah G, Peele KA, Krupanidhi S, Kumar RB, Venkateswarulu TC. Identification of bioactive compounds in leaf extract of *Avicennia alba* by GC-MS analysis and evaluation of its in-vitro anticancer potential against MCF7 and HeLa cell lines. J King Saud Univ Sci. 2019;32(1):1–4.

Faivre EJ, Lange CA. Progesterone receptors upregulate Wnt-1 to induce epidermal growth factor receptor transactivation and c-Src-dependent sustained activation of Erk1/2 Mitogen-Activated Protein Kinase in breast cancer cells. Mol Cell Biol. 2007;27(2):466-480.

Farid MM, Hussein SR, Ibrahim LF, El Desouky MA, Elsayed AM, El Oqlah AA, et al. Cytotoxic activity and phytochemical analysis of *Arum palaestinum* Boiss. Asian Pac J Trop Biomed. 2015;5(11):944–947.

Farmani F, Moein M, Amanzadeh A, Kandelous M, Ehsanpour Z, Salimi M. Antiproliferative evaluation and apoptosis induction in MCF-7 cells by *Ziziphus spina christi* leaf extracts. Asian Pac J Cancer Prev. 2016;17(1):315–321.

Farombi EO, Owoeye O. Antioxidative and chemopreventive properties of *Vernonia amygdalina* and *Garcinia biflavonoid*. Int J Environ Res Public Health. 2011;8(6):2533–2555.

Fermor BF, Masters JRW, Wood CB, Miller J, Apostolov K, Habib NA. Fatty acid composition of normal and malignant cells and cytotoxicity of stearic, oleic and sterculic acids in vitro. Eur J Cancer. 1992;28(6–7):1143–1147.

Fernández MA, De Las Heras B, Garcia MD, Sáenz MT, Villar A. New insights into the mechanism of action of the anti-inflammatory triterpene lupeol. J Pharm Pharmacol. 2001;53(11):1533–1539.

Fernando IPS, Sanjeewa KKA, Ann YS, Ko CI, Lee SH, Lee WW, et al. Apoptotic and antiproliferative effects of Stigmast-5-en-3-ol from *Dendronephthya gigantea* on human leukemia HL-60 and human breast cancer MCF-7 cells. Toxicol in Vitro. 2018;52:297–305.

Forabosco A, Chiarella S, De Pol A, Vizzotto L, Marzona L, Ferrario VF. Morphometric study of the human neonatal ovary. Anat Rec. 1991;231(2):201–208.

Furman BL. Goserelin. In Reference module in biomedical sciences. New York: Elsevier Inc. 2017. p. 1–3.

Gabay O, Sanchez C, Salvat C, Chevy F, Breton M, Nourissat G, et al. Stigmasterol: a phytosterol with potential anti-osteoarthritic properties. Osteoarthr Cartil. 2010;18(1):106–116.

Ghatage DD, Gosavi SR, Ganvir SM, Hazarey VK. Apoptosis: molecular mechanisms. J Orofac Sci. 2012;4(2):103–107.

Global Biodiversity Information Facility, *Andrographis paniculata* Nees [internet] 2017a [cited 2018 Sep 20]. Available from: https://www.gbif.org/species/3173178.

Global Biodiversity Information Facility, *Ziziphus spina-christi (L.) Desf* [internet] 2017b [cited 2018 Sep 20]. Available from: https://www.gbif.org/species/8228089.

Global Biodiversity Information Facility, *Vernonia extensa Wall. ex DC* [internet] 2017c [cited 2019 September 2019]. Available from: https://www.gbif.org/species/5397808.

Gómez-Sintes R, Hernández F, Lucas JJ, Avila J. GSK-3 mouse models to study neuronal apoptosis and neurodegeneration. Front Mol Neurosci. 2011;4(45):1–11.

Gougeon A. Regulation of ovarian follicular development in primates: Facts and hypotheses. Endocr Rev. 1996;17(2):121–155.

Gougeon A. Dynamics of human follicular growth: morphologic, dynamic, and functional aspects. In The Ovary. Second Ed. San Diego: Elsevier. 2004.p.25–43.

Gunalan G, Vijayalakshmi K, Tamilvannan T, Hopper W. Anti-cancer activity of secondary metabolites from *Bauhinia variegata* Linn. Leaf–an *in silico* approach. Indo Am J Pharm Res Pharmcoepid Appr. 2016;6(7):6299–6311.

Habib MR, Karim MR. Antimicrobial and cytotoxic activity of Di-(2-ethylhexyl) Phthalate and Anhydrosophoradiol-3-acetate isolated from *Calostropis gigantea* (Linn.) flower. Mycobiol. 2009;37(1):31-36.

Hafiz TA, Mubaraki MA. The potential role of *Ziziphus spina-christi* leaf extracts against *Plasmodium berghei*-induced liver and spleen injury. *Biomedical Research (India)*. 2016;27(4):1027–1032.

Ho SM. Estrogen, progesterone and epithelial ovarian cancer. Reprod Biol Endocrinol. 2003;1:1–8.

Hodroj MH, Jardaly A, Raad SA, Zouein A, Rizk S. Andrographolide potentiates the antitumor effect of topotecan in acute myeloid leukemia cells through an intrinsic apoptotic pathway. Cancer Manag Res. 2018;10:1079–1088.

Holanda Pinto SA, Pinto LMS, Cunha GMA, Chaves MH, Santos FA, Rao VS. Anti-inflammatory effect of α, β-Amyrin, a pentacyclic triterpene from *Protium heptaphyllum* in rat model of acute periodontitis. Inflammopharmacology. 2008;16(1):48–52.

Holliday DL, Speirs V. 2011. Choosing correct breast cancer cell line. Breast Cancer Res. 2011;13(4):1–7.

Hotchkiss RS, Strasser A, McDunn JE, Swanson PE. Cell death in disease: mechanisms and emerging therapeutic concepts. N Engl J Med. 2009;361(16):1570–1583.

Howard CB, Johnson WK, Pervin S, Izevbigie EB. Recent perspectives on the anticancer properties of aqueous extracts of Nigerian Vernonia *amygdalina*. Botanics. 2015;5:65–76.

Huang M, Lu JJ, Huang MQ, Bao JL, Chen XP, Wang YT. Terpenoids: natural products for cancer therapy. Expert Opin Inv Drug. 2012;21(12):1801–1818.

Hui LM, Zhao GD, Zhao, JJ. δ-Cadinene inhibits the growth of ovarian cancer cells via caspase-dependent apoptosis and cell cycle arrest. International J Clin Exp Pathol. 2015;8(6):6046–6056.

Hunter DJ, Kraft P, Jacobs KB, Cox DG, Yeager M, Hankinson SE, et al. A genome-wide association study identifies alleles in FGFR2 associated with risk of sporadic postmenopausal breast cancer. Nat Genet. 2012;39(7):870–874.

Idowu O, Ojo O. Antimicrobial activity and fatty acids from *Ipomea ochraceae*. Med Chem. 2017;7(10):299–301.

Igile G, Oleszek W, Jurzysta M. Vernoniosides D and E, two novel saponins from *Vernonia amygdalina*. J Nat Prod. 1995;58(9):1438–1443.

Igile GO, Oleszek W, Jurzysta M, Burda S, Fafunso M, Fasanmade AA. 1994. Flavonoids from *Vernonia amygdalina* and their antioxidant Activities. J Agr Food Chem. 1994;42(11):2445–2448.

Ioachim HL, Dorsett BH, Sabbath M, Barber HRK. 1975. Electron microscopy, tissue culture, and immunology of ovarian carcinoma. J Natl Cancer Inst Monographs. 1975;42:45-62.

Ishihara Y, Matsunaga K, Iijima H, Hasegawa G, Suzuki T, Sato A, et al. The combination of 5-FU, leucovorin and CPT-11 (FOLFIRI) prolongs survival through inhibition of metastasis in an orthotopic model of colon cancer. Anticancer Res. 2010;30(2):403–408.

Iwu MW. Handbook of African medicinal plants by CRC PRESS. ICC. New York. 1993. p.256.

Izevbigie EB, Opata M, Bryan JL. Deleterious side effects of tamoxifen may be ameliorated by aqueous *Vernonia amygdalina* leaf extracts. Am Soc Nutrition J Nutr (Poster Abstracts). 2005;135(12):3048S.

Jada SR, Subur GS, Matthews C, Hamzah AS, Lajis NH, Saad MS, et al. Semisynthesis and *in vitro* anticancer activities of andrographolide analogues. Phytochem. 2007;68(6), pp. 904–912.

Jada SR, Matthews C, Saad MS, Hamzah AS, Lajis NH, Stevens MFG, et al. Benzylidene derivatives of andrographolide inhibit growth of breast and colon cancer cells in vitro by inducing G1 arrest and apoptosis. Br J Pharmacol. 2008;155(5), pp. 641–654.

Jafarian A, Zolfaghari, B, Shirani K. Cytotoxicity of different extracts of arial parts of *Ziziphus spina-christi* on Hela and MDA-MB-468 tumor cells. Adv Biomed Res. 2014;3(1):38.

Jamshidpoor A, Ahmadi R, Mazloomifar H, Mahdavi E. 2015. The effects of Konar extract on kidney cell line in cell culture. Int J Adv Chem Eng Biol Sci. 2015;2(1):57–58.

Jayasekeran V, Holt B, Bourke M. 2013. Normal adult colonic anatomy in colonoscopy. Vid J Encycl GI End. Elsevier GmbH. 2013;1(2):390–392.

Ji L, Liu T, Liu J, Chen Y, Wang Z. Andrographolide inhibits human hepatoma-derived Hep3B cell growth through the activation of c-Jun N-terminal kinase. Planta Med. 2007;73(13):1397–1401.

Jiang CG, Li JB, Liu FR, Wu T, Yu M, Xu HM. Andrographolide inhibits the adhesion of gastric cancer cells to endothelial cells by blocking E-selectin expression. Anticancer Res, 2007;27:2439–2448.

Jisaka M, Ohigashi H, Takagaki T, Nozaki H, Tada T, Hirota M, et al. Bitter steroid glucosides, vernoniosides A1, A2, and A3, and related B1 from a possible medicinal plant, *Vernonia amygdalina*, used by wild chimpanzees. Tetrahedron. 1992;48(4):625–632.

Jung CH, Ro SH, Cao J, Otto NM, Kim DH. MTOR regulation of autophagy. FEBS Lett. 2010;584(7):1287–1295.

Kaewsa-ard S, Liawruangrath B, Liawruangrath S, Teerawutgulrag A, Pyne SG. Chemical constituents and antioxidant and biological activities of the essential oil from leaves of *Solanum spirale*. Nat Prod Comm. 2012;7(7):955–958.

Kalimuthu R, Yegiyants SS, Brenzek C. Anatomy of the breast, axilla, and chest wall. In AI Riker. Breast Disease. New York: Springer. 2015. p.1-12.

Kanehisa Laboratories, Breast cancer – Homo sapiens (human) [internet] 2018a [cited 2019 Jan 25]. Available from: https://www.genome.jp/kegg-bin/show_pathway?hsa05224.

Kanehisa Laboratories, Colorectal cancer – Homo sapiens (human) [internet] 2018b [cited 2019 Jan 25]. Available from: https://www.genome.jp/kegg-bin/show_pathway?hsa05210.

Kangsamaksin T, Chaithongyot S, Wootthichairangsan C, Hanchaina R, Tangshewinsirikul C, Svasti J. Lupeol and stigmasterol suppress tumor angiogenesis and inhibit cholangiocarcinoma growth in mice via downregulation of tumor necrosis factor-a. PLoS ONE. 2017;12(12):1–16.

Kathiravan MK, Khilare MM, Nikoomanesh K, Chothe AS, Jain KS. Topoisomerase as target for antibacterial and anticancer drug discovery. J Enzyme Inhib Med Ch. 2013;28(3):419–434.

Khaidakov M, Manjanatha MG, Aidoo A. Molecular analysis of mitochondrial DNA mutations from bleomycin-treated rats. Mutat Res-Fund Mol M. 2002;500(1–2):1–8.

Khan I, Khan F, Farooqui A, Ansari IA. Andrographolide exhibits anticancer potential against human colon cancer cells by inducing cell cycle arrest and programmed cell death via augmentation of intracellular reactive oxygen species level. Nutr Cancer. Taylor & Francis. 2018;70(5):787-803.

Kim C, Cho SK, Kapoor S, Kumar A, Vali S, Abbasi T, et al. β-Caryophyllene oxide Inhibits Constitutive and Inducible STAT3 Signaling Pathway Through Induction of the SHP-1 Protein Tyrosine Phosphatase. Mol Carcinog. 2013;53(10):793-806.

Kim SJ, Chung WS, Kim SS, Ko SG, Um JY. Antiinflammatory effect of *Oldenlandia diffusa* and its constituent, hentriacontane, through suppression of caspase-1 activation in mouse peritoneal macrophages. Phytother Res. 2011;25(10):1537–1546.

Kiplimo JJ, Everia CA, Koorbanally NA. Novel polyene from *Vernonia urticifolia* (Asteraceae). J Med Plant Res. 2011;5(17):4202–4211.

Koopman G, Reutelingsperger CPM, Kuijten GAM, Keehnen RMJ, Pals ST, van Oers MHJ. Annexin V for flow cytometric detection of phosphatidylserine expression on B cells undergoing apoptosis. Blood. 1994;84(5): 1415-1420.

Kooti W, Daraei N. A review of the antioxidant activity of Celery (*Apium graveolens* L). J Evid-Based Compl Alt Med. 2017;22(4):1029–1034.

Korkaya H, Wicha MS. Breast cancer stem cells: We've got them surrounded. Clin Cancer Res. 2013;19(3):511–513.

Kreuger MRO, Farias BG, Moreira J, Blind LZ, Amoah SKS, Leite AS, et al. Effects of the topical application of an ethylacetate fraction from *Vernonia scorpioides* on excisional wounds infected with *Staphylococcus aureus* in rats. Br J Pharmacog. 2011;22(1):123–130.

Krief S, Hladik CM, Haxaire C. Ethnomedicinal and bioactive properties of plants ingested by wild chimpanzees in Uganda. J Ethnopharm. 2005;101(1–3):1–15.

Ku SK, Lee IC, Kim JA, Bae JS. Anti-septic Effects of Pellitorine in HMGB1-Induced Inflammatory Responses In Vitro and In Vivo. Inflammation. 2014;37(2):338–348.

Kumar PP, Kuttan G. 2009. *Vernonia cinerea* L. scavenges free radicals and regulates nitric oxide and proinflammatory cytokines profile in carrageenan induced paw edema model. *Immunopharmacology and Immunotoxicology*, 2009;31(1):94–102.

Kumar RA, Sridevi K, Kumar NV, Rajagopal NS. Anticancer and immunostimulatory compounds from *Andrographis paniculata*. J Ethnopharmacol. 2004;92(2–3):291–295.

Kumari N, Menghani E, Mithal R. GCMS analysis of compounds extracted from actinomycetes AIA6 isolates and study of its antimicrobial efficacy. Indian J Chem Technol. 2019;26(4):362–370.

Kunwar RM, Shrestha KP, Bussmann RW. Traditional herbal medicine in Far-west Nepal: A pharmacological appraisal. J Ethnobiol Ethnomed. 2010;6:1–18.

Lampi AM, Kataja L, Kamal-Eldin A, Vieno P. Antioxidant activities of α- and γ-tocopherols in the oxidation of rapeseed oil triacylglycerols. J Am Oil Chem Soc. 1999;76(6):749–755.

Lasfargues EY, Ozzello L. Cultivation of human breast carcinomas. J Natl Cancer Inst. 1958;21(6):1131–1147.

Leary A, Dowsett M. Combination therapy with aromatase inhibitors: The next era of breast cancer treatment?. Br J Cancer. 2006;95(6):661–666.

Lee H, Jeong AJ, Ye S. Highlighted STAT3 as a potential drug target for cancer therapy. BMB Reports. 2019;52(7):415–423.

Lee IM. Physical activity and cancer prevention - data from epidemiologic studies. Med Sci Sports Exerc. 2003;35(11):1823–1827.

Lee JY, Kim YS, Shin DH. Antimicrobial synergistic effect of linolenic acid and monoglyceride against *Bacillus cereus* and *Staphylococcus aureus*. J Agr Food Chem. 2002;50(7):2193–2199.

Leelaprakash G, Mohan Dass S, Sivajothi V. Antioxidant and hepatoprotective activities of *Vernonia cinerea* extract against CCL4 induced hepatotoxicity in albino rats. Int J Pharm Sci Rev Res. 2011;10(2):30–34.

Lei CS, Hou YC, Pai MH, Lin MT, Yeh SL. Effects of quercetin combined with anticancer drugs on metastasis-associated factors of gastric cancer cells: *in vitro* and *in vivo* studies. J Nutr Biochem. 2018;51:105–113.

Leibovitz A, Stinson JC, McCombs WB, McCoy CE, Mazur KC, Mabry ND. Classification of human colorectal adenocarcinoma cell lines. Cancer Res. 1976;36(12):4562–4569.

Leslie A, Carcy FA, Pratt NR, Steele RJC. The colorectal adenoma-carcinoma sequence. Br J Surg. 2002;89(7):845–860.

Liang FP, Lin CH, Kuo CD, Chao HP, Fu SL. Suppression of v-Src transformation by andrographolide via degradation of the v-Src protein and attenuation of the Erk signaling pathway. J Biol Chem. 2007;283(8):5023–5033.

Li C, Jing H, Ma G, Liang P. Allicin induces apoptosis through activation of both intrinsic and extrinsic pathways in glioma cells. Mol Med Rep. 2018b;17(4): 5976-5981.

Li CL, Chang L, Guo L, Zhao D, Lin HB, Wang QS, et al. β-elemene induces caspase-dependent apoptosis in human glioma cells in vitro through the upregulation of bax and Fas/FasL and downregulation of Bcl-2. Asian Pac J Cancer Prev. 2014;15(23):10407–10412.

Li D, Wu X, Liang X. The inhibitory effect of β-elemene alone or combined with chemotherapy on diffuse large B cell lymphoma cell strain OCI-LY8 in vitro. Biomed Res. 2017;28(12):5418–5422.

Li K, Yuan D, Yan R, Meng L, Zhang Y, Zhu K. 2018. Stigmasterol exhibits potent antitumor effects in human gastric cancer cells mediated via inhibition of cell migration, cell cycle arrest, mitochondrial mediated apoptosis and inhibition of JAK/STAT signalling pathway. J BUON. 2018a;23(5):1420–1425.

Lim JCW, Jeyaraj EJ, Sagineedu SR, Wong WSF, Stanslas J. SRS06, a new semisynthetic andrographolide derivative with improved anticancer potency and selectivity, inhibits nuclear factor-κB nuclear binding in the A549 non-small cell lung cancer cell line. Pharmacol. 2015;95:70–77.

Lin FL, Wu SJ, Lee SC, Ng LT. Antioxidant, antioedema and analgesic activities of *Andrographis paniculata* extracts and their active constituent andrographolide. Phyother Res. 2009;23(7):958-964.

Liu G, Chu H. Andrographolide inhibits proliferation and induces cell cycle arrest and apoptosis in human melanoma cells. Oncol Lett. 2018;15(4):5301–5305.

Liu J, Liu Y, Si Y, Yu S, Qu J, Xu S, et al. New vernocuminosides from the stem barks of *Vernonia cumingiana* Benth. Steroids. 2009;74(1):51–61.

Liu J, Wang ZT, Ji LL. *In vivo* and *in vitro* anti-inflammatory activities of neoandrographolide. Am J Chinese Med. 2007;35(2):317-328.

Liu Y, Yin T, Feng Y, Cona MM, Huang G, Liu J, et al. Mammalian models of chemically induced primary malignancies exploitable for imaging-based preclinical theragnostic research. Quant Imag Med Surg. 2015;5(5):708–70829.

Llor X, Pons E, Xicola RM, Castells A, Alenda C, Piñol V, et al. Differential features of colorectal cancers fulfilling Amsterdam criteria without involvement of the mutator pathway. Clin Cancer Res. 2005;11(20):7304–7310.

Logan K, Zhang J, Davis EA, Ackerman S. Drug Inhibitors of RNA Polymerase II Transcription. DNA. 1989;8(8):595–604.

Loi S, Haibe-Kains B, Desmedt C, Lallemand F, Tutt AM, Gillet C, et al. Definition of clinically distinct molecular subtypes in estrogen receptor-positive breast carcinomas through genomic grade. J Clin Oncol. 2007;25(10):1239–1246.

Lopes JLC. Sesquiterpene lactones from *Vernonia jugalis*. Mem Inst Oswaldo Cruz. 1991;86(11):227–230.

Lowe HIC, Daley-Beckford D, Toyang NJ, Watson C, Hartley S, Bryant J. The anti-cancer activity of *Vernonia divaricata* Sw against leukaemia, breast and prostate cancers in vitro. West Indian Med J. 2014;63(4):285–288.

Lu X, Yu H, Ma Q, Shen S, Das UN. Linoleic acid suppresses colorectal cancer cell growth by inducing oxidant stress and mitochondrial dysfunction. Lipids Health Dis. 2010;9:106.

Luo X, Luo W, Lin C, Zhang L, Li Y. Andrographolide inhibits proliferation of human lung cancer cells and the related mechanisms. Int J Clin Exp Med. 2014;7(11):4220–4225.

Madlum KN, Galib RA, Ghazi FM, Ali ZH. The effects of Zizyphus stem bark and termite shelter tubes on HeLa cell growth. Res J Pharm Biol Chem Sci. 2015;6(6) 620–626.

Makhafola TJ, Elgorashi EE, McGaw LJ, Awouafack MD, Verschaeve L, Eloff JN. Isolation and characterization of the compounds responsible for the antimutagenic activity of *Combretum microphyllum* (Combretaceae) leaf extracts. BMC Complem Altern Med. 2017;17(1):1–8.

Malahubban M, Alimon AR, Sazili AQ, Fakurazi S, Zakry FA. Phytochemical analysis of *Andrographis paniculata* and *Orthosiphon stamineus* leaf extracts for their antibacterial and antioxidant potential. Trop Biomed. 2013;30(3):467–480.

Malek SNA, Shin SK, Wahab NA, Yaacob. Cytotoxic components of *Pereskia bleo* (Kunth) DC. (Cactaceae) leaves. Molecules. 2009;14(5):1713–1724.

Manikam SD, Stanslas J. Andrographolide inhibits growth of acute promyelocytic leukaemia cells by inducing retinoic acid receptor-independent cell differentiation and apoptosis. J Pharm Pharmacol. 2009;61(1):69–78.

Martin AM, Weber BL. Genetic and hormonal risk factors in breast cancer. J Natl Cancer Inst. 2000;92(14):1126–1135.

Masi G, Allegrini G, Cupini S, Marcucci L, Cerri E, Brunetti I, et al. First-line treatment of metastatic colorectal cancer with irinotecan, oxaliplatin and 5-fluorouracil/leucovorin (FOLFOXIRI): results of a phase II study with a simplified biweekly schedule. Ann Oncol. 2004;15(12):1766–1772.

Mazumder UK, Gupta M, Manikandan L, Bhattacharya S, Haldar PK, Roy S. Evaluation of anti-inflammatory activity of *Vernonia cinerea* Less. extract in rats. Phytomed. 2003;10(2–3):185–188.

McIlwain DR, Berger T, Mak TW. Caspase functions in cell death and disease. Cold Spring Harb Perspect Biol. 2013;5(4):a008656.

Mcpherson K, Steel CM, Dixon JM. Breast cancer - epidemiology, risk factors, and genetics Risk factors for breast cancer. Br Med J. 2000;321(7261):624-628.

Medina V, Edmonds B, Young GP, James R, Appleton S, Zalewski PD. Induction of caspase-3 protease activity and apoptosis by butyrate and trichostatin a (Inhibitors of histone deacetylase): Dependence on protein synthesis and synergy with a mitochondrial/cytochrome c-dependent pathway. Cancer Res. 1997;57(17):3697–3707.

Mehmood RK. Review of cisplatin and oxaliplatin in current immunogenic and monoclonal antibodies perspective. Oncol Rev. 2014;8(2).

Mendiola JA, Santoyo S, Cifuentes A, Reglero G, Ibánez E, Señoráns FJ. Antimicrobial activity of sub- and supercritical CO_2 extracts of the green alga *Dunaliella salina*. J Food Protect. 2008;71(10):2138–2143.

Mihailović V, Vuković N, Nićiforović N, Solujić S, Mladenović M, Mašković P, et al. Studies on the antimicrobial activity and chemical composition of the essential oils and alcoholic extracts of *Gentiana asclepiadea* L. J Med Plants Res. 2011;5(7):1164–1174.

Miscia S, Marchisio M, Grilli A, Di Valerio V, Centurione L, Sabatino G, et al. Tumor necrosis factor α (TNF-α) activates Jak1/Stat3-Stat5B signaling through TNFR-1 in human B cells1. Cell Growth Diff. 2002;13:13–18.

Mishra SK, Sangwan NS, Sangwan RS. Phcog Rev.: Plant Review *Andrographis paniculata* (Kalmegh): A Review. Pharmacog Rev. 2007;1(2):283–298.

Mohammad RM, Muqbil I, Lowe L, Yedjou C, Hsu HY, Lin LT, et al. Broad targeting of resistance to apoptosis in cancer. Semin Cancer Biol. 2015;35(0):S78-S103.

Mohansrinivasan V, Subathra DC, Meenakshi D, Ananya B, Jemimah NS. Exploring the anticancer activity of grape seed extract on skin cancer cell lines A431. Br Arch Biol Technol. 2015;58(4):540–546.

Monien BH, Herrmann K, Florian S, Glatt H. Metabolic activation of furfuryl alcohol: Formation of 2-methylfuranyl DNA adducts in *Salmonella typhimurium* strains expressing human sulfotransferase 1A1 and in FVB/N mice. Carcinogenesis. 2011;32(10):1533–1539.

Montecucco A, Zanetta F, Biamonti G. Molecular mechanisms of etoposide. Exp Clin Sci J. 2015;14:95–108.

Morah FNI, Uduagwu DN. Chemical composition, antioxidant and larvicidal activity of *Alchornea laxiflora* (Benth) leaf extracts. Edorium J Pharmacol. 2017;1:1–8.

Mota CS, Freitas RB, Athayde ML, Boligon AA, Augusti PR, Somacal S. Effect of *Vernonia cognata* on oxidative damage induced by ethanol in rats. Hum Exp Toxicol. 2011;30(7):675–684.

Motiwala MN, Rangari VD. Combined effect of paclitaxel and piperine on a MCF-7 breast cancer cell line *in vitro*: Evidence of a synergistic interaction. Synergy. 2015;2(1):1–6.

Moushumi Priya A, Jayachandran, S. Induction of apoptosis and cell cycle arrest by Bis (2-ethylhexyl) phthalate produced by marine *Bacillus pumilus* MB 40. Chem Biol Interact. 2012;195(2):133–143.

Mutch DG, Prat J. 2014 FIGO staging for ovarian, fallopian tube and peritoneal cancer. Gynecol Oncol. 2014;133(3):401–404.

National Cancer Institute, NIH visuals online [internet] 2011 [cited 2019 Jan 22]. Available from: https://visualsonline.cancer.gov/details.cfm?imageid=7127.

National Cancer Institute, Immunotherapy to treat cancer [internet] 2019c [cited 2020 May 28]. Available from: https://www.cancer.gov/about-cancer/treatment/types/immunotherapy.

National Cancer Institute. Radiation therapy to treat cancer [internet] 2019b [cited 2020 May 28]. Available from: https://www.cancer.gov/about-cancer/treatment/types/radiation-therapy.

National Cancer Institute, Risk of breast cancer death is low after a diagnosis of Ductal Carcinoma in Situ [internet] 2015a [cited 2019 Jan 22]. Available from: https://www.cancer.gov/news-events/cancer-currents-blog/2015/dcis-low-risk.

National Cancer Institute, Salpingo – Ovarian & peritoneal functional anatomy [internet] 2018 [cited 2019 Jan 25]. Available from: https://training.seer.cancer.gov/ovarian/anatomy/.

National Cancer Institute, Rectal cancer treatment (PDQ®)-Patient Version [internet] 2019a [cited 2019 Jan 22]. Available from: https://www.cancer.gov/types/colorectal/patient/rectal-treatment-pdq.

National Cancer Institute, Surgery to treat cancer [internet] 2015b [cited 2020 May 28]. Available from: https://www.cancer.gov/about-cancer/treatment/types/surgery.

National Cancer Institute, Targeted therapy to treat cancer [internet] 2020 [cited 2020 May 28]. Available from: https://www.cancer.gov/about-cancer/treatment/types/targeted-therapies.

National Center for Advancing Translational Sciences, Genetic and rare diseases information center, Peutz-Jeghers syndrome [internet] 2015 [cited 2019 Jan 22]. Available from: https://rarediseases.info.nih.gov/diseases/7378/peutz-jeghers-syndrome.

Niranjan A, Tewari SK, Lehri A. Biological activities of Kalmegh (*Andrographis paniculata* Nees) and its active principles-A review. Indian J Nat Prod Res. 2010;1(2):125–135.

Nithya M, Ragavendran C, Natarajan D. Antibacterial and free radical scavenging activity of a medicinal plant *Solanum xanthocarpum*. Int J Food Prop. Taylor & Francis. 2018;21(1):328–342.

Niwa AM, de Paula NA, Vesenick DC, Sartori D, Maistro EL, Ribeiro LR, et al. Evaluation of lignan (-)-cubebin extracted from Piper cubeba on human colon adenocarcinoma cells (HT29). J Toxicol Environ Health Part A. 2016;79(2):92–100.

Nkafamiya II, Shagal MH, Haruna M. Potential of *Ziziphus spina-christi* seed ethanolic extract on inhibition of microbial growth. Acad J Biotech. 2013;1(4), pp. 53–56.

Nugrahaningsih, Sarjadi, Dharmana E, Subagjo HW. *Andrographis paniculata* extract induced apoptosis of adenocarcinoma mammae in C3H mice. Univ Med. 2013;32(2):99–107.

Nyeem MAB, Abdul Mannan M, Nuruzzaman M, Kamrujjaman KM, Das SK. Indigenous king of bitter (*Andrographis paniculata*): A review. J Med Plants Stud. 2017;5(2):318–324.

OECD Directorate for Science, Technology and Industry [internet] 2007 [cited 2019 Feb 21]. Available from: http://www.oecd.org/dataoecd/7/13/38777417.pdf.

Okhuarobo A, Falodun JE, Erharuyi O, Imieje V, Falodun A, Langer P. Harnessing the medicinal properties of *Andrographis paniculata* for diseases and beyond: a review of its phytochemistry and pharmacology. Asian Pac J Trop Dis. 2014;4(3):213-222.

Olajuyigbe OO, Onibudo TE, Coopoosamy RM, Ashafa AOT, Afolayan AJ. Bioactive compounds and in vitro antimicrobial activities of ethanol stem bark extract of *Trilepisium madagascariense* DC. Int J Pharmacol. 2018;14(7):901–912.

Padmalochana K. Anticancer properties of *Andrographis paniculata* Nees. Int J Pharm Biosci Biochem. 2017;8(2):865–868.

Paplomata E, O'regan R. The PI3K/AKT/mTOR pathway in breast cancer: Targets, trials and biomarkers. Ther Adv Med Oncol. 2014;6(4):154–166.

Pardini B, Kumar R, Naccarati A, Novotny J, Prasad RB, Forsti A, et al. 5-Fluorouracil-based chemotherapy for colorectal cancer and MTHFR/MTRR genotypes. Br J Clin Pharmacol. 2011;72(1):162–163.

Paridens R, Biganzoli L, Bruning P, Klijn JGM, Gamucci T, Houston S, et al. Paclitaxel versus doxorubicin as first-line single agent chemotherapy for metastatic breast cancer: a European organization for research and treatment of cancer randomized study with cross-over. J Clin Oncol. 2000;18(4):724–733.

Parihar G, Balekar N. Isolation and characterisation of Stigmast-5-en-ol (beta-sitosterol) from *Calotropis procera* latex ethyl acetate fraction for immunomodulatory activity. Int J Pharm Sci Res. 2017;8(3):1375–1380.

Park SH, Kim DS, Kim S, Lorz LR, Choi E, Lim HY, et al. Loliolide presents antiapoptosis and antiscratching effects in human keratinocytes. Int J Mol Sci. 2019;20(3).

Pasdaran A, Pasdaran A, Atanassova M, Ahmad MA. Chemical compounds, antibacterial and insecticidal activity of lipophilic extract of *Scrophularia amplexicaulis* Benth and *Scrophularia oxysepala* Boiss. Der Pharma Chem. 2018;10(4):84–88.

Patel BB, Sengupta R, Qazi S, Vachhani H, Yu Y, Rishi AK, et al. Curcumin enhances the effects of 5-fluorouracil and oxaliplatin in mediating growth inhibition of colon cancer cells by modulating EGFR and IGF-1R. Int J Cancer. 2008;122(2):267–273.

Pattingre S, Tassa A, Qu X, Garuti R, Liang XH, Mizushima N, et al. Bcl-2 antiapoptotic proteins inhibit Beclin 1-dependent autophagy. Cell. 2005;122(6):927–939.

Pédeboscq S, Rey C, Petit M, Harpey C, De Giorgi F, Ichas F, et al. Non-antioxidant properties of α-tocopherol reduce the anticancer activity of several protein kinase inhibitors in vitro. PLoS ONE. 2012;7(5).

Pérez-Herrero E, Fernández-Medarde A. Advanced targeted therapies in cancer : Drug nanocarriers , the future of chemotherapy. Eur J Pharm Biopharm. 2015;93:52–79.

Pietras RJ, Márquez-Garbán DC. Membrane-associated estrogen receptor signaling pathways in human cancers. Clin Cancer Res. 2007;13(16):4672–4676.

Pillay P, Vleggaar R, Maharaj VJ, Smith PJ, Lategan CA, Chouteau F, et al. Antiplasmodial hirsutinolides from *Vernonia staehelinoides* and their utilization towards a simplified pharmacophore. Phytochem. 2007;68(8):1200–1205.

Pitchai D, Roy A, Ignatius C. In vitro evaluation of anticancer potentials of lupeol isolated from *Elephantopus scaber* L. on MCF-7 cell line. J Adv Pharm Tech Res. 2014;5(4):179–184.

Poma P, Labbozzetta M, Notarbartolo M, Bruno M, Maggio A, Rosselli S, et al. Chemical composition, in vitro antitumor and pro-oxidant activities of *Glandora rosmarinifolia* (Boraginaceae) essential oil. PLoS ONE. 2018;13(5):1–11.

Ponglux D, Wongseripipatana S, Aimi N, Oya N, Hosokawa H, Haginiwa J, et al. Structures of two new bitter principles isolated from a Thai medicinal plant, *Vernonia extensa* D.C. Chem Pharm Bull. 1992;40(2):553–555.

Pongrakhananon V. Anticancer Properties of Cardiac Glycosides. In Rangel, L. (ed.) Cancer Treatment - Conventional and Innovative Approaches. InTech, 2013. p.65–83.

Prasad R, Prasad SB. Antitumor activity of rutin-cisplatin in combination and its protective effect against hematotoxicity. Res J Life Sci Bioinform Pharm Chem Sci. 2018;4(6):42–56.

Prat A, Adamo B, Cheang MCU, Anders AK, Carey LA, Perou CM. Molecular characterization of basal-like and non-basal-like triple-negative breast Cancer. Oncologist. 2013;18(2):123–133.

Prat A, Pineda E, Adamo B, Galván P, Fernández A, Gaba L, et al. Clinical implications of the intrinsic molecular subtypes of breast cancer. Breast J. 2015;24(2015):S26–S35.

Pratheeshkumar P, Kuttan G. Protective role of *Vernonia cinerea* L. against gamma radiation-induced immunosupression and oxidative stress in mice. Hum Exp Toxicol. 2010;30(8):1022–1038.

Ptak A, Hoffmann M, Rak A. The ovary as a target organ for bisphenol a toxicity bisphenol an exposure and health risks. In Bisphenol A Exposure and Health Risks. InTech, 2017. p. 57–73.

Rabe T, Mullholland D, Van Staden J. 2002. Isolation and identification of antibacterial compounds from *Vernonia colorata* leaves. J Ethnopharmacol. 2002;80(1), pp. 91–94.

Ragasa CY, De Luna RD, Hofilena JG. Antimicrobial terpenoids from *Pterocarpus indicus.* Nat Prod Res. 2005;19(4):305–309.

Rajagopal S, Ajaya Kumar R, Deevi DS, Satyanarayana C, Rajagopalan R. Andrographolide, a potential cancer therapeutic agent isolated from *Andrographis paniculata*. J Exp Ther Oncol. 2003;3(3):147–158.

Rajeshkumar S, Nagalingam M, Ponnanikajamideen M, Vanaja M, Malarkodi C. Anticancer activity of *Andrographis Paniculata* leaves extract against Neuroblastima (IMR-32) and human colon (HT-29) cancer cell line. World J Pharm Pharm Sci. 2015;4(6):1667–1675.

Raman VB, Samuel LA, Pardha SM, Narashimha RB, Naga VKA, Sudhakar M, et al. Antibacterial, antioxidant activity and GC-MS analysis of *Eupatorium odoratum*. Asian J Pharm Clin Res. 2012;5(2):99–106.

Ramirez-González JA, Vaamondelemos R, Cunha-Filho JS, Varghese AC, Swanson RJ. Overview of the female reproductive system. in Vaamonde D, du Plessis S, Agarwal A. (eds) Exercise and human reproduction: induced fertility disorders and possible therapies. New York, NY: Springer, 2016. p.1–351.

Ratnasooriya WD, Deraniyagala SA, Peiris SKJS. Antinociceptive potential of the Sri Lankan endemic plant *Vernonia zeylanica*. Pharm Biol. 2007;45(7):525–532.

Ravi L, Krishnan K. Cytotoxic potential of N-hexadecanoic acid extracted from *Kigelia pinnata* leaves. Asian J Cell Biol. 2016;12(1):20–27.

Reddy VLN, Reddy SM, Ravikanth V, Krishnaiah P, Goud TV, Rao TP. A new BIS-andrographolide ether from *Andrographis paniculata* Nees and evaluation of anti-HIV activity. Nat Prod Res. 2005;19(3):223–230.

Redondo-Blanco S, Fernández J, Gutiérrez-del-Rio I, Villar CJ, Lombó F. New insights toward colorectal cancer chemotherapy using natural bioactive compounds. Front Pharmacol. 2017;8:1–22.

Reed JC, Pellecchia M. Review in translational hematology Apoptosis-based therapies for hematologic malignancies. Blood. 2005;106(2):408–418.

Rimon-Dahari N, Yerushalmi-Heinemann L, Alyagor L, Dekel N. Ovarian Folliculogenesis. In Piprek, R. (ed.) Molecular mechanisms of cell differentiation in gonad development, results and problem in cell differentiation. New York, NY: Springer, 2016. p.167–190.

Rohin MAKB, Ridzwan N, Jumli MN, Abd Hadi N, Johari SATT, Latif AZA. Cytotoxicity study and morphological changes of different extraction for bismillah leaf (*Vernonia amygdalina*) in human glioblastoma multiforme cell line (u-87). Biomed Res. 2017;28(4):1472–1478.

Romero-Estrada A, Maldonado-Magaña A, González-Christin J, Bahena SM, Garduño-Ramirez ML, Rodríguez-López V, et al. Anti-inflammatory and antioxidative effects of six pentacyclic triterpenes isolated from the Mexican copal resin of *Bursera copallifera*. *BMC* Complemen Altern Med. 2016;16(1):1–10.

Roos G, Prawat H, Walter CU, Klaiber I, Vogler B, Guse JH, et al. New sesquiterpene lactones with antibacterial activity from *Vernonia fastigiata.* Planta Med. 1998;64(7):673–674.

Rose PG. First-Line Chemotherapy for Ovarian Cancer: Inferences From Recent Studies. Oncologist. 2016;21(11):1286–1290.

Rosenfeldt MT, Ryan KM. The role of autophagy in tumour development and cancer therapy. Exp Rev Mol Med. 2009;11:1–20.

Ryu NH, Park KR, Kim SM, Yun HM, Nam D, Lee SG, et al. A hexane fraction of guava leaves (*Psidium guajava L*.) induces anticancer activity by suppressing AKT/mammalian target of rapamycin/ribosomal p70 S6 kinase in human prostate cancer cells. J Med Food. 2012;15(3):231–241.

Sagadevan P, Suresh SN, Rathishkumar S, Gayathri S, Eswari DV. Anticancer activity of methanolic leaf extracts of *Andrographis paniculata* (Nees) and *Cardiospermum halicacabum* (Linn) against human breast cancer cell line (MCF-7). Int J Pharm Life Sci. 2013;4(9):2983–2986.

Saied AS, Gebauer J, Hammer K, Buekert A. 2008. *Ziziphus spina-christi* (L.) Willd.: A multipurpose fruit tree. Genet Resour Crop Ev. 2008;55(7):929–937.

Sak K. Chemotherapy and Dietary Phytochemical Agents. Chemother Res Pract. 2012;2012. 1–11.

Sakthivel R, Malar DS, Devi KP. Phytol shows anti-angiogenic activity and induces apoptosis in A549 cells by depolarizing the mitochondrial membrane potential. Biomed Pharmacother. 2018;105:742–752.

Samy RP, Thwin MM, Gopalakrishnakone P, Ignacimuthu S. Ethnobotanical survey of folk plants for the treatment of snakebites in Southern part of Tamilnadu, India. J Ethnopharmacol. 2008;115:302–312.

Santos-Sánchez NF, Salas-Coronado R, Villanueva-Cañongo C, Hernández-Carlos B. Antioxidant compounds and their antioxidant mechanism. In Antioxidants. IntechOpen, 2019. 1–28.

Sarkar S, Gopal PK, Paul S. Andrographolide induced apoptosis in NALM-6 cells mediated through the cell cycle arrest and nuclear fragmentation. Pharmacog J. 2018;10(2):210–214.

Satyanarayana C, Deevi DS, Rajagopalan R, Srinivas N, Rajagopal S. DRF 3188 a novel semi-synthetic analog of andrographolide: Cellular response to MCF 7 breast cancer cells. BMC Cancer. 2004;4:1–8.

Schellens JHM. Capecitabine. Oncologist. 2007;12(2):152–155.

Sghaier MB, Skandrani I, Nasr N, Franca MGD, Chekir-Ghedira L, Ghedira K. Flavonoids and sesquiterpenes from *Tecurium ramosissimum* promote antiproliferation of human cancer cells and enhance antioxidant activity: A structure-activity relationship study. Environ Toxicol Pharmacol. 2011;32(3):336–348.

Shah MD, Iqbal M. Antioxidant activity, phytochemical analysis and total polyphenolics content of essential oil, methanol extract and methanol fractions from *Commelina nudiflora*. Int J Pharm Pharm Sci. 2018;10(8):36.

Shahat AA, Pieters L, Apers S, Nazeif NM, Abdel-Azim N, Berghe DV, et al. Chemical and biological investigations on *Zizyphus spina-christi* L. Phytother Res. 2001;15(7):593–597.

Shahbaz K. Pharmenzymonetics and pharmgeonetics: a new door in pharmacology. World J Pharm Pharm Sci. 2016;5(2):1424–1432.

Shamsi MS, Tibb-e-Nabawi: Medical Guidance & Teachings of Prophet Muhammed [internet] 2016 [cited 2018 Aug 28]. Available from: http://www.tib-e-nabi-for-you.com/documents/part 1 final.pdf.

Sharma P, Jha AB, Dubey RS, Pessarakli M. Reactive oxygen species, oxidative damage, and antioxidative defense mechanism in plants under stressful conditions. J Bot. 2012:1–26.

Sheeja K, Shihab PK, Kuttan G. Antioxidant and anti-inflammatory activities of the plant *Andrographis paniculata* nees. Immunopharmacol Immunotoxicol. 2006;28(1):129–140.

Shi MD, Lin HH, Lee YC, Chao JK, Lin RA, Chen JH. Inhibition of cell-cycle progression in human colorectal carcinoma Lovo cells by andrographolide. Chem Biol Interact. 2008;174(3):201–210.

Singhamahapatra A, *Andrographis paniculata* [internet] 2019a [cited 2020 Mar 26]. Available from: https://www.inaturalist.org/photos/30695568.

Singhamahapatra A, *Andrographis paniculata* [internet] 2019b [cited 2020 Mar 26]. Available from: https://www.inaturalist.org/photos/30695387.

Singh S, Mehta A, Baweja S, Ahirwal L, Mehta P. Anticancer activity of *Andrographis paniculata* and *Silybum marianum* on five human cancer cell lines. J Pharmacol Toxicol. 2013;8(1):42–48.

Siripong P, Kongkathip B, Preechanukool K, Picha P, Tunsuwan K, Taylor WC. Cytotoxic diterpenoid constituents from *Andrographis paniculata* Nees. leaves. J Sci Soc Thailand. 1992;18:187–194.

Sørlie T, Perou CM, Tibshirani R, Aas T, Geisler S, Johnsen H, et al. Gene expression patterns of breast carcinomas distinguish tumor subclasses with clinical implications. PNAS. 2001;98(19):10869–10874.

Sriwiriyajan S, Ninpesh T, Sukpondma Y, Nasomyon T, Graidist P. Cytotoxicity screening of plants of genus Piper in breast cancer cell lines. Trop J Pharm Res. 2014;13(6):921–928.

Sriwiriyajan S, Sukpondma Y, Srisawat T, Madla S, Graidist P. (-)-Kusunokinin and piperloguminine from *Piper nigrum*: An alternative option to treat breast cancer. Biomed Pharmacother. 2017;92:732–743.

Sriwiriyajan S, Tedasen A, Lailerd N, Boonyaphiphat, Nitiruangjarat A, Deng Y, et al. Anticancer and cancer prevention effects of piperine-free *Piper nigrum* extract on n-nitrosomethylurea-induced mammary tumorigenesis in rats. Cancer Prev Res. 2016;9(1):74–82.

Stacey SN, Manolescu A, Sulem P, Rafnar T, Gudmundsson J, Gudjonsson SA, et al. Common variants on chromosomes 2q35 and 16q12 confer susceptibility to estrogen receptor-positive breast cancer. Nat Genet. 2007;39(7):865–869.

Subik K, Lee JF, Baxter L, Strzepek T, Costello D, Crowley P, et al. The expression patterns of ER, PR, HER2, CK5/6, EGFR, KI-67 and AR by immunohistochemical analysis in breast cancer cell lines. Breast Cancer: Basic and Clinical Research. 2010;4(1):35–41.

Sukardiman H, Widyawaruyanti A, Zaini NC. Apoptosis inducing effect of andrographolide on TD-47 human breast cancer cell line. Afr J Tradit Complement Altern Med. 2007;4(3):345–351.

Sukardiman, Studiawan H, Rahman A, Santosa MH, Pratama FA. Ethyl acetate fraction of *Andrographis paniculata* Nees increases cytotoxic effect of 5-Fluorouracil on human cancer cell lines. Int J Pharm Pharm Sci. 2014;6(5):1–5.

Sukumari-Ramesh S, Bentley N, Laird MD, Singh N, Vender JR, Dhandapani KM. Dietary phytochemicals induce p53- and caspase-independent cell death in human neuroblastoma cells. Int J Dev Neurosci. 2011;29(7):1–22.

Suliman MB, Mohammed AA. Preliminary phytochemical screening and antibacterial activity of ethanolic and aqueous extracts of Sudanese medicinal plant *Ziziphus spina-christi* L leaves. Arab J Med Aromat Plants. 2018;4(1):35–44.

Sun YF, Wink M. Tetrandrine and fangchinoline, bisbenzylisoquinoline alkaloids from *Stephania tetrandra* can reverse multidrug resistance by inhibiting P-glycoprotein activity in multidrug resistant human cancer cells. Phytomed. 2014;21(8–9):1110–1119.

Sundarraj S, Thangam R, Sreevani V, Kaveri K, Gunasekaran P, Achiraman S, et al. γ-Sitosterol from *Acacia nilotica* L. induces G2/M cell cycle arrest and apoptosis through c-Myc suppression in MCF-7 and A549 cells. J Ethnopharmacol. 2012;141(3):803–809.

Suriani MN, Nurul AAZ, Jamaliah H, Normah M, Goon SC, Nor Haliza S, et al. Cytotoxicity activity of *Andrographis paniculata* ethanolic extract against Vero cell line and chicken embryo fibroblast cells. In 25th Veterinary Association Malaysia Congress. Kota Tinggi, Johor, Malaysisa, 2013. p.25–27.

Suwito H, Heffen WL, Cahyana H, Suwarso WP. Isolation, transformation, anticancer, and apoptosis activity of lupeyl acetate from Artocarpus integra. In AIP Conference Proceedings. American Institute of Physics. 2016. p.080004-1–080004-8

Suzuki R, Matsushima Y, Okudara N, Sakagami H, Shirataki Y. Cytotoxic components against human oral squamous cell carcinoma isolated from *Andrographis paniculata*. Anticancer Res. 2016;36(11):5931–5936.

Swamy TA, Obey J, Mutuku NC. Phytochemical analysis of *Vernonia adoensis* leaves and roots used as a traditional medicinal plant in Kenya. Int J Pharm Biol Sci. 2013;3(3):46–52.

Swantara MD, Rita WS, Suartha N, Agustina KK. Anticancer activities of toxic isolate of *Xestospongia testudinaria* sponge. Vet World. 2019;12(9):1434–1440.

Sy GY, Cissé A, Nongonierma RB, Sarr M, Mbodj NA, Faye B. Hypoglycaemic and antidiabetic activity of acetonic extract of *Vernonia colorata* leaves in normoglycaemic and alloxan-induced diabetic rats. J Ethnopharmacol. 2005;98(1–2):171–175.

Syamala G, Prasad K. Anatomical Study of Sigmoid Colon. IOSR J Dent Med Sci. 2016;15(08):26–30.

Tagne RS, Telefo BP, Talla E, Nyemb JN, Njina SN, Asrar M, et al. Bio-guided fractionation of methanol extract of *Ziziphus mauritiana* Lam. (bark) and effect of the most active fraction on cancer cell lines. Asian Pac J Trop Dis. 2015;5(4):307–312.

Talib WH. Regressions of breast carcinoma syngraft following treatment with piperine in combination with thymoquinone. Sci Pharm. 2017;85(3):1–11.

Tan CP, Lu YY, Ji LN, Mao ZW. Metallomics insights into the programmed cell death induced by metal-based anticancer compounds. Metallomics. 2014;6(5):978–995.

Tan MCS, Oyong GG, Shen CC, Ragasa CY. Chemical constituents of *Andrographis paniculata* (Burm. f.) Nees. Int J Pharmacog Phytochem Res. 2016;8(8):1398–1402.

Tan ML, Kuroyanagi M, Sulaiman SF, Najimudin N, Muhammad T. Cytotoxic activities of major diterpenoid constituents of *Andrographis paniculata* in a panel of human tumor cell lines. Pharm Biol. 2005;43(6):501–508.

Tchimene MK, Nwaehujor CO, Ezenwali M, Okoli CC, Iwu MM. Free radical scavenging activity of lupeol isolated from the methanol leaf extract of *Crateva adansonii* oliv. (Capparidaceae). Int J Pharmacog Phytochem Res. 2016;8(3):419–426.

Tchinda AT, Tsopmo A, Tane P, Ayafor JF, Connolly JD, Sterner. Vernoguinosterol and vernoguinoside, trypanocidal stigmastane derivatives from *Vernonia guineensis* (Asteraceae). Phytochem. 2002;59(4):371–374.

Tedasen A, Khoka A, Madla S, Sriwiriyajan S, Graidist P. Anticancer effects of piperine-free *Piper nigrum* extract on cholangiocarcinoma cell lines. Pharmacog Mag. 2020;16(68):28-38.

Thakur RS, Puri HS, Husain A. Major Medicinal Plants of India. Central Institute of Medicinal and Aromatic Plants. Lucknow. 1989. p.61.

The Global Cancer Observatory, Thailand [internet] 2019 [cited 2020 April 20]. Available from: https://gco.iarc.fr/today/data/factsheets/populations/764-thailand-fact-sheets.pdf.

The World Ovarian Cancer Coalition. The World Ovarian Cancer Coalition Atlas: Global Trends in Incidence, Mortality and Survival. 2018.

Thomas E, Gopalakrishnan V, Somasagara RR, Choudhary B, Raghavan SC. Extract of *Vernonia condensata*, inhibits tumor progression and improves survival of tumor-allograft bearing mouse. Sci Rep. Nature Publishing Group. 2016;6:23255.

Thongnest S, Chawengrum P, Keeratichamroen S, Lirdprapamongkol K, Eurtivong C, Boonsombat J, et al. Vernodalidimer L, a sesquiterpene lactone dimer from *Vernonia extensa* and anti-tumor effects of vernodalin, vernolepin, and vernolide on HepG2 liver cancer cells. Bioorg Chem. 2010;92:1-10.

Uma B, Parvathavarthini R. Antibacterial effect of hexane extract of sea Urchin, *Temnopleurus alexandri* (Bell,1884). Int J Pharmtech Res. 2010;2(3):1677–1680.

Underhill BML. Intestinal Length in Man. Br Med J. 1955;2(4950):1243–1246.

Vandenabeele P, Galluzzi L, Berghe TV, Kroemer G. Molecular mechanisms of necroptosis: An ordered cellular explosion. Nat Rev Mol Cell Biol. 2010;11(10):700–714.

Varma A, Padh H, Shrivastava N. Andrographolide: A new plant-derived antineoplastic entity on horizon. Evid-Based Compl Alt Med. 2011;2011.

Vergara M, Olivares A, Altamirano C. Antiproliferative evaluation of tall-oil docosanol and tetracosanol over CHO-K1 and human melanoma cells. Electron J Biotechnol. 2015;18(4):291–294.

Wada-Hiraike O, Yano T, Nei T, Matsumoto Y, Nagasaka K, Takizawa S, et al. The DNA mismatch repair gene hMSH2 is a potent coactivator of oestrogen receptor α. Br J Cancer. 2005;92(12):2286–2291.

Wang J, Song H, Wu X, Zhang S, Gao X, Li F, et al. Steroidal saponins from *Vernonia amygdalina* Del. and their biological activity. Molecules. 2018;23(3):1–11.

Wang W, Guo W, Li L, Fu Z, Liu W, Gao J, et al. Andrographolide reversed 5-FU resistance in human colorectal cancer by elevating BAX expression. Biochem Pharm. 2016;121:8–17.

Wang X, Zhang H, Chen X. Drug resistance and combating drug resistance in cancer. Cancer Drug Res. 2019;2:141-160.

Wang Y, Hong D, Qian Y, Tu Xuezi, Wang K, Yang X, et al. Lupeol inhibits growth and migration in two human colorectal cancer cell lines by suppression of Wnt-β-catenin pathway. Oncotargets Ther. 2018;11:7987-7999.

Wang ZJ, Liang CL, Li GM, Yu CY, Yin M. Stearic acid protects primary cultured cortical neurons against oxidative stress. Acta Pharmacol Sin. 2007;28(3):315–326.

Wei Q, Ma X, Zhao Z, Zhang S, Liu S. Antioxidant activities and chemical profiles of pyroligneous acids from walnut shell. J Anal Appl Pyrol. 2010;88(2):149–154.

Wen, S., Gu, D, Zeng, H. Antitumor effects of beta-amyrin in Hep-G2 liver carcinoma cells are mediated via apoptosis induction, cell cycle disruption and activation of JNK and P38 signalling pathways. J BUON. 2018;23(4):965–970.

Widyawati T. Aspek farmakologi sambiloto (*Andrographis paniculata* Nees) (In Indonesia). Majalah Kedokteran Nusantara. 2007;40(3):216–222.

Wilson AC, Meethal SV, Bowen RL, Atwood CS. Leuprolide acetate: A drug of diverse clinical applications. Exp Opin Inv Drugs. 2007;16(11):1851–1863.

Wlodkowic D, Telford W, Skommer J, Darzynkiewicz Z. Apoptosis and beyond: cytometry in studies of programmed cell death. Methods Cell Biol. 2011;103:55–98.

Wong FC, Woo CC, Hsu A, Tan BKH. The anti-cancer activities of *Vernonia amygdalina* extract in human breast cancer cell lines are mediated through caspase-dependent and p53-independent pathways. PLoS ONE. 2013;8(10):e78021.

World Health Organization, Breast Cancer [internet] 2018b [cited 2019 Jan 22]. Available from: https://gco.iarc.fr/today/data/factsheets/cancers/20-Breast-fact-sheet.pdf.

World Health Organization, *Indonesia* [internet] 2019 [cited 2019 Jan 22]. Available from: http://gco.iarc.fr/today/data/factsheets/populations/360-indonesia-fact-sheets.pdf.

Xu XH, Li T, Fong CMV, Chen X, Chen XJ, Wang YT, et al. Saponins from chinese medicines as anticancer agents. Molecules. 2016;21(10):1–27.

Yang L, Wu D, Luo K, Wu S, Wu P. Andrographolide enhances 5-fluorouracil-induced apoptosis via caspase-8-dependent mitochondrial pathway involving p53 participation in hepatocellular carcinoma (SMMC-7721) cells. Cancer Lett. 2009;276(2):180–188.

Yayli N, Güleç C, Üçüncü O, Yaşar A, Ülker S, Coşkunçelebi K, et al. 2006. Composition and antimicrobial activities of volatile components of *Minuartia meyeri*. Turk J Chem. 2006;30(1):71–76.

Yildirim I, Kutlu T. Anticancer agents: Saponin and tannin. Int J Biol Chem. 2015;9(6):332–340.

Yoshida Y, Niki E. Antioxidant effects of phytosterol and its components. J Nutr Sci Vitaminol. 2003;49(4):277–280.

Yu J, Ma Y, Drisko J, Chen Q. Antitumor activities of *Rauwolfia vomitoria* extract and potentiation of carboplatin effects against ovarian cancer. Curr Ther Res Clin Exp. Elsevier. 2013;75:8–14.

Yuan H, Sun B, Gao F, Lan M. Synergistic anticancer effects of andrographolide and paclitaxel against A549 NSCLC cells. Pharm Biol. 2016;54(11):2629–2635.

Yuan M, Meng W, Liao W, Lian S. Andrographolide antagonizes TNF-α-induced IL-8 via inhibition of NADPH Oxidase/ROS/NF-κB and Src/MAPKs/AP-1 axis in human colorectal cancer HCT116 cells. J Agr Food Chem. 2018;66(20):5139–5148.

Yusuf RZ, Duan Z, Lamendola DE, Penson RT, Seiden MV. Paclitaxel resistance: molecular mechanisms and pharmacologic manipulation. Curr Cancer Drug Targets. 2003;3:1–19.

Zafaryab M, Fakhri KU, Khan MA, Hajela K, Rizvi MMA. *In vitro* assessment of cytotoxic and apoptotic potential of Palmitic acid for breast cancer treatment. Int J Life Sci Res. 2019;7(1):166–174.

Zheng CJ, Yoo JS, Lee TG, Cho HY, Kim YH, Kim WG. Fatty acid synthesis is a target for antibacterial activity of unsaturated fatty acids. FEBS Letters. 2005;579(23):5157–5162.

Zulkapli R, Abdul Razak F, Zain RB. Vitamin e (α-Tocopherol) exhibits antitumour activity on oral squamous Carcinoma Cells ORL-48. Integr Cancer Ther. 2017;16(3):414–425.

APPENDIX A

1. Solution used in cell culture

1.1 RPMI-1640 or DMEM medium

RPMI-1640 or DMEM medium (final concentration. 1.04% w/v)	10.4	g
$NaHCO_3$ (sodium bicarbonate) for RPMI-1640	2	g
$NaHCO_3$ (sodium bicarbonate) for DMEM	3.8	g

After RPMI and $NaHCO_3$ were dissolved. The pH was adjusted with 1 N HCl to give final pH around 7.4. The distilled water was added to medium solution until reach 1 L.

The medium solution was aseptically supplemented with:

Fetal Bovine Serum (final concentration 10% v/v)	100	ml
Penicillin/Streptomycin (final concentration 1% v/v)	10	ml
(10,000 U/ml of Penicillin, 10,000 μg/ml Streptomycin)		
200 mM, 100X L-glutamine (final concentration 2 mM, 1X)	10	ml

1.2 10X PBS

NaCl (sodium chloride)	80	g
KCl (potassium chloride)	2	g
Na_2HPO_4 (sodium hydrogen phosphate)	14.4	g
KH_2PO_4 (potassium dihydrogen phosphate)	2.4	g

800 ml DI water was used to dissolve the compounds using magnetic stirrer until completely dissolved. pH (potential hydrogen) was adjusted using pH paper indicator which should be in 7–8. The DI water was added and adjusted until 1000 ml. This solution was mentioned as 10X PBS. As the needed PBS was 1X PBS, the 10X PBS was dissolved by adding 100 ml of 10X PBS in 900 ml DI water.

APPENDIX B

1. Character of cell lines

1.1 Human breast carcinoma cell line

Two different human breast cancer cell lines MCF-7 and MDA-MB-231 were exploited in current research. The characters of each cell are displayed in Table 26 and Table 27.

Table 26. Biological properties of MCF-7 cells

Category	**Biological properties**
Cat No.	ATCC®HTB-22™
Organism	Homo sapiens, human
Disease	Adenocarcinoma
Tissue origin	Mammary gland, breast; derived from pleural effusion
Cell type	Epithelial, adherent
Hormone receptor expression	Estrogen receptor, expressed
Gene expression	Insulin-like growth factor binding proteins (IGFBP) BP-2; BP-4; BP-5
Cell duplication time	29 h
Comments	The MCF-7 cell line process estradiol via cytoplasmic estrogen receptors and form domes. The cells express the WNT7B oncogene. Growth of MCF-7 cells is inhibited by tumor necrosis factor alpha (TNF alpha). Secretion of IGFBP's can be modulated by treatment with anti-estrogens.
Culture medium and condition	RPMI-1640, supplemented with 10% fetal bovine serum, 1% Penicillin/Streptomycin (+10,000 Units/ml Penicillin, +10,000 µg/ml Streptomycin)
Cryopreservation	Culture medium supplemented with 5% (v/v) DMSO or fetal bovine serum in 5% (v/v) DMSO. Freeze cells were kept at liquid nitrogen vapor phase.
Image	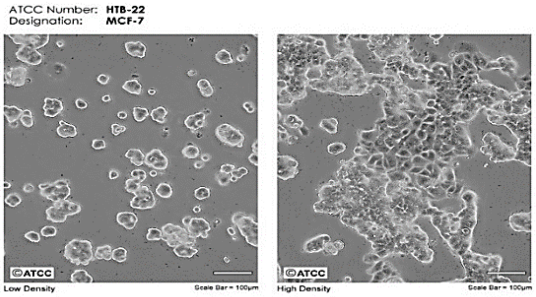

Table 27. Biological properties of MDA-MB-231 cells

Category	**Biological properties**
Cat No.	ATCC®HTB-26™
Organism	Homo sapiens, human
Disease	Adenocarcinoma
Tissue origin	Mammary gland, breast; derived from metastatic site: pleural effusion
Cell type	Epithelial, adherent
Receptor expression	Epidermal growth factor (EGF), expressed Transforming growth factor alpha (TGF alpha), expressed
Gene expression	The cells express the WNT7B oncogene
Cell duplication time	38 h
Culture medium and condition	DMEM, supplemented with 10% fetal bovine serum, 1% Penicillin/Streptomycin (+10,000 Units/ml Penicillin, +10,000 µg/ml Streptomycin)
Cryopreservation	Culture medium supplemented with 5% (v/v) DMSO or fetal bovine serum in 5% (v/v) DMSO. Freeze cells were kept at liquid nitrogen vapor phase.
Image	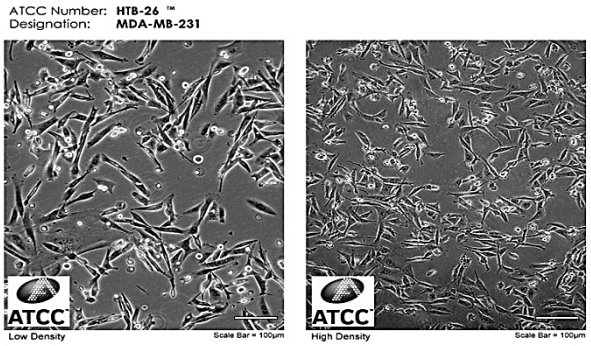

1.2 Human colorectal carcinoma cell line

Two different human colorectal cancer cell lines HT-29 and SW-620 were exploited in current research. The characters of each cell are displayed in Table 28 and Table 29.

Table 28. Biological properties of HT-29 cells

Category	**Biological properties**
Organism	Homo sapiens, human
Disease	Colorectal adenocarcinoma
Tissue origin	Colon
Cell type	Epithelial, adherent
Receptor expression	The cells express human adrenergic alpha2A, urokinase receptor (u-PAR), vitamin D (moderate expression)
Gene expression	The cells express transforming growth factor beta binding protein; mucin, myc, ras, myb, fos, sis, p53.
Cell duplication time	23 h
Comments	Ultrastructural features reported for HT-29 cells include microvilli, microfilaments, large vacuolated mitochondria with dark granules, smooth and rough endoplasmic reticulum with free ribosomes, lipid droplets, few primary and many secondary lysosomes. The cells express urokinase receptors but do not have detectable plasminogen activator activity. HT-29 cells are negative for CD4, but there is cell surface expression of galactose ceramide (a possible alternative receptor for HIV).
Culture medium and condition	DMEM, supplemented with 10% fetal bovine serum, 1% Penicillin/Streptomycin (+10,000 Units/ml Penicillin, +10,000 µg/ml Streptomycin)
Cryopreservation	Culture medium supplemented with 5% (v/v) DMSO or fetal bovine serum in 5% (v/v) DMSO. Freeze cells were kept at liquid nitrogen vapor phase.
Image	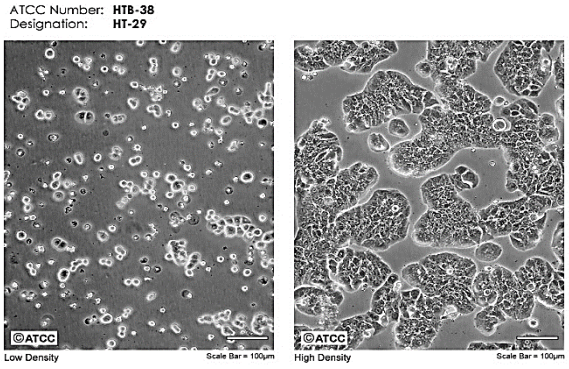

Table 29. Biological properties of SW-620 cells

Category	**Biological properties**
Organism	Homo sapiens, human
Disease	Dukes type C, Colorectal adenocarcinoma
Tissue origin	Colon; derived from metastatic site: lymph node
Cell type	Epithelial, adherent
Gene expression	The cells express carcinoembryogenic antigen, transforming growth factor alpha (TGF alpha), c-myc, K-ras, H-ras, N-ras, myb, sis and fos oncogenes.
Cell duplication time	20 h
Comments	SW-620 is a recurrence of the malignancy consequence in a wide-spread metastasis from the colon to an abdominal mass. The established cell line comprises mainly of individual small spherical and bipolar cells lacking microvilli. The cells were derived from a metastasis of the same tumor from which the SW480 was derived.
Culture medium and condition	DMEM, supplemented with 10% fetal bovine serum, 1% Penicillin/Streptomycin (+10,000 Units/ml Penicillin, +10,000 µg/ml Streptomycin)
Cryopreservation	Culture medium supplemented with 5% (v/v) DMSO or fetal bovine serum in 5% (v/v) DMSO. Freeze cells were kept at liquid nitrogen vapor phase.
Image	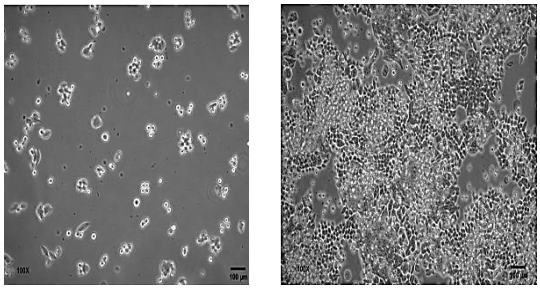 Low density High density

1.3 Human ovarian carcinoma cell line

Two different human colorectal cancer cell lines A2780 and SKOV-3 were exploited in current research. The characters of each cell are displayed in Table 30 and Table 31.

Table 30. Biological properties of A2780 cells

Category	**Biological properties**
Cat No.	C0017002 (Addexbio)
Organism	Homo sapiens, human
Disease	Ovarian carcinoma
Tissue origin	Ovary
Cell type	Epithelial, adherent
Cell duplication time	16 h
Culture medium and condition	RPMI-1640, supplemented with 10% fetal bovine serum, 1% Penicillin/Streptomycin (+10,000 Units/ml Penicillin, +10,000 μg/ml Streptomycin)
Cryopreservation	Culture medium supplemented with 5% (v/v) DMSO or fetal bovine serum in 5% (v/v) DMSO. Freeze cells were kept at liquid nitrogen vapor phase.
Image	 Source: author's sample

Table 31. Biological properties of SKOV-3 cells

Category	**Biological properties**
Cat No.	ATCC® HTB-77™
Organism	Homo sapiens, human
Disease	Adenocarcinoma
Tissue origin	Ovary: ascites
Cell type	Epithelial, adherent
Gene expression	The cells express blood type B; Rh+
Cell duplication time	30 h
Comments	SKOV-3 cells are resistant to tumor necrosis factor and to several cytotoxic drugs including diphtheria toxin, cis-platinum and Adriamycin.
Culture medium and condition	RPMI-1640, supplemented with 10% fetal bovine serum, 1% Penicillin/Streptomycin (+10,000 Units/ml Penicillin, +10,000 µg/ml Streptomycin)
Cryopreservation	Culture medium supplemented with 5% (v/v) DMSO or fetal bovine serum in 5% (v/v) DMSO. Freeze cells were kept at liquid nitrogen vapor phase.
Image	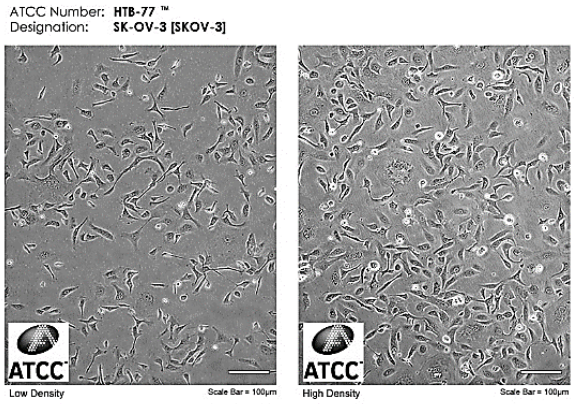

1.4 Non-cancerous cell line

Two different non-cancerous cancer cell lines Vero and L929 were exploited in current research. The characters of each cell are displayed in Table 32 and Table 33.

Table 32. Biological properties of Vero cells

Category	**Biological properties**
Cat No.	ATCC® CCL-81™
Organism	Cercopithecus aethiops (African green monkey)
Disease	-
Tissue origin	Kidney
Cell type	Epithelial, adherent
Cell duplication time	24 h
Applications	Vero cells can be used for detecting verotoxin, testing therapeutics, studying malaria biology, testing media, testing the mycoplasma, transfecting virus, detecting virus in ground beef.
Culture medium and condition	RPMI-1640, supplemented with 10% fetal bovine serum, 1% Penicillin/Streptomycin (+10,000 Units/ml Penicillin, +10,000 µg/ml Streptomycin)
Cryopreservation	Culture medium supplemented with 5% (v/v) DMSO or fetal bovine serum in 5% (v/v) DMSO. Freeze cells were kept at liquid nitrogen vapor phase.
Image	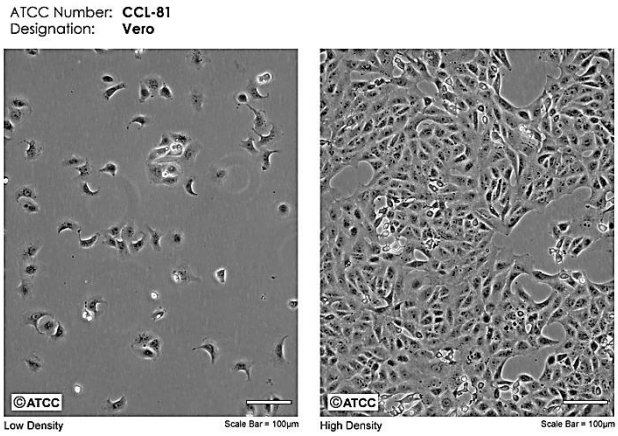

Table 33. Biological properties of L-929 cells

Category	**Biological properties**
Organism	Mouse
Disease	Normal
Tissue origin	Adipose
Cell type	Fibroblast, adherent
Cell duplication time	14 h
Description	The parent L strain was derivative of normal subcutaneous areolar and adipose tissue of a 100-day-old-male C3H mouse. NCTC clone 929 Clone of strain L.
Culture medium and condition	DMEM, supplemented with 10% fetal bovine serum, 1% Penicillin/Streptomycin (+10,000 Units/ml Penicillin, +10,000 µg/ml Streptomycin)
Cryopreservation	Culture medium supplemented with 5% (v/v) DMSO or fetal bovine serum in 5% (v/v) DMSO. Freeze cells were kept at liquid nitrogen vapor phase.
Image	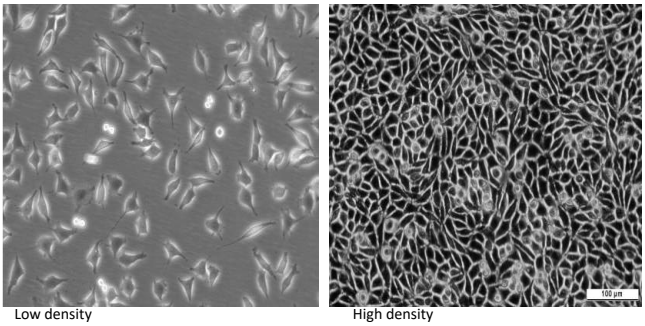 Low density High density

VITAE

Name Muhammad Faisal

Student ID 6110320004

Educational Attainment

Degree	Name of Institution	Year of Graduation
S.Si (Biological Sciences)	Andalas University	2017

Scholarship Awards during Enrolment

Thailand Education Hub for ASEAN countries for Prince of Songkla University

PSU GS. Financial Support for Thesis, Graduate School, Prince of Songkla University.

Work – Position and Address

-

List of Publication and Proceeding

Poster Presentation

Faisal M, Liu X, Tedasen A, Rattanaburee T, Graidist P. Antiproliferative assessment induced by different extracts of *Andrographis paniculata*, *Zizphus spina-christi* and *Vernonia extensa* leaves on cancer cell lines. The International Conference on Molecular Diagnostics and Biomarker Discovery 2019 (MDBD2019). Penang, Malaysia. 25-26 September 2019.